2020-09-11

Regulation of Innate Immunity in the C. elegans Intestine by Olfactory Neurons

Kyle J. Foster
University of Massachusetts Medical School

REGULATION OF INNATE IMMUNITY IN THE *C. ELEGANS* INTESTINE BY

OLFACTORY NEURONS

A Dissertation Presented By:

KYLE J. FOSTER

Submitted to the Faculty of the

University of Massachusetts Graduate School of Biomedical Sciences, Worcester

in partial fulfillment of the requirements for the degree of

DOCTOR OF PHILOSOPHY

September 11, 2020

Program in Innate Immunity

REGULATION OF INNATE IMMUNITY IN THE *C. ELEGANS* INTESTINE BY

OLFACTORY NEURONS

A Dissertation Presented

By

KYLE J. FOSTER

This work was undertaken in the Graduate School of Biomedical Sciences

Interdisciplinary Graduate Program

Under the mentorship of

_____

Read Pukkila-Worley M.D., Thesis Advisor

_____

Cole Haynes Ph.D., Member of Committee

_____

Beth McCormick Ph.D., Member of Committee

_____

Mark Alkema Ph.D., Member of Committee

_____

Alex Soukas M.D., External Member of Committee

_____

Neal Silverman Ph.D., Chair of Committee

_____

Mary Ellen Lane, Ph.D.,
Dean of the Graduate School of Biomedical Sciences
September 11, 2020

Acknowledgements

I would first like to wholeheartedly thank my PI Read Pukkila-Worley for taking me on as his very first graduate student during his UMass Career. He took a risk on me and I took a risk on him – and looking back, choosing to walk into his office and asking him to be my Ph.D. mentor was one of best decisions I made during my academic career. His support and encouragement during my time at UMass molded me into the scientist I am today. I would also like to thank my fellow lab members Hilary, Sarah, Nick and Sammy for all their help and support throughout my graduate studies. Our lab is a team, and I couldn't have asked for a better team to work with for the past 5 years.

I'd like to recognize my TRAC committee members Cole Haynes, Mark Alkema, and Beth McCormick for always challenging me during our meetings and helping me to grow as a scientist and as a critical thinker. Their suggestions and critiques have helped me considerably to refine and improve my story. I would also like to acknowledge the support of my committee chair, Neal Silverman, who was always there to help me along the way throughout my journey in graduate school. He was the first faculty member I interviewed with when I was trying to get accepted into UMass, and it's only fitting that his signature is one of the last on my dissertation.

Dedications

Throughout my life, I have received an enormous amount of support from my family. They taught me when I was young how to develop a good work ethic and to always strive to be the best I could be. My success as a student and as a scientist is a direct result of their love and guidance throughout my academic career. I hope that I continue to grow as a scientist and that I never lose my strong desire to always ask questions about the world around me.

Thank you for always believing in me.

I would like to dedicate this dissertation to my parents, Gary and Jeanine, and to my grandparents Doris, James, and Barbara.

Published Works

The work presented in Chapter II of this thesis has been adapted from:

Foster, K., Cheesman, H., Liu, P., Peterson, N., Anderson, S., Pukkila-Worley, R. (2020). Innate Immunity in the C. elegans Intestine Is Programmed by a Neuronal Regulator of AWC Olfactory Neuron Development. Cell reports 31(1), 107478.

The work presented in Appendix I of this thesis has been adapted from:

Peterson, N., Cheesman, H., Liu, P., Anderson, S., Foster, K., Chhaya, R., Perrat, P., Thekkiniath, J., Yang, Q., Haynes, C., Pukkila-Worley, R. (2019). The nuclear hormone receptor NHR-86 controls anti-pathogen responses in C. elegans. PLoS genetics 15(1), e1007935.

The work presented in Appendix II of this thesis has been adapted from:

Foster, K., McEwan, D., Pukkila-Worley, R. (2020). Measurements of Innate Immune Function in C. elegans. Methods in molecular biology (Clifton, N.J.) 2144(), 145-160.

Abstract

The intestinal epithelium represents one of the first lines of defense against pathogenic bacteria. Immune regulation at this critical barrier is necessary to maintain organismal fitness, and mis-regulation here has been linked to numerous debilitating diseases. Functional relationships between the nervous system and immune system have been found to be critical in the proper coordination of immune defenses at barrier surfaces, however the precise mechanisms underlying theses interactions remains unclear.

Through conducting a forward genetic screen utilizing the model organism *Caenorhabditis elegans, we* uncovered a surprising requirement for the olfactory neuron gene *olrn-1* in the regulation of intestinal epithelial immunity. During nematode development, *olrn-1* is required to program the expression of odorant receptors in the AWC olfactory neuron pair. Here, we show that *olrn-1* also functions in AWC neurons in the cell non-autonomous suppression of the canonical p38 MAPK PMK-1 immune pathway in the intestine. Low activity of OLRN-1, which activates the p38 MAPK signaling cassette in AWC neurons during larval development, also de-represses the p38 MAPK PMK-1 pathway in the intestine to promote immune effector transcription, increased clearance of an intestinal pathogen and resistance to bacterial infection. However, derepression of the p38 MAPK PMK-1 pathway also results in severe developmental and reproductive defects, demonstrating the critical function of OLRN-1 to both prime *C. elegans* intestinal epithelial cells for the induction of anti-pathogen responses, and to limit the deleterious effects of immune hyper-activation. These data reveal an unexpected connection between olfactory

receptor development and innate immunity, as well as demonstrate how neuronal regulation of immune responses within the intestinal epithelium is critical for both reproductive and developmental fitness.

Table of Contents

Table of Tables

Table of Figures

List of Online Files

The following tables referenced in chapter 2 of this thesis are located on the publisher's website and can be downloaded by following the included links:

Table 2.1. The List of *olrn-1*-Regulated Genes from the mRNA-Seq Experiment, Related to Figure 2.2.

https://ars.els-cdn.com/content/image/1-s2.0-S2211124720303569-mmc2.xlsx

Table 2.2. Sample Sizes, Mean Lifespan, and p Values for Assays Presented in This Article, Related to STAR Methods.

https://ars.els-cdn.com/content/image/1-s2.0-S2211124720303569-mmc3.xlsx

Chapter 1: Introduction

1.1 *C. elegans* as a Model of Host-Microbe Interactions

Caenorhabditis elegans is a free-living soil-dwelling bacterivore that can be found ubiquitously in the environment where it primarily feeds on microbes found on decomposing organic matter. Over the past two decades, it has been discovered that nematodes possess a genetically tractable innate immune system that has allowed *C. elegans* to become a popular research model commonly used in the study of host-microbe interactions and immune regulation (Foster, Cheesman, et al., 2020; D. H. Kim et al., 2002; Peterson et al., 2019; Pukkila-Worley et al., 2011; Pukkila-Worley & Ausubel, 2012a, 2012b). The constant exposure to microbe-rich environments has created a selective pressure for *C. elegans* to develop specialized intestinal defense mechanisms to protect themselves from ingested pathogenic bacteria and fungi.

Functionally, the intestine of *C. elegans*, much like in mammals, serves as one of the first critical physical and immunological barriers to ingested pathogens. The *C. elegans* gut contains 20 non-renewable intestinal epithelial cells that are positioned as bilaterally
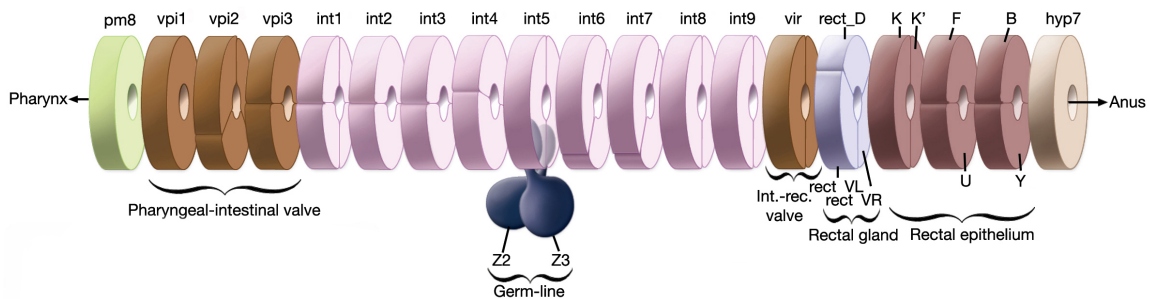
Figure 1.1: The Cells of the *C. elegans* intestine.

symmetric pairs that form a tube around the intestinal lumen. The one exception is the anteriormost intestinal ring, which is made up of four epithelial cells that are morphologically distinct and have notably different gene expression profiles compared to the neighboring more posteriorly intestinal epithelial cells (Figure 1.1). Even though *C. elegans* lacks the diverse array of specialized intestinal epithelial cells that line the human intestinal tract (i.e. Paneth cells, goblet cells, and neuroendocrine cells), the basic organization of the *C. elegans* intestine is markedly similar to that of higher chordates. Individual intestinal epithelial cells, which closely resemble enterocytes, each have a well-defined apical domain (including a microvillar brush border), basolateral domain, and basement membrane. Gap junctions located on the lateral cell membranes connect each epithelial cell to its neighbor, allowing small molecules to transit freely between cells. In addition to the morphological similarities that exist between the nematode and mammalian intestine, both also function similarly regarding the ability to mount innate immune responses. Many potent non-specific innate immune mechanisms that are necessary to protect intestinal epithelial cells against invading pathogens are evolutionarily conserved between nematodes and mammals; however, all adaptive immune mechanisms are notably absent from *C. elegans*. Thus, while not a perfect model, the conserved core structural and functional elements of the *C. elegans* intestine makes it an incredibly useful model in the study of host-pathogen interactions.

In a laboratory setting, there are numerous key features that make *C. elegans* a convenient research model in the study of host-pathogen interactions. Firstly, as *C. elegans* is encased in a transparent cuticle, it is extraordinarily simple to observe complex core

biological processes with limited difficulty. When utilizing *C. elegans* as an infection model, one can easily observe feeding, intestinal colonization, and morphological changes in intestinal epithelial cells, all while utilizing a low powered differential contrast (DIC) microscope. Secondly, numerous powerful genetic tools are readily available for use in *C. elegans*, such as the ability to selectively target and knock down genes of interest via RNAi, and the ability to manipulate gene function by taking advantage of the powerful CRISPR Cas9 system (Fire et al., 1998; Friedland et al., 2013). Harnessing these tools makes it possible to determine precisely which genes are required for adequate immune function and regulation (Anderson et al., 2019; Cheesman et al., 2016; Fire et al., 1998; Peterson et al., 2019). Third, the utilization of fluorescently tagged transcriptional and translational reporters enables cellular processes to be monitored in real time (Anderson et al., 2019; Chalfie et al., 1994; Cheesman et al., 2016; Foster, Cheesman, et al., 2020; Peterson et al., 2019; Pukkila-Worley et al., 2014). This unique ability provides researchers with the ability to quantify gene expression, determine protein localization and stability, and observe how those each may change in response to environmental and pathogenic stressors. Lastly, while the immune system of *C. elegans* significantly predates the intricate immune system present in mammals, many components of core immune signaling pathways are evolutionarily conserved (Pukkila-Worley et al., 2014; Pukkila-Worley & Ausubel, 2012b; Troemel et al., 2006). Thus, working with *C. elegans* gives insight into complex signaling pathways that would otherwise be much more challenging to characterize in higher order species.

For all the above reasons, *C. elegans* remains a valuable tool for characterizing the complex biological relationships nematodes have with microbial counterparts. To date, investigators have developed infection models using numerous human pathogens including *Pseudomonas aeruginosa* (Conery et al., 2014; Kirienko et al., 2014; Powell & Ausubel, 2008) *Serratia marcescens* (Mallo et al., 2002; Pujol et al., 2001), Salmonella enterica (Aballay et al., 2003; Kerry et al., 2006), Enterococcus faecalis (Kerry et al., 2006; Moy et al., 2009), and fungi such as *Cryptococcus neoformans* (Alspaugh et al., 2002; Means et al., 2009; Pukkila-Worley et al., 2005), and *Candida albicans* (Pukkila-Worley et al., 2009, 2011) . As innate immune systems of high order chordates have evolved from these simple invertebrate species, the information gained from studying host-microbe interactions using accessible and tractable model organisms like *C. elegans* allows for a more comprehensive understanding basic biological principles underlying mechanism of innate immunity in mammals.

1.2 Chemosensation and Behavioral Avoidance in *C. elegans*

The ability to locate nutritious food sources and avoid toxic compounds and pathogenic microbes is vital to the longevity and evolutionary fitness and all organisms (Peters & Harper, 1985; Sanahuja & Harper, 1962). As *C. elegans* thrives in bacteria laden environments, the ability to dynamically respond to environmental conditions, such as the presence or absence of food sources, the quality of food sources, or the existence of pathogens is of critical importance. Thus, nematodes rely upon a highly developed chemosensory system in order to collect and process input gathered from its surrounding

in order to influence core biological processes such as foraging behaviors, pathogen avoidance, and immune activation for the purpose of maximizing the odds of surviving in hostile habitats (C. Bargmann, 2006; Ha et al., 2010; Hao et al., 2018; K C Reddy et al., 2009)

1.2.1 Chemosensation in *C. elegans*

For *C. elegans* to navigate its microbe rich habitat, it must be able to discriminate nutritious food sources from potentially harmful pathogens. One important mechanism by which nematodes are able to integrate environmental cues is by utilizing a highly specialized system of chemosensory and olfactory neurons (C. Bargmann, 2006; C. I. Bargmann et al., 1993; Rankin, 2006; Troemel et al., 1997; Zhang et al., 2005) . In fact, an estimated 5% or all nematode genes are involved in the recognition of environmental stimuli. *C. elegans* contains 32 chemosensory neurons - the vast majority of these neurons (22 out of 32) are paired neurons of the amphid sensilla, four are paired neurons of the phasmid sensilla, and six are IL2 neurons of the inner labial sensilla (Table 1). Sensory dendrites from chemosensory neurons protrude through openings in the body formed by neighboring glial cells where they make direct contact with the environment (S. Ward et al., 1975; Ware et al., 1975).

	Function
ASE	• Chemotaxis to water soluble attractants
AWA	• Chemotaxis to diacetyl, pyrazine, trimethylthiazole • Required for sexual attraction in males
AWB	• Avoidance from 2-nonanone, 1-octanol • Light sensation • Electro sensory navigation
AWC	• Chemotaxis to volatile odorants • Induction of local search behavior and promoting turns • Thermosensation • Electro sensory navigation • Modulation of innate immune responses to pathogenic bacteria
ASH	• Nociception, • Avoidance responses from noxious stimuli • Light sensation • Electro sensory navigation • Modulation of innate immune responses to pathogenic bacteria • Plays role in establishment of asymmetric fates of AWCL/R
ASI	• Control entry into dauer stage: sole source of DAF-7/TGF-β • Induction of local search behavior, promoting turns, and reversals • Chemotaxis to lysine • Thermosensory • Pheromone sensing • Modulation of innate immune responses to pathogenic bacteria
ADF	• Only serotonergic sensory neurons • Dauer formation, • Chemotaxis (minor) to cAMP, biotin, Cl$^-$, and Na$^+$
ADF	• Chemotaxis to water soluble attractants • Control entry into dauer stage • Lifespan regulation
ASJ	• Control entry into and exit from dauer stage • Light sensation • Electro sensory navigation
ASK	• Chemotaxis to LYS • Avoidance from protons, detergents, alkaloids • Pheromone sensing • Light sensation • Electro sensory navigation
ADL	• Avoidance behavior from heavy metals • Social feeding behavior • Pheromone sensing
URX	• Oxygen/aerotaxis • Social feeding • Lifespan regulation • Suppression of innate immunity
AQR	• Oxygen/aerotaxis • Social feeding • Suppression of innate immunity
PQR	• Oxygen/aerotaxis • Social feeding • Suppression of innate immunity • Mate-searching behavior of males
PHA	• Chemorepulsion behavior • Mate-searching behavior of males
PHB	• Chemorepulsion behavior

Table 1: Chemosensory Neurons and their reported functions

Chemosensory neurons generally exist as bilateral structurally symmetric pairs (annotated as left and right), however several gene expression studies have discovered numerous examples of asymmetrical gene expression patterns between left and right pairs of neurons within the same class (Chuang & Bargmann, 2005; Huang et al., 2007; Sagasti et al., 2001; S. Yu et al., 1997). The two ASE neurons, for example, are functionally discrete, with the ASER neuron able to detect chloride and potassium ions whereas the ASEL neuron detects sodium ions (S. Yu et al., 1997) . Similarly, AWC olfactory neurons display notable asymmetric distribution of chemoreceptors. While both AWC neurons can detect benzaldehyde and isoamyl alcohol, the volatile odorants butanone and 2,3-pentanedione are only detected by one or the other. This functional asymmetry that exists within AWC neurons is required for odor differentiation and behavioral responses that result upon recognitions of these odors (Huang et al., 2007; Troemel et al., 1999; Wes & Bargmann, 2001) .

As the chemosensory system functions to detect environmental stimuli, it has been shown to be tightly integrated with both behavioral and locomotive responses. Studies performed using numerous volatile organic compounds demonstrated that in fact, each specific sensory neuron elicits a specific and reproducible behavioral response (Wes & Bargmann, 2001). Some neurons, such as AWC, and AWA neurons are chemoattractive, whereas AWB is linked to repulsion (Wes & Bargmann, 2001). Interestingly, if chemoreceptors normally expressed in neurons linked to chemoattraction are instead expressed in neurons linked to repulsive responses, the corresponding odorant becomes repulsive to *C. elegans* (Wes & Bargmann, 2001). This suggests that each sensory neuron

induces a preferential behavioral response upon activation that is independent of chemoreceptor expression. By systematically receiving input for the environment, *C. elegans* is able to make complex decisions in order to productively navigate its surroundings.

1.2.2 Food Preference and Behavioral Avoidance

All living organisms must carefully select their food in order to meet specific dietary requirements that promote developmental and reproductive fitness (Peters & Harper, 1985; Sanahuja & Harper, 1962). The two primary steps of food acquisition include locating and subsequently evaluating the quality of available food sources in the environment. *C. elegans* thrive in microbe rich environments where it is especially critical to differentiate between nutritious and potentially pathogenic food sources in order to ensure survival. The presence and quality of bacterial food sources can dramatically affect *C. elegans* behavior, inducing or repressing actions such as feeding, locomotion, thermotaxis, and aerotaxis (Rankin, 2006; Shtonda & Avery, 2006). When given a choice between high- and low-quality bacteria, worms will almost always choose to feed on lawns of high-quality bacteria (Rankin, 2006; Shtonda & Avery, 2006). High quality food in this case is defined as bacteria that is known to support robust growth and development. Not only will worms gravitate towards higher quality food, but they also display different behaviors while feeding on more nutritious food sources, characterized by a decrease in roaming behaviors (straight rapid forward movement), and an increase in dwelling behavior (frequent direction changes and reversals). On poor quality food sources, *C.*

elegans tends to display just the opposite behavior, increasing roaming and decreasing dwelling. While worms always tend to ultimately prefer high quality food sources over time, the process of developing food presence is typically a learned process. In fact, even the odors associated with pathogenic bacteria usually requires initial exposure before inducing an aversive response (Zhang et al., 2005). Initial studies attempting to understand the precise biological mechanisms influencing food preference behaviors concluded that serotonin plays a critical role in pathogen induced olfactory learning and that the specific neurons involved in this circuit are NSM and AFD neurons; with NSM mediating an attractive response and AFD mediating a repulsive response. Downstream AIY and AIZ interneurons, upon activation by serotonin release have been shown to subsequently modulates aversive learning behavior. Further complicating the story, follow-up studies by Avery et al. determined that AIY interneurons also appear to play an important role in suppressing roaming-to-dwelling transitions, resulting in longer food-seeking periods (Zhang et al., 2005). Thus, behavioral leaning and food preference is a complex process that integrates both motor-sensory cues, olfactory cues and aversive learning behavior in order to make complex decisions.

Behavioral avoidance not only assists in the search of nutritious food, but also is a vital defense strategy to avoid pathogenic food sources. *C. elegans* has been shown to employ both learned and, less commonly, innate avoidance behaviors in order to reduce exposure to potentially toxic or pathogenic food sources (Ballestriero et al., 2016; Chang et al., 2011; Meisel & Kim, 2014; Schulenburg & Ewbank, 2007; Styer et al., 2008; Zhang et al., 2005). Innate avoidance behavior is when *C. elegans* displays aversion to a pathogen

without having had any prior contact. A prime example of *C. elegans* innate behavioral avoidance can be observed upon exposure to numerous dodecanoic acid secreting *Streptomyces* species (Tran et al., 2017). Dodecanoic acid, a nematicide which is sensed by the seven-transmembrane receptor SRB-6, causes rapid avoidance behavior in *C. elegans* (Tran et al., 2017). SRB-6 has been shown to be expressed in both phasmid and aphid chemosensory neurons, including PHA, PHB, ASH, ADL and ADF. Interestingly, *C. elegans* also exhibits a strong innate aversion to decanoic acid, another potent nematicide that does not appear to be secreted from *Streptomyces* (Tran et al., 2017). This observation potentially indicates that *C. elegans* has evolved to sense a diverse array of toxic compounds - some secreted by bacteria and others outside the context of pathogen exposure. Another study by Ballestriero et al. found that *C. elegans* displays innate avoidance behavior to toxic bacterial metabolite tambjamine YP1, which is secreted by a broad set of bacterial strains commonly found in soil and freshwater environments (Ballestriero et al., 2016). Less well understood is why some compounds induce immediate innate avoidance behavior, while others involve olfactory learning and subsequent adaptation.

Learned avoidance behavior, unlike innate avoidance behavior, requires an initial exposure to a toxic stimulus in order to induce future avoidance. A well-studied bacterial pathogen that elicits a notable learned avoidance phenotype is the gram-negative, opportunistic pathogen *Pseudomonas aeruginosa* (Chang et al., 2011; Meisel et al., 2014; Styer et al., 2008). Under optimal growth conduction and high cell density, *Pseudomonas Aeruginosa* produces two potent toxins: phenazine-1-carboximide and pyochelin. Upon

initial exposure to *Pseudomonas Aeruginosa*, *C. elegans* is strongly attracted to the bacterial lawn. However, soon after this initial attraction, animals begin to display a strong aversion to the bacterial lawn and can be observed fleeing the lawn (Chang et al., 2011; Meisel et al., 2014; Styer et al., 2008). This process of learned aversion to *Pseudomonas* has been shown to be dependent upon DAF-7 neuroendocrine signaling originating from ASJ neurons (Meisel et al., 2014). Upon exposure to *Pseudomonas aeruginosa*, the secreted toxins phanazine-1-carboximide and pyochelin activate the expression *daf-7* in ASJ neurons, which in turn, signals to DAF-1 in adjacently located RIM/RIC interneurons. This process has been shown to alter aerotaxis and ultimately promotes a lawn-leaving behavior (Meisel et al., 2014).

An exciting recent discovery relating to nematode aversive learning has found evidence of multi-generation pathogen avoidance. Progeny of *C. elegans* exposed to lawns of *P. aeruginosa* have been found to more strongly avoid lawns of *P. aeruginosa* when they encounter it, compared to controls whose parents have never encountered the pathogen (Moore et al., 2019). This suggests that not only is decision making regarding pathogen avoidance a complex process in the confines of a single generation, but multi-generational epistatic changes may need to be accounted for when trying to accurately characterize behavioral responses to microbes. Further work will need to be conducted in order to characterize precisely how trans-generational inheritance may influence the decision-making process that regulates behavioral avoidance to pathogens.

1.3 Molecular Immunity in *C. elegans*

1.3.1 Introduction to innate immunity in *C. elegans*

The innate immune system is an ancient defense mechanism that provides the first line of protection against pathogen infection after behavioral avoidance mechanisms fail. Studies first performed in *Drosophila* have demonstrated that numerous primitive mechanisms of pathogen detection and the subsequent activation of innate defense responses are broadly conserved across a wide range of organisms (Christophides et al., 2002; Medzhitov & Janeway, 1998; Sackton et al., 2007). Canonical innate immune activation results after pathogen recognition occurs, typically through detection of pathogen-associated molecular patterns (PAMPs), such as bacterial wall components, or through detection of damage-associated molecular patterns (DAMPs), such as the release of nuclear or cytoplasmic material into the extra cellular space. Upon detection of a threat, core sets of signal transduction pathways are activated typically involving defined families of proteins including protein kinases and phosphates which activate transcriptional regulators to induce protective transcriptional responses. While adaptive immunity typically involved a pathogen specific immunological response, the innate immune system relies on a quick and robust, though non-specific response to general environmental and pathogenic stressors.

As *C. elegans* does not possess an adaptive immune system, it therefore relies solely on the innate immune system to provide adequate protection against pathogens and other environmental assaults (D. H. Kim et al., 2002; Pukkila-Worley & Ausubel, 2012a;

Troemel et al., 2006). Even so, numerous innate immune signaling components conserved across many species appear to be absent from *C. elegans*. Early studies in Drosophila characterized the role of Toll-like signaling pathways in pathogen detection, a process by which specific molecular patterns present on pathogens are recognized by toll-like receptors (TLRs) and subsequently initiate signaling cascades resulting in the induction of distinct patterns of gene expression which promote pathogen clearance (Belvin & Anderson, 1996; Nüsslein-Volhard & Wieschaus, 1980; SUN & FAYE, 1992; Wasserman, 1993). TLR signaling pathways are notably absent in *C. elegans*, as is NF-κB, the transcription factor that induces the transcription of numerous pro-inflammatory molecules upon TLR activation in many metazoans. Interestingly, *C. elegans* does in fact contain one Toll homolog, *tol-1*, which has been shown to be important during pharyngeal invasion of *S. enterica*, however numerous studies have failed to demonstrate that it plays an important role in the detection of PAMPs (Pujol et al., 2001; Tenor & Aballay, 2008). Thus, *C. elegans* must rely on a very limited ancient innate immune repertoire to effectively mitigate pathogenic infection.

1.3.2 The p38 PMK-1 Innate Immune Pathway

At the core of *C. elegans* immunity to bacterial pathogens, lies the evolutionarily conserved PMK-1 p38 MAPK pathway. MAPK signaling pathways are highly conserved across a broad range of species and serve as transducers of extracellular stimuli, relaying important environmental information into the cell in order to produce appropriate transcriptional response (Arthur & Ley, 2013; Feng & Li, 2011). MAPK pathways have

been shown to regulate many important physiological processes in numerous evolutionarily diverse organisms, such as development, growth, cell proliferation, stress response and immunity (Keshet & Seger, 2010; Morrison, 2012). Identified during a forward genetic screen seeking to determine genes required for *C. elegans* survival during pathogen infection, the PMK-1 p38 MAPK pathway was found to be a core requirement for *C. elegans* immunity (D. H. Kim et al., 2002). The *C. elegans* PMK-1 p38 MAPK pathway consists of a kinase cascade including the MAPKKK *nsy-1*, the MAPKK *sek-1*, and the p38 MAPK gene *pmk-1*, and is orthologous to the human ASK-1/MKK-3/6 MAPK pathway (Figure 1.2). Animals harboring loss-of-function mutations in any of the core kinases within the PMK-1 p38 MAPK pathway results in notable hyper-susceptibility to killing by a wide gamut of bacterial and fungal pathogens, suggesting that *C. elegans* relies heavily upon this signaling pathway for immunity to diverse microorganisms (Bolz et al., 2010; Cheesman et al., 2016; D. H. Kim et al., 2002; Pukkila-Worley et al., 2014; Troemel et al., 2006). Subsequent studies aimed at further characterizing this pathway identified TIR-1, the only TIR-domain adapter protein in *C. elegans*, as being positioned directly upstream of the NSY-1-SEK-1-PMK-1 signaling cassette and determined it to be required for pathway activation (Liberati et al., 2004). TIR-1 domains are intracellular signaling domains present on many mammalian immune signaling intermediates such as MyD88, IL-1R, and toll receptors. As the *C. elegans* genome does not encode any of these functional immune elements, it remains unclear precisely how TIR-1 is activated and what upstream signaling components may exist to initiate the PMK-1 p38 MAPK pathway.

Upon activation, the PMK-1 p38 MAPK pathway results in the sequential phosphorylation of NSY-1, SEK-1, and finally PMK-1 at conserved serine/threonine residues (D. H. Kim et al., 2002; Troemel et al., 2006). Phosphorylated, active PMK-1 subsequently phosphorylates the CREB/ATF bZIP transcription factor, ATF-7 (Pukkila-Worley et al., 2012; Shivers et al., 2010). Under basal conditions, ATF-7 functions as a transcriptional repressor, however upon phosphorylation by active PMK-1, ATF-7 becomes a transcriptional activator of PMK-1-regulated genes in response to *P. aeruginosa* infection (Shivers et al., 2010). In fact, subsequent studies have concluded that over 50% of all genes differentially upregulated in response to *Pseudomonas aeruginosa* infection rely upon ATF-7 for their transcriptional activation. ChIP-seq analysis confirmed this, by showing direct binding of ATF-7 at the promotors of a significant subset of pseudomonal-response genes, demonstrating that upon pathogen infection, ATF-7 functions as a direct transcriptional regulator downstream of the p38 PMK-1 pathways responsible for coordinating the induction of a broad assortment of protective defense genes required for *C. elegans* immunity (Shivers et al., 2008, 2010).
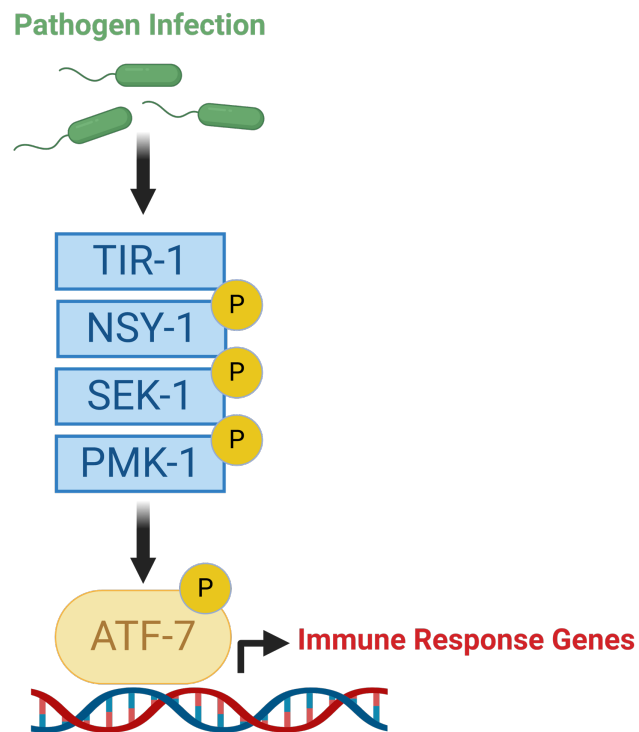
Figure 1.2: The *C. elegans* p38 PMK-1 MAPK Pathway

Activation of the p38 PMK-1 pathway elicits the transcription of a wide assortment of antimicrobial peptides (AMPs) that function to mitigate pathogen infection by promoting pathogen clearance (Cheesman et al., 2016; Foster, Cheesman, et al., 2020; Peterson et al., 2019; Pukkila-Worley et al., 2012; Pukkila-Worley & Ausubel, 2012b; Troemel et al., 2006). There are several primary classes of AMPs that are commonly induced upon exposure to pathogenic microbes such as: defensins, which cause permeabilization of the pathogen membrane, lysozymes, which digest peptidoglycans within in bacterial cell walls, and putative immune effectors including CUB-like domain proteins and C-type lectins (Irazoqui et al., 2010; Mallo et al., 2002; Murphy et al., 2003;

Pujol, Zugasti, et al., 2008; Pukkila-Worley et al., 2011). Generally speaking, antimicrobial peptides interact in a non-specific manner with invading pathogens, and usually target general structural elements of pathogens rather than microbe-specific moieties.

Conservation of the p38 MAPK pathway across a broad range of metazoans - from *C. elegans* to mammals - and its relevance in human disease, makes it a particularly lucrative area of research. Four p38 MAP kinases have been identified in humans, p38-α, p38-β p38-γ, and p38-δ. Collectively, p38 MAP kinases in humans have been shown to regulate a plethora of biological processes including cell differentiation, apoptosis, autophagy, and coordinate responses to stress stimuli, such as cytokines, heat shock, and osmotic shock . Abnormal activity of p38 MAP kinases has been linked to the onset of numerous diseases such as cancer, cardiovascular disease, inflammatory bowel disease, and neurological conditions such as Alzheimer's disease (Hollenbach et al., 2004; Iwasa et al., 2003; Johnson & Bailey, 2003; Wang et al., 2002; Xia et al., 1995; Zarubin & Han, 2005). Thus, there is currently and unmet medical need to learn more about precisely how p38 MAPK pathways are activated and subsequently regulated in order to properly address their role in clinically relevant human disease.

1.4 Mechanisms to Promote Immune Homeostasis in *C. elegans*

1.4.1 Aberrant immune activation is toxic to *C. elegans*

Immune responses are necessary for all organisms to protect themselves against environmental stressors, pathogens, and xenobiotic agents. *C. elegans* must be able to

swiftly and potently respond to threats as they are constantly exposed to a plethora of potentially dangerous bacteria and fungi in their natural habitat. While these inducible defense responses are beneficial and promote longevity upon exposure to pathogenic organisms, inappropriate activation of immune responses can have disastrous consequences on organismal fitness (Cheesman et al., 2016; Foster, Cheesman, et al., 2020; Richardson et al., 2010). The additional stress placed on *C. elegans* during immune activation is especially felt within the endoplasmic reticulum, where immune effector proteins must be folded and exported efficiently to ensure a robust defense response is initiated in a timely manner. A study by Richardson et al. was the first to clearly show that pathogen infection causes a significant increase in ER stress during pathogen infection. This added organismal stress was found to be toxic in developing animals, so much so that it led to larval lethality in animals lacking XBP-1, a key component of a compensatory unfolded protein response pathway that functions to maintain ER homeostasis (Richardson et al., 2010). A related study published by Cheesman et al., subsequently demonstrated that constitutive induction of the p38 PMK-1 MAPK pathway was noticeably toxic to developing animals. Mutants harboring gain-of-function (gf) mutations in the MAPKKK *nsy-1* were found to robustly induce PMK-1-dependent immune responses, which resulted in a notable survival advantage when survival assays were conducted using *P. aeruginosa* (Cheesman et al., 2016) However, under normal conditions *nsy-1(gf)* animals were significantly smaller, thinner and developed at a much slower rate relative to wild-type animals. Furthermore, the reproductive fitness of these mutants was also affected, as they tended to lay significantly smaller broods. Cheesman et al. also utilized an immuno-

stimulatory molecule previously reported to induce the p38 PMK-1 MAPK pathway in the absence of pathogen exposure to demonstrate that similar developmental delays occurred in the context of artificial immune hyper-activation (Cheesman et al., 2016). These studies indicate that a careful balance that must be established and maintained between toxic immune activation and core developmental and reproductive processes in order to promote longevity and organismal fitness. Recent studies have built upon this observation, by working to elucidate mechanisms of immune regulation *C. elegans* employs in order to carefully coordinate activation of its immune defenses in order to provide adequate protection against environmental pathogens, while at the same time limiting the deleterious consequences that result from immune hyper-activation (Aballay, 2009; Foster, Cheesman, et al., 2020; Liu et al., 2016; Sellegounder et al., 2019; Sowa et al., 2020; Y. Yu et al., 2016). Described in the sections to follow are the various strategies *C. elegans* utilizes to regulate protective defense mechanisms in order to maintain immune homeostasis and thus limit the potentially deleterious consequences of aberrant immune activation.

1.4.2 Proteostasis: The IRE1-XBP1 Unfolded Protein Response Pathway

The endoplasmic reticulum is the site where protein folding and export, post-translational protein processing, and lipid synthesis occur. As all translated proteins must traffic through the ER, it is critically important that a balance is maintained between cellular demand and the capacity of the organelle to fold, process and export proteins. The Unfolded Protein Response (UPR) functions as a protective mechanism that maintains homeostasis within the ER by balancing protein import into and export out of the organelle

(Calfon et al., 2002; Shen et al., 2001). Under normal physiological conditions, the UPR can be thought of as a surveillance mechanism that prevents misfolded proteins from being exported to the golgi. However, under conditions of environmental stress, such as during pathogen infection when there is a rapid transcriptional up-regulation of immune defenses and detoxification genes, this sudden increase in protein processing demand places significant stress on the ER, inducing the UPR as a protective response aimed to alleviate organelle stress.

In *C. elegans*, upon sensing an increase in ER stress, the kinase IRE-1 excises an intron from *xbp-1* (X-box binding protein-1) mRNA by means of an unconventional splicing event (Calfon et al., 2002; Richardson et al., 2010). This splicing event of *xbp-1* causes a frame shift that results in the translation of a truncated *xbp-1* isoform that functions as a transcription factor which subsequently activates the expression of numerous ER-associated chaperones and degradation proteins. Interestingly, *xbp-1*-independent functions of *ire-1* have similarly been shown to reduce ER-stress during times of environmental stress. In addition to targeting *xbp-1*, ire-1 targets and causes the degradation of numerous other mRNA substrates, typically encoding proteins containing signal peptides and transmembrane domains that are particularly difficult for ER machinery to fold in the context of ER stress. Additionally, *ire-1* has been implicated in the activation of cell death machinery and in the formation of autophagosomes in a manner that is independent on XBP-1.

Translation inhibition is another common cellular strategy aimed at reducing the burden on the ER during times of excessive organismal stress. The mechanism by which

this occurs is anchored by the serine/threonine kinase, PEK-1 (Richardson et al., 2011; Shen et al., 2001). ER stress causes PEK-1-dependent phosphorylation of the alpha subunit of eIF2, subsequently leading to the inhibition of ribosome assembly and translation initiation. Additionally, translational inhibition has been shown to induce a potent avoidance response, potentially providing evidence that maintenance of proteostasis and avoidance behaviors are inherently linked, and work in tandem to reduce ER stress upon pathogen exposure (Melo & Ruvkun, 2012). Ultimately each of the aforementioned mechanisms causes a reduction in host translation of immune and stress-responsive molecules as a means to maintain proteostasis during pathogen infection or exposure to environmental stressors.

1.4.3 FSHR-1: A sensor of reactive oxygen species

Pattern recognition receptors (PRRs) are germ-line encoded pathogen sensor that respond to invading pathogens by activating immune defense signaling cascades. In mammals, PRR's respond to two main classes of molecules, pathogen-associated molecular patterns (PAMPs) and damage-associated molecular patterns (DAMPs). PAMPs activate protective defenses by sensing non-self-molecules such as bacterial lipopolysaccharides, endotoxins, and the presence of cytoplasmic DNA that are indicative of an active infection. DAMPs on the other hand activate the immune and inflammatory responses by sensing endogenous molecular signatures that are released from dead and dying cells, such as chromatin organization and heat-shock proteins, or a buildup of

reactive oxygen species (ROS). A commonality among many PRR's is the presence of a leucine-rich repeat (LRR), a structural motif that is highly conserved in vertebrates, invertebrates, and plants.

While *C. elegans* lack many canonical PRR's such as TLRs and NOD-like receptors, screens of LRRs-containing proteins have found that LRR-containing proteins may contribute to the regulation of immune defense responses in *C. elegans*. Powell et all, reported that animals lacking the LRR-containing GPCR FSHR-1 exhibited hyper susceptibility to both gram negative and gram-positive bacteria. FSHR-1, which contains sequence similarity to mammalian follicle stimulating hormone, thyroid-stimulating hormone and luteinizing hormone receptors, has been shown to control the induction of both PMK-1-dependent and PMK-1-independent genes within the intestinal lumen (Powell et al., 2009). It was initially hypothesized that FHSR-1 might function either as a canonical pattern recognition receptor and directly senses secreted pathogen-related molecules, or as an intestinal hormone receptor, responsible for initiating transcriptional responses within tissues that make direct contact with ingested pathogens. Further research however, indicated that FSHR-1 appears to respond to oxidative stress, eliciting the production of transcriptional responses aimed at detoxifying reactive oxygen species (ROS) (Miller et al., 2015). ROS production is a conserved mechanism of pathogen virulence, however oxidative stress can also result from exposure to damaging xenobiotic agents and other environmental stressors, therefore FSHR-1 was postulated to be a DAMP sensor that coordinates numerous protective defense mechanisms in response to oxidative stress. Interestingly, Miller et al. also observed that the intestinal expression of FSHR-1 appeared

to be requirement for pathogen induced avoidance, suggesting that FSHR-1 responds to intestinal bacterial colonization by eliciting both microbial and behavioral immune responses (Miller et al., 2015).

1.4.4 Surveillance Immunity

A new paradigm emerging in the realm of immune activation and regulation in *C. elegans* is the concept of "surveillance immunity". During a pathogenic infection, there are numerous core cellular processes that can become interrupted (Dunbar et al., 2012; Haynes & Ron, 2010; McEwan et al., 2012; A M Nargund et al., 2012; Pukkila-Worley, 2016b). The concept of surveillance immunity is that in addition to sensing specific pathogen associated signatures directly, animals also monitor the function of core cellular processes that may be perturbed upon microbial infection as a surrogate. As *C. elegans* lacks many of the canonical microbe-associated molecular patterns (MAMP) sensors, worms might instead rely more heavily upon atypical mechanisms of pathogen recognition and immune regulation.

It has been observed that pathogen infection often leads to disruption of mitochondrial homeostasis, due in part to the bacterial secretion of mitochondrial toxins that compromise mitochondrial function (Kirienko et al., 2015). As mitochondrial function is a core biological process commonly targeted by pathogens, numerous mitochondrial homeostatic mechanisms have been found to be linked to immune regulatory processes. One key example of this involves the transcription factor ATFS-1, a key regulator of the mitochondrial UPR (UPR^{mt}). Under normal physiological conditions, ATFS-1 is readily

imported into the mitochondria and rapidly degraded. However, it in times of mitochondrial dysfunction, which commonly occurs during pathogen infection or environmental stress, import of ATFS-1 into the mitochondria is inhibited, thus allowing it to remain cytosolic where it ultimately translocates into the nucleus and initiates the transcription of numerous stress-response genes (Haynes & Ron, 2010; A M Nargund et al., 2012; Pellegrino et al., 2014). During bacterial infection in particular, it has been observed that ATFS-1 elicits the production of putative anti-microbial peptides and immune effectors found to be required for defenses against bacterial pathogens, thus mitochondrial stress is functionally a surrogate sensor of infection.

Disruption of core cellular processes not only results in the induction of immune response genes, but also has been shown to induce behavioral avoidance, suggesting that not only does *C. elegans* utilize sensory input to monitor the external environment for potential threats, but sensory signals originating within an animal's internal tissues are also used to induce behavioral changes. By genetically disrupting fundamental cellular activities such as protein translation, mitochondrial functions, the proteasome, vacuolar ATPases, the tubulin and actin *cytoskeletons*, mRNA processing, chromatin packaging, central metabolism, and the molting program in *C. elegans*, Melo et al. discovered that animals elicited strong behavioral avoidance responses, similar to what is typically observed when worms are subjected to pathogenic food sources (Melo & Ruvkun, 2012). Thus, *C. elegans* takes advantage of a plethora of both endogenous and exogenous sensory cues in order to influence complex behavioral and immunological processes during times of stress.

1.4.5 Neuronal regulation of Innate Immunity in *C. elegans*

Rapid induction of protective defense mechanisms upon pathogen recognition is necessary in order to provide adequate protection again invading microbes. An increasing body of evidence suggests that the nervous system, which can quickly respond to environmental stimuli, has the ability to carefully coordinate the induction and subsequent regulation of host immune responses (Aballay, 2009; Foster, Cheesman, et al., 2020; Liu et al., 2016; K C Reddy et al., 2009; J Sun et al., 2011). Understanding how the nervous system is tightly integrated with the immune system has been made possible by taking advantage of the numerous genetic tools available in *C. elegans*.

The *C. elegans* nervous system is relatively simplistic, containing only 302 neurons and 52 glial cells, which communicate through approximately 6400 chemical synapses. Additionally, the connectome of *C. elegans* has been completely mapped, providing comprehensive information about precisely how neurons interact with each other and with organ systems (White et al., 1986). It is for these reasons that *C. elegans* has become a powerful model for dissecting the relationship between the nervous system and the regulation of host defenses.

1.4.5.1 Insulin signaling

The highly conserved *daf-2/daf-16* insulin-like signaling pathway in *C. elegans* regulates a wide array of biological processes including lifespan, development, entry into

dauer, and stress resistance (Evans, Chen, et al., 2008; Henderson & Johnson, 2001; Miyata et al., 2008; Murphy et al., 2003; Ookuma et al., 2003; V. Singh & Aballay, 2009; Vowels & Thomas, 1992). It was also one of the first pathways found to be a part of a neuronal circuit involved in the coordination of immune defenses in *C. elegans*. When an agonist binds to the insulin-like growth factor 1 (IGF-1) receptor, DAF-2, a kinase cascade is initiated involving the AKT-1/AKT-2 and PDK-1 which ultimately results in the phosphorylation and cytoplasmic retention of the FOXO transcription factor, DAF-16. In the presence of an antagonist, the DAF-2/IGF-1 receptor is deactivated, and subsequent downstream phosphorylation events do not occur (Evans, Chen, et al., 2008). Non-phosphorylated DAF-16 then translocates into the nucleus where it acts as a transcriptional activator of numerous stress response and longevity promoting genes. The initial characterization of the DAF-2/DAF-16 pathway resulted following the observation that daf-2 mutants displayed significant extended lifespans relative to wildtype animals (Kenyon 1993), which at the time was the first mutant ever identified displaying such a significant lifespan extension. This observation eventually led to the question of whether longevity and immunity were inherently linked processes, and whether the DAF-2/DAF-16 pathway also functioned to regulate immune defenses in *C. elegans*. Early studies by Troemel et al. concluded that unlike the PMK-1 which functions as the backbone of *C. elegans* immunity against pathogens, DAF-16 regulated immune genes as part of "a more general stress response" (Troemel et al., 2006). However, not soon after this initial characterization, work by Evans et al. concluded the neurosecretory activity of dense core vesicles (DCVs) influenced the activity of the DAF-2/DAF-16 resulting in transcriptome

changes enriched for immune defense genes (Evans, Kawli, et al., 2008). Specifically, it was found that by either reducing or eliminating DCV secretions, the insulin-like-peptide encoding gene *ins-7* was downregulated and subsequently signaled via the DAF-2/DAF-16 pathway to induce the transcription of antimicrobial peptides within intestinal epithelial cells (Evans, Kawli, et al., 2008). This model was one of the first to demonstrate a direct regulatory role for the nervous system in the coordination of immune defenses in *C. elegans*. Interestingly, this mechanism appears to also be a virulence strategy used by *P. aeruginosa*, whereby upon infection, *ins-7* is induced and subsequently inhibits downstream signaling cascades responsible for upregulating immune defense genes. These discoveries not only provided important evidence that the *C. elegans* immune system is carefully controlled by elements of the nervous system, but also demonstrated that neuro-immune regulatory elements can be hijacked by pathogens in order to increase pathogenicity.

1.4.5.2 NPR-1: A Link Between Behavioral Avoidance and Innate Immunity

Soon after initial discoveries were made implicating the *C. elegans* nervous system as a key immune regulator, mutants in NPR-1, a neuronal GPCR and putative neuropeptide receptor orthologous to the mammalian Neuropeptide Y receptor, were found to display increased susceptibility to *P. aeruginosa*, *S. enterica*, and *E. faecalis*, demonstrating that *npr-1* is required for immunity against a wide range of microbes (Aballay, 2009; Styer et al., 2008). NPR-1 is expressed in AQR, PQR and URX neurons, and is required for the behavioral integration of numerous environmental cues, including responses to changes in

oxygen levels. NPR-1 loss-of-function mutants display hyperoxia avoidance, and as a result, can typically be observed displaying a lawn "bordering" phenotype in addition to clumping. While these behavioral abnormalities could independently explain the increased pathogen susceptibility of *npr-1* mutants, transcriptome analyses have revealed that many genes misregulated in *npr-1* mutants are similarly misregulated in *pmk-1* mutants (Aballay, 2009; Styer et al., 2008). Additionally, PMK-1 phosphorylation has been shown to be significantly decreased in NPR-1 mutants, suggesting that NPR-1 plays a key role in coordinating p38-dependent immune defenses. Many of the genes observed to be dependent on *npr-1* are genes known to be required for defense against *P. aeruginosa* and are expressed in specific intestinal cells that are in direct contact with pathogenic microbe during infection (Styer et al., 2008). These observations provide strong evidence that *npr-1* is not only required for promoting behavioral changes in response to oxygen availability, but also plays an important role in the modulation of innate immune responses during pathogen infection.

1.4.5.3 The Octopaminergic Immuno-inhibitory Pathway

Maintenance of proteostasis, as previously mentioned, is vitally important for maintaining both cell integrity and immune homeostasis. ER folding capacity can be modulated during the course of pathogen infection when there is a notable increase in protein folding demand placed on the organelle by inducing chaperones through activation of the unfolded protein response (UPR). Interestingly, recent evidence indicates in addition

to responding to increase in protein folding demand, UPR activation can be modulated directly by nervous system in response to environmental stimuli to coordinate the induction of immune pathways as a means to maintain immune homeostasis (Aballay, 2013; Jingru Sun et al., 2012). The first evidence of this phenomenon was the observation that OCTR-1, one of three *C. elegans* octopamine receptors expressed in ASH, ASI, and AIY neurons, functions as a negative regulator of p38-dependent immune responses. OCTR-1 mutant animals display notable resistance to pathogen and up regulate many pathogen response genes. The precise mechanism of this regulation was unclear until the observation was made that OCTR-1 was also found to suppress numerous genes within the *abu (activated in blocked unfolded protein response)* gene family, which are under the control of the non-canonical UPR (Jingru Sun et al., 2012). Interestingly, many *abu* genes are similarly differentially regulated in response to *P. aeruginosa*, suggesting that the non-canonical UPR is an important element of pathogen defense. Utilizing tissue-restricted OCTR-1 rescue lines, Sun et al. concluded that OCTR-1-esxpressing ASI and ASH negatively regulate innate immunity by controlling the activation of the non-canonical UPR. Subsequent studies built upon this model, showing that in addition to modulating the non-canonical UPR, OCTR-1 also gains control of the canonical, *xbp-1*-mediated UPR post-developmentally. OCTR-1 was shown to inhibit key translation machinery, such as the protein synthesis factor RPS-1 and the translation initiation factor EIF3.J, which ultimately results in the down regulation of immune defense responses in *C. elegans* (Liu et al., 2016). Further studies conducted by Sellegounder et al., were able to demonstrate that RIC neurons, which produce exogenous octopamine, are tonically active under normal

conditions and subsequently lead to the activation of the OCTR-1-dependent octopaminergic immuno-inhibitory pathway (Sellegounder et al., 2018). Upon exposure to the pathogenic bacteria *P. aeruginosa*, RIC neurons are deactivated, leading to the repression of the octopaminergic immune-inhibatory pathway and transcriptional activation of immune effectors (Sellegounder et al., 2018).

1.4.5.4 NPR-8 and the Regulation of Cuticular Collagens

Intestinal epithelial cells in *C. elegans* constitute the primary physical barrier nematodes use to prevent ingested pathogens from entering the body. As previously described, inducible defense mechanisms within the intestine are critically important in the clearance of these microbes from the intestinal lumen. The intestine, however, is not the only physical barrier that protects against pathogen attack. *C. elegans* are encased within a flexible, durable, collagenous cuticle that enables locomotion, growth by molting, and serves as a resilient exoskeleton that protects animals from environmental threats. Like the intestinal epithelial barrier, the cuticle and associated epidermis are in nearly constant contact with environmental microbes and as a result have specialized immune defense mechanisms that are initiated upon pathogen recognition (Bolz et al., 2010; Pujol, Cypowyj, et al., 2008; Zugasti & Ewbank, 2009a, 2009b). Numerous fungi, such as *D. coniospora* penetrate the *C. elegans* cuticle by extending hyphal projections directly into the epidermal tissue (Dijksterhuis et al., 1990). This invasive fungal infection leads to the rapid up regulation of numerous antimicrobial peptides that have been shown to be dependent upon the neuropeptide-like-protein NLP-29, suggesting that much like intestinal

immunity, epidermal immunity is tightly integrated with the nervous system (Engelmann et al., 2011; Pujol, Cypowyj, et al., 2008). Recently, alternative mechanisms of epidermal immune defense have been postulated. One such mechanism, published by Sellegounder et al., suggests that rather than inducing immune effectors, pathogen exposure results in the restructuring of the cuticle itself in order to maintain barrier integrity (Sellegounder et al., 2019). A common virulence mechanism employed by numerous pathogenic bacteria is the secretion of extracellular proteases. These proteases can lead to the degradation of the *C. elegans* cuticle, thus reducing its ability to function as a barrier to infection. For example, when exposed to the gram-negative bacterium *Pseudomonas aeruginosa* the *C. elegans* cuticle becomes wrinkled and resembles the cuticle of older animals. Interestingly, it was discovered that mutants harboring a loss-of-function allele of NPR-8, a GPCR within the neuropeptide Y subfamily of cellular receptors, have cuticles that are far more resistant to infection-dependent cuticle damage (Sellegounder et al., 2019). Further analysis of NPR-8 mutants revealed that NPR-8 functions in AWB, ASJ, and AWC aphid sensory neurons to cell non-autonomously to suppresses the induction of cuticular college genes. Not only does this finding suggest that there are both physical and microbial defenses working in unison in order to maintain epidermal barrier integrity, but the regulatory involvement of NPR-8 in this process further demonstrates how tightly defense mechanisms are integrated with the nervous system.

1.4.5.5 NPR-9 and the Intersection of Foraging and Immunity

A complex assortment of sensory cues gathered from the environment influences a specific set of forging behavioral states in *C. elegans*. When exposed to food, *C. elegans* will typically roam in the forward direction, followed by brief pauses and slow backward movement (Shtonda & Avery, 2006). Eventually, upon evaluating the food source, worms will transition to a state called "dwelling" whereby movement will slow, and animals will begin making more frequent turns. This highly regulated foraging behavior is an example of *C. elegans* locomotory behavior being influenced by sensory cues from environmental stimuli. As described previously, *C. elegans* utilizes numerous GPCRs expressed in sensory neurons to probe the environment and subsequently integrate these chemical cues with numerous biological systems influencing behavior, locomotion, feeding, and development.

An increasing body of work suggests that many neuronal GPCRs also play important roles in immune regulation. From a screen of putative neuropeptide receptors, Bendena et al. observed that NPR-9, an allatostatin/galanin-like receptor expressed in AIB neurons, is essential for *C. elegans* to properly respond to diverse environmental stimuli (Bendena et al., 2008; Campbell et al., 2016). Interestingly, further research into this mechanism yielded the discovery that not only does NPR-9 function within AIB neurons to modulate behavioral responses to sensory cues, but NPR-9 also regulates innate immunity. NPR-9 mutants were found to be more resistant to infection with *Pseudomonas aeruginosa* and induced numerous immune-related genes such as *dod-22*, *irg-4* and *pqm-1*. The mechanism by which NPR-9 coordinates the induction of immune effectors upon

pathogen infection has been found to be dependent upon the ability of NPR-9 to antagonize the function of AIB interneurons. Thus, NPR-9 appears to function within a specialized neuronal circuit that utilizes sensory cues to regulate both *C. elegans* foraging behavior and immunity to pathogens, suggesting that neuronal GPCRs can influence numerous interconnected biological processes.

1.4.5.6 Neurotransmitter-dependent Immune Regulation

Neurotransmitters are endogenous singling molecules released from neurons that transmit signals across chemical synapses and regulate numerous psychological processes in mammals including the regulation of mood and behavior, appetite, motor function, and have been shown to be critical for cardiovascular and function. Behavioral studies conducted on *C. elegans* have indicated that monoamine neurotransmitters are necessary for integrating sensory information with behavioral responses (Rankin, 2006; Schulenburg & Ewbank, 2007; Zhang et al., 2005). Upon encountering a nutritious food source, *C. elegans* demonstrates a slowing behavior known as the "basal slowing response" in order to maximize the time spent feeding. Interestingly, this behavior was found to be dependent upon serotonin and dopamine signaling, as mutants in genes within the biogenic amine synthesis pathway were found to display defecting basal slowing responses in the presence of nutritious food sources (Sawin et al., 2000). This observation indicates that neurotransmission plays an important role in local search behavior of *C. elegans*. In alignment with these observations, recent evidence has suggested that bacterially produced neuro-modulatory molecules can alter host behavior and may even function as possible

bacterial virulence mechanism (O'Donnell et al., 2019). O' Donnell et al observed that tyrosine produced by the commensal bacteria *Providencia* upon colonizing the *C. elegans* intestine is able to circumvent endogenous tyrosine biosynthesis and is subsequently covered to octopamine, which signals through the octopamine receptor OCTR-1 in ASH neurons to suppress aversion behavior to volatile compounds (O'Donnell et al., 2020).

In addition to modulating behavior, dopamine and serotonin also function in the regulation of immune responses to pathogens. Dopamine release from CEP neurons, the only dopaminergic neurons in the *C. elegans* nervous system, modulates immunity to pathogenic bacteria by suppressing the PMK-1 MAPK pathway (Cao & Aballay, 2016). This regulatory pathway was shown to be dependent upon the D1-like dopamine receptor DOP-4 expression in chemosensory ASG neurons. This suggests that a complex dopamine-dependent neuronal signaling network exists between multiple sensory neurons and functions to modulate immunity to ingested pathogens by fine tuning the expression of immune effectors within the intestine.

1.4.5.7 Acetylcholine and the Wnt Pathway

Numerous complex biological processes occur during metazoan embryonic development to ensure proper formation of and spatial organization of critical tissues and organ systems. These key developmental programs such as cell fate specification, cell migration, cell polarity, and body axis patterning, rely on the evolutionarily conserved Wnt family of secreted, lipid-modified glycoproteins (Komiya & Habas, 2008). Originally characterized in *Drosophila melanogastor*, Wnt proteins are highly conserved across

species, including *C. elegans*, zebrafish, mice, and humans. Post-developmentally, Wnt signaling in humans has been shown to play important roles in the proliferation and maintenance of nearly all human stem cell populations, and is required in cells with high turnover rates, such as intestinal epithelial cells (Flanagan et al., 2018). Regulation of Wnt signaling is crucially important to properly maintain a balance between hypo- and hyper-proliferative states. Due to the important roles Wnt proteins play in cell proliferation of organization, misregulation of Wnt signaling in humans is commonly associated with cancers, including colon and hepatocellular carcinomas, leukemia, and melanoma (Ng et al., 2019).

Recent discoveries made using *C. elegans* have demonstrated that in addition to playing key roles in developmental processes, Wnt signaling is also involved in pathogen sensing and immune regulation. Work by Labed et al., suggests a new signaling axis between acetylcholine-releasing neurons and Wnt-expressing intestinal epithelial cells that is required for adequate immunological defense against *S. aureus* (Labed et al., 2018). In response to intestinal colonization by *S. aureus*, acetylcholine is released by cholinergic neurons where it subsequently functions as a neuroendocrine signaling molecule to activate muscarinic receptors located within the intestinal epithelium. Activation of these muscarinic receptors, results in increased expression of Wnt and its cognate receptor Frizzled within the intestinal epithelium, ultimately causing activation of Wnt signaling and transcription of immune defense genes such as C-type lectins and lysozymes (Labed et al., 2018). The signaling axis described by Labed et al., demonstrates that the nervous

system is able to quickly and robustly respond to pathogen ingestion, and can rapidly elicit protective immune responses at distal sights of infection.

1.5 Perspectives

C. elegans lives in a microbe rich environment where the quick and robust activation of immune defenses is necessary to defend against a wide array of pathogenic threats. The complex integration of sensory information gathered from *C. elegans* elaborate sensory system functions as the first critical barrier to pathogen infection by enabling numerous environmental cues to influence core biological processes, such as foraging and avoidance behavior. When basic avoidance mechanisms prove futile, *C. elegans* has evolved to respond to pathogen infection by eliciting potent immune defense mechanisms that non-specifically target invading microbes. At the core of *C. elegans* immunity is the p38 MAPK pathway, which responds to a host of bacterial and fungal stressors. The induction of immune defenses comes at a cost however, and numerous studies have demonstrated that without proper regulation, immune defenses pose significant threats to developing animals and can lead to severe fitness and reproductive defects. Thus, it is vital that protective mechanisms are tightly regulated in order maintain effectiveness against invading microorganisms, while simultaneously acting to limit potential deleterious consequences of immune activation. Numerous mechanisms of immune regulations have so far been characterized in *C. elegans*, further demonstrating the importance of maintaining immune homeostasis. The nervous system is becoming increasingly recognized as a core regulator of *C. elegans* innate immunity, due to its ability to quickly

and robustly react to stimuli. While strides have been made in recent years in characterizing numerous neuronal circuits that are tightly integrated with the immune system, many questions remain regarding precisely these circuits work together to influence immunity as a whole. Further insight gained by continuing to study the model organism *C. elegans* will help to elucidate all of the intricacies that exist between the nervous and immune systems and will lay the foundation for future work in more advanced species.

In this graduate thesis, I characterize a novel neuronally-regulated signaling axis that modulates p38 PMK-1-dependent immune responses within the intestine of *C. elegans*. OLRN-1, a previously characterized negative regulator of the PMK-1 pathway in AWC sensory neurons, was found to also act cell non-autonomously coordinate the induction of the PMK-1 pathway in the intestinal epithelium, thus controlling physiologically relevant transcriptional responses to pathogenic stressors. The regulatory control OLRN-1 has over the PMK-1 pathway in the intestine was found to be a necessary requirement for development and reproductive fitness, suggesting that the nervous system of *C. elegans* is inherently intertwined with both innate immune and developmental processes, that work together to ensure productive growth and organismal fitness in microbe rich habitats. These findings add to a growing body of evidence that suggests neuronal control of innate immunity within the intestine is an evolutionarily conserved process across all metazoans.

Chapter 2: Innate Immunity in the *C. elegans* Intestine Is Programmed by a Neuronal Regulator of AWC Olfactory Neuron Development

2.1 Abstract

Olfactory neurons allow animals to discriminate nutritious food sources from potential pathogens. From a forward genetic screen, we uncovered a surprising requirement for the olfactory neuron gene *olrn-1* in the regulation of intestinal epithelial immunity in *Caenorhabditis elegans*. During nematode development, *olrn-1* is required to program the expression of odorant receptors in the AWC olfactory neuron pair. Here, we show that *olrn-1* also functions in AWC neurons in the cell non-autonomous suppression of the canonical p38 MAPK PMK-1 immune pathway in the intestine. Low activity of OLRN-1, which activates the p38 MAPK signaling cassette in AWC neurons during larval development, also de-represses the p38 MAPK PMK-1 pathway in the intestine to promote immune effector transcription, increased clearance of an intestinal pathogen and resistance to bacterial infection. These data reveal an unexpected connection between olfactory receptor development and innate immunity, and show that anti-pathogen defenses in the intestine are developmentally programmed.

2.2 Introduction

The expression of a diverse array of olfactory receptors within sensory neurons is essential for metazoans to survive in microbe rich environments. For example, amphid neurons in the head of the nematode *C. elegans* sample the environment and program rapid changes in locomotion, which allows nematodes to forage decomposing organic matter for bacterial food sources and avoid potential pathogens. Thus, *C. elegans* provide an

experimental platform to understand how the development of sensory neurons is integrated with the physiology of the organism as a whole.

In addition to learned behavioral aversion responses to bacterial pathogens, innate immune defenses in intestinal epithelial cells allow nematodes to survive challenge from environmental pathogens (D. H. Kim, 2018; Pukkila-Worley, 2016a). The canonical immune pathway in intestinal cells is anchored by the p38 Mitogen-Activated Protein Kinase (MAPK) PMK-1 (D. H. Kim et al., 2002; Troemel et al., 2006). p38 MAPK PMK-1 functions as part of a classical MAPK signaling cassette, which is activated by the MAPKKK NSY-1 and the MAPKK SEK-1, homologs of mammalian ASK1 and MKK3/6, respectively (D. H. Kim et al., 2002), and by TIR-1, a Toll/Interleukin-1 Receptor (TIR) domain protein (Liberati et al., 2004). The p38 MAPK PMK-1 pathway ensures the basal expression of immune effectors in the absence of pathogen (Peterson et al., 2019; Troemel et al., 2006). Thus, mechanisms that adjust basal levels of p38 MAPK PMK-1 pathway activity could act as a rheostat for immune effector expression, functioning both to prime *C. elegans* intestinal epithelial cells for the induction of anti-pathogen responses and to limit the deleterious effects of immune hyperactivation.

Here, we conducted a forward genetic screen to identify endogenous regulators of the p38 MAPK PMK-1 pathway. Genetic analyses of mutants identified in this screen uncovered a signaling axis between amphid wing C (AWC) sensory neurons and the intestinal epithelium that promotes immune homeostasis by suppressing the canonical p38 MAPK PMK-1 immune pathway. Interestingly, *olrn-1*, the newly discovered neuronal regulator of this pathway, was previously shown to control the expression of olfactory

receptors in AWC sensory neurons (Huang et al., 2007). During neuronal development, *olrn-1* acts cell autonomously in AWC neurons to suppress the TIR-1/ NSY-1/ SEK-1 cassette, which signals redundantly through the p38 MAP kinases PMK-1 or PMK-2 (Chuang & Bargmann, 2005; Huang et al., 2007; Pagano et al., 2015b; Troemel et al., 1999). Modulation of p38 MAPK pathway activity by OLRN-1 in AWC neurons leads to differentiation of olfactory receptor expression, a developmental step that is required for *C. elegans* to detect specific chemoattractive odors (Wes & Bargmann, 2001). We show that neuronal *olrn-1* also functions cell non-autonomously to suppress the p38 MAPK PMK-1 innate immune pathway in the intestine. Low *olrn-1* activity in AWC neurons, as recapitulated in multiple *olrn-1* loss-of-function mutant strains, de-represses the p38 MAPK PMK-1 pathway in the intestine, which promotes immune effector transcription, increased clearance of an intestinal pathogen and resistance to bacterial infection. Interestingly, *olrn-1* and p38 MAPK *pmk-1*-dependent immune effectors are enriched among genes that are induced during larval development in wild-type nematodes. These data suggest that low activity of neuronal OLRN-1 de-represses the p38 MAPK PMK-1 pathway to prime the immune response in the intestine to handle challenges from bacterial pathogens encountered during larval development.

2.3 Results

2.3.1 Loss-of-function mutations in *olrn-1* cause constitutive immune activation

We conducted a forward genetic screen to identify endogenous regulators of the p38 MAP kinase PMK-1 innate immune pathway. The innate immune reporter, P*irg-4*(F08G5.6)::GFP was used for this experiment to provide a convenient readout of innate immune activation (Pukkila-Worley et al., 2014). *irg-4* is a putative *C. elegans* immune effector whose basal expression is under the control of the p38 MAPK PMK-1 innate immune pathway (Anderson et al., 2019; Peterson et al., 2019; Pukkila-Worley & Ausubel, 2012b; Troemel et al., 2006). In addition, *irg-4* is upregulated during infection by multiple bacterial pathogens and is required for host defense against the bacterial pathogen *Pseudomonas aeruginosa* (Anderson et al., 2019; Nandakumar & Tan, 2008; Peterson et al., 2019; Troemel et al., 2006). Previously, we screened the F1 progeny of mutagenized P*irg-4::GFP* for dominant mutations that cause constitutive immune activation and identified *nsy-1(ums8)*, a gain-of-function mutation in the MAPKKK that functions upstream of p38 MAPK *pmk-1* (Cheesman et al., 2016). Thus, this approach can identify mutations that affect the activity of the p38 MAPK PMK-1 pathway.

To identify regulators of immune activation in *C. elegans*, we screened the F2 progeny of approximately 40,000 mutagenized P*irg-4::GFP* haploid genomes for recessive mutations that caused constitutive P*irg-4::GFP* expression, and identified two mutant alleles: *ums9* and *ums11* (**Figure 2.1A**). Whole genome sequencing of pooled F2 recombinants, homozygous for the mutant phenotype following two outcrosses to wild-

type N2 animals, was performed to identify the mutations that caused constitutive P*irg-4::GFP* expression. Sequencing revealed that both *ums9* and *ums11* contain different recessive mutations in *olrn-1*, a neuronally-expressed protein with putative transmembrane domains (Huang et al., 2007; Torayama et al., 2007). *ums9* is a nonsense mutation (Q497*) and *ums11* is a mutation that disrupts an *olrn-1* splice acceptor site **(Figure 2.1B)**. Several experiments demonstrated that loss-of-function mutations in *olrn-1* causes constitutive activation of P*irg-4::GFP*. First, expression of *olrn-1* under the control of its own promoter in three independent extrachromosomal arrays rescued the constitutive activation of P*irg-4::GFP* in the *ums9* mutant **(Figure 2.1A)**. Second, a previously characterized loss-of-function allele, *olrn-1(ky626)* [a missense mutation (G473E) mutation], also caused constitutive activation of P*irg-4::GFP* **(Figures 2.1A and 2.1B)** (Bauer Huang et al., 2007). Finally, we outcrossed *olrn-1(ums9)* to wild-type six times and confirmed that P*irg-4::GFP* was still constitutively activated **(Figure 2.1A).**
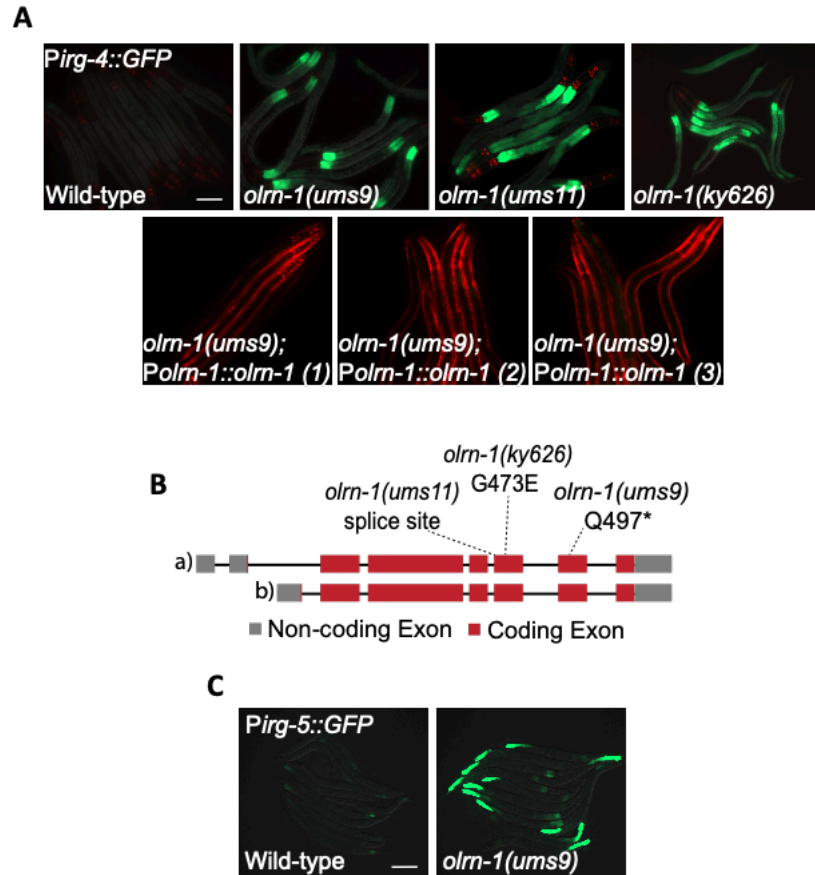
Figure 2.1: Loss-of-function mutations in *olrn-1* cause constitutive immune activation.

(A) Images of *olrn-1* mutants and three independent rescue lines with *olrn-1* expressed under the control of its own promoter in the P*irg-4::GFP* immune reporter background are shown. Red pharyngeal expression is the P*myo-2::mCherry* co-injection marker, which confirms the presence of the P*irg-4::GFP* transgene. The P*myo-3::mCherry* co-injection marker confirms expression of the P*olrn-1::olrn-1* construct in the rescue lines. **(B)** A schematic of the *olrn-1* locus with the locations of the *ums9*, *ums11* and *ky626* mutations is shown. **(C)** The immune reporter P*irg-5::GFP* in the *olrn-1(ums9)* background is shown. Presence of the P*irg-5::GFP* transgene was confirmed by assaying for the Rol phenotype. qRT-PCR data of *irg-4*

A second transcriptional reporter for a different innate immune effector, P*irg-5(F35E12.5)::GFP*, is also constitutively activated in the intestine of *olrn-1(ums9)* mutants **(Figure 2.1C)**. Like *irg-4*, *irg-5* is an immune effector that is required for host defense during *P. aeruginosa* infection and is a target of the p38 MAPK PMK-1 pathway (Bolz et

al., 2010; Peterson et al., 2019; Troemel et al., 2006). Together, *irg-4* and *irg-5* are useful readouts of innate immune activation in the *C. elegans* intestine. Endogenous *irg-4* and *irg-5* were transcriptionally induced to comparable levels in *olrn-1(ums9)*, *olrn-1(ums11)* and *olrn-1(ky626)* mutants, and reintroduction of *olrn-1* under the control of its own promoter rescued the constitutive activation of these genes in the *olrn-1(ums9)* mutant background (**Figures 2.2A-E)**
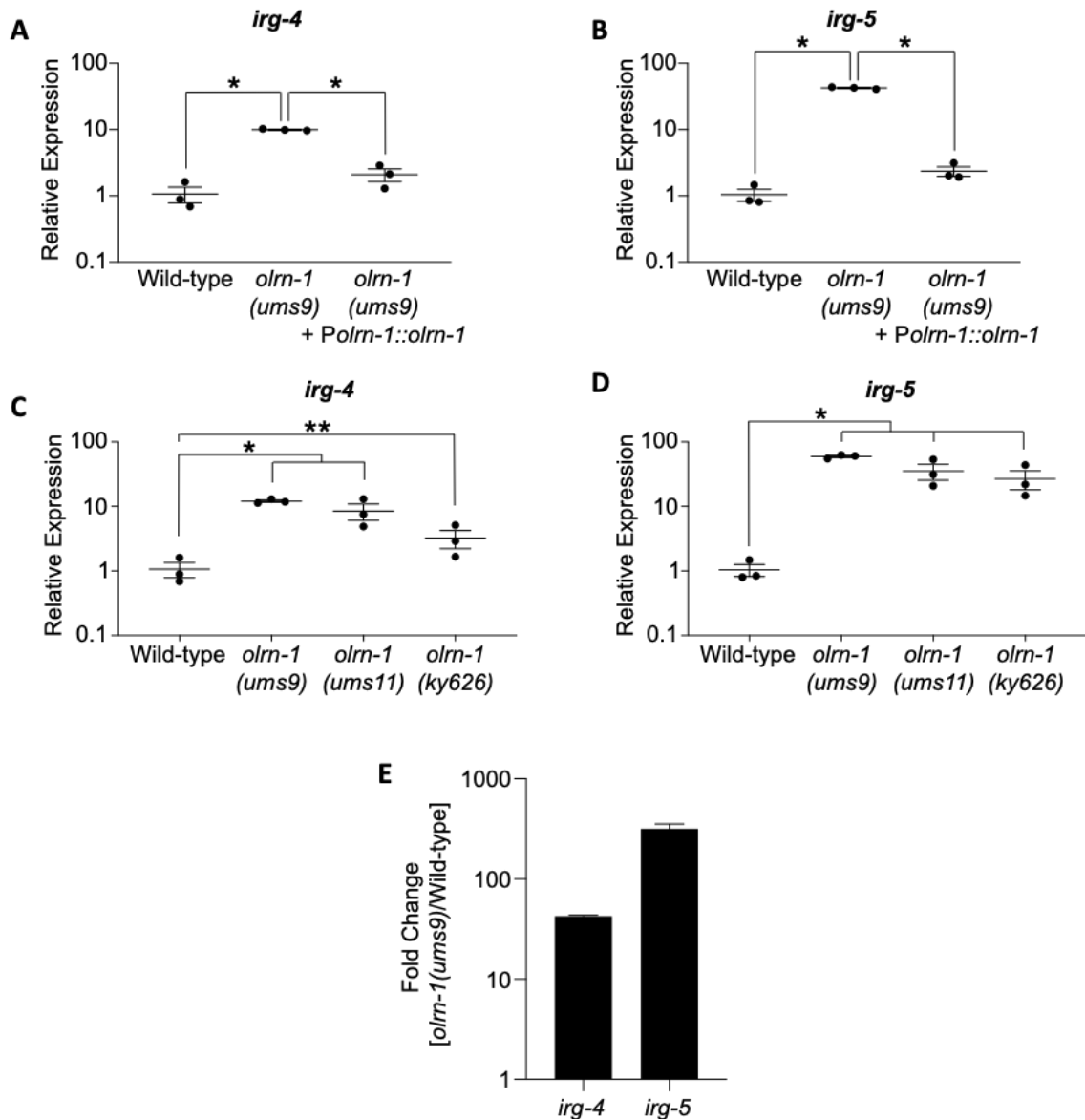
Figure 2.2 Loss-of-function mutations in olrn-1 cause constitutive activation of PMK-1 dependent immune effectors.

qRT-PCR data of irg-4 **(A)** and irg-5 **(B)** of the indicated genotypes is presented. Data are the average of three independent replicates, each normalized to a control gene with error bars representing SEM, and are presented as the value relative to the average expression from all replicates of the indicated gene in wild-type animals. * equals $p<0.05$ by one-way ANOVA for the indicated comparison. qRT-PCR data of irg-4 **(C)** and irg-5 **(D)** in wild-type, olrn-1(ums9), olrn-1(ums11) and olrn-1(ky626) is presented. Data are the average of three independent replicates, each normalized to the control gene snb-1 with error bars representing SEM, and are presented as the value relative to the average expression from all replicates of the indicated gene in wild-type animals. * equals $p<0.05$ by one-way ANOVA for the indicated comparison. **$p=0.10$ by one-way ANOVA and $p<0.05$ by two-tailed t-test. **(E)** Data from a nanoString analysis of irg-4 and irg-5 expression, presented as the fold change of gene expression in olrn-1(ums9) mutants versus wild-type animals. Data are the average of two independent replicates for olrn-1(ums9) and one sample for wild-type, each normalized to three control genes (snb-1, ama-1 and act-1) with error bars representing SEM.

Consistent with the constitutive activation of innate immune effector transcription in *olrn-1* loss-of-function animals, *olrn-1* mutants displayed increased resistance to infection by *P. aeruginosa* **(Figure 2.3A).** Importantly, we confirmed that loss-of-function of *olrn-1* modulates the susceptibility of *C. elegans* to *P. aeruginosa* infection by testing the pathogen susceptibility of the three independent *olrn-1* rescue lines described above **(Figure 2.3B)**. Expression of *olrn-1* under the control of its own promoter rescued the pathogen-resistance phenotype of the *olrn-1(ums9)* mutant **(Figure 2.3B).** We considered that *olrn-1* mutants may be resistant to *P. aeruginosa* infection because they are better able to avoid the pathogen than wild-type animals. However, *olrn-1(ums9), olrn-1(ums11)* and *olrn-1(ky626)* mutants were resistant to *P. aeruginosa* infection in a pathogenesis assay conducted with a lawn of bacteria that was spread to the edges of the agar, which negates the contribution of behavioral avoidance to the pathogen-resistance phenotype **(Figure 2.3A)** (K C Reddy et al., 2009; Styer et al., 2008; J Sun et al., 2011). In addition, the *olrn-*

1(ums9) mutant did not have an increased propensity to avoid a small lawn of *P. aeruginosa* compared to wild-type **(Figure 2.3C)**.

Interestingly, *olrn1(ums9)* mutant animals accumulated significantly less *Pseudomonas aeruginosa* in their intestine compared to wild-type animals **(Figure 2.3D).** Reintroduction of *olrn-1* under the control of its own promoter complemented this *olrn-1(ums9)* mutant phenotype **(Figure 2.3D)**. Of note, there was no difference in pharyngeal pumping rates between wild-type and *olrn-1(ums9)* mutants **(Figure 2.3E)**. In addition, *olrn-1(ums9)* and *olrn-1(ky626)* mutants each have a lifespan that is similar to wild-type animals **(Figure 2.3F)**. Together, these data demonstrate that *olrn-1(ums9)* mutants drive a transcriptional response that promotes clearance of bacteria from the intestine and resistance to *P. aeruginosa* infection, without pleiotropic effects on feeding behavior or nematode lifespan.
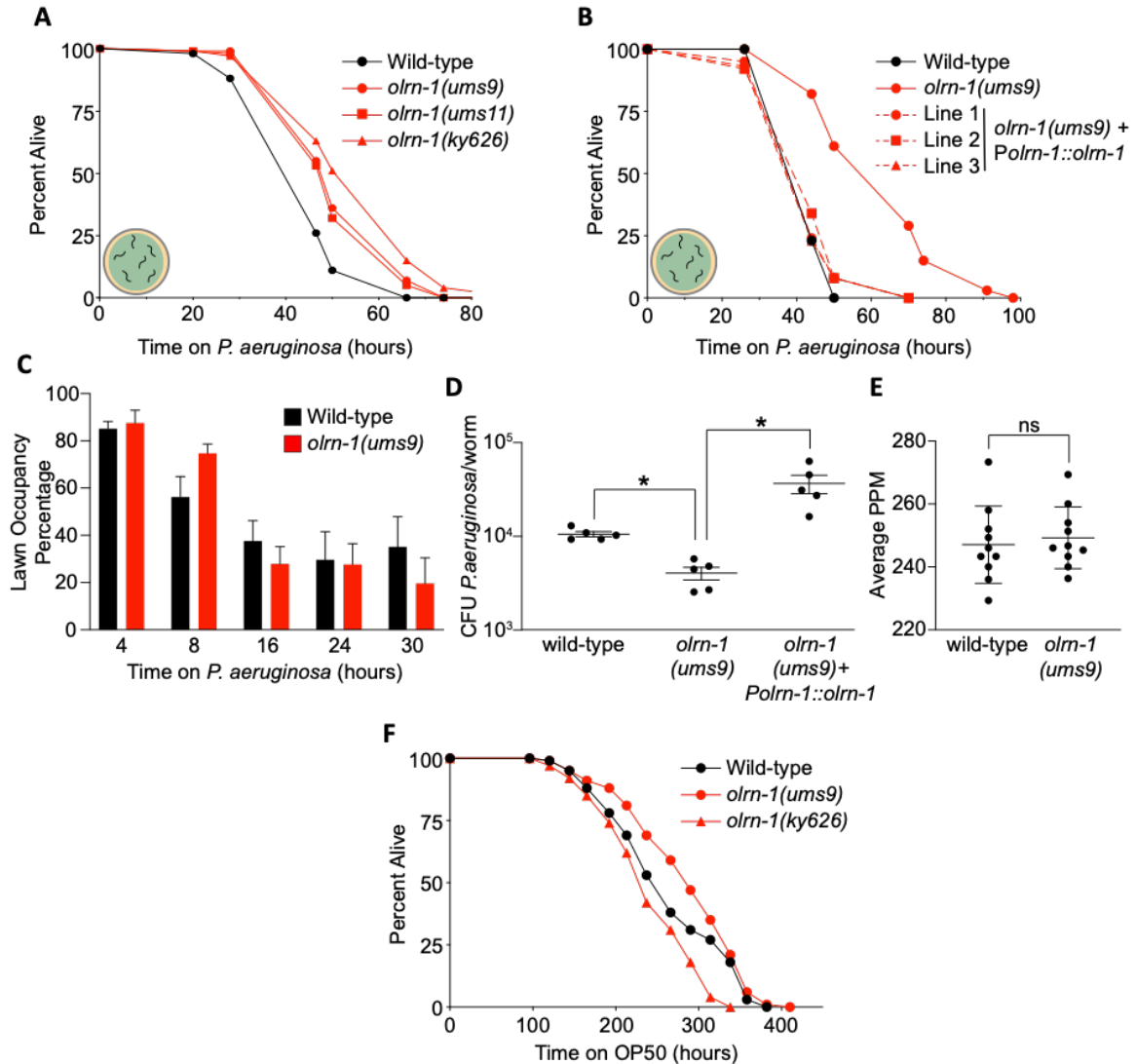
Figure 2.3 *olrn-1* loss-of-function mutants are resistant to the *Pseudomonas aeruginosa*.

(A, B) *C. elegans* pathogenesis assay conducted with a large lawn of *P. aeruginosa* and *C. elegans* of indicated genotypes at the L4 larval stage is shown. Data are representative of three trials. The Kaplan-Meier method was used to estimate the survival curves for each group, and the log rank test was used for all statistical comparisons. Sample sizes, mean lifespan and p-values for all trials are shown in Table 2.2. **(C)** Quantification of the propensity of *olrn-1(ums9)* and wild-type animals to avoid a lawn of *P. aeruginosa* is shown. Data are presented as the average number of animals that were on a small lawn of *P. aeruginosa* from three separate replicates with error bars representing SEM. There is no significant difference by one-way ANOVA between these mutants, except at the 8-hour time point. **(D)** *P. aeruginosa,* isolated from the intestines of animals with the indicated genotypes, were quantified after 24 hours of bacterial infection. Data are colony forming units (CFU) of *P. aeruginosa* and are presented as the average of five separate replicates with each replicate containing 10-11 animals. * equals p<0.05 by one-way ANOVA for the indicated comparison. **(E)** Data are the pharyngeal pumping rates, recorded as pumps per minute (PPM), of 10 individual young adult *C. elegans* feeding on non-pathogenic OP50 in wild-type and *olrn-1(ums9)* mutants with error bars representing SEM. 'ns' equals no significant difference by one-way ANOVA for the indicated

comparison. Scale bars in Figures 1A and 1C are 100 μm. **(F)** The lifespan of olrn-1(ums9) and olrn-1(ky626) mutant animals is shown relative to wild-type animals.

2.3.2 OLRN-1 suppresses the p38 MAPK PMK-1 innate immune pathway

To characterize the full spectrum of genes regulated by *olrn-1*, we performed RNA-seq. The transcriptomes of wild-type and *olrn-1(ums9)* mutant animals growing in standard culture conditions (*i.e.,* in the absence of pathogen challenge) were profiled. In *olrn-1(ums9)* mutants, 549 genes were upregulated compared to wild-type (greater than 2-fold, $p<0.05$) **(Figure 2.4A)**. Analysis of these differentially expressed transcripts revealed a significant enrichment for innate immune genes **(Figure 2.4B)**, including *irg-4* and *irg-5* **(Figure 2.4A)**. Indeed, 41 of the 236 genes that are induced during *Pseudomonal* infection (Miller et al., 2015) are also constitutively upregulated in the *olrn-1(ums9)* mutant (hypergeometric p-value 2.80e-21)**(Figure 2.4C)**.

Loss-of-function *olrn-1* mutants demonstrated constitutive activation of P*irg-4::GFP* **(Figure 2.1A)** and P*irg-5::GFP* **(Figure 2.1C)** in the intestinal epithelial cells of *C. elegans*, the tissue that directly interfaces with ingested pathogens. In the RNA-seq experiment, 171 of the 549 *olrn-1*-repressed genes are expressed in intestinal epithelial cells (hypergeometric p-value 1.16e-32) (Haenni et al., 2012). Together, these data indicate that *olrn-1* suppresses the transcription of genes that are expressed in the intestine, which includes a significant number of immune effectors.

Interestingly, the RNA-seq experiment also revealed that *olrn-1* negatively regulates a significant number of genes that are known targets of the p38 MAPK PMK-1 pathway (Bond et al., 2014; Troemel et al., 2006). Of the 549 genes that are upregulated in

olrn-1(ums9) mutants, 139 are dependent on *pmk-1* for their basal transcription (hypergeometric p-value 3.61e-69) **(Figures 2.4A and 2.4D)** (Bond et al., 2014). To determine if *olrn-1* controls the activity of the p38 MAPK PMK-1 pathway, we performed western blot experiments with antibodies that recognize the doubly-phosphorylated TGY motif of activated PMK-1 and the total PMK-1 protein. Both the *olrn-1(ums9)* and *olrn-1(ky626)* loss-of-function mutants have an increased ratio of phosphorylated PMK-1 relative to total PMK-1 compared to wild-type controls, as quantified from four biological replicates **(Figures 2.4E and 2.4F).**
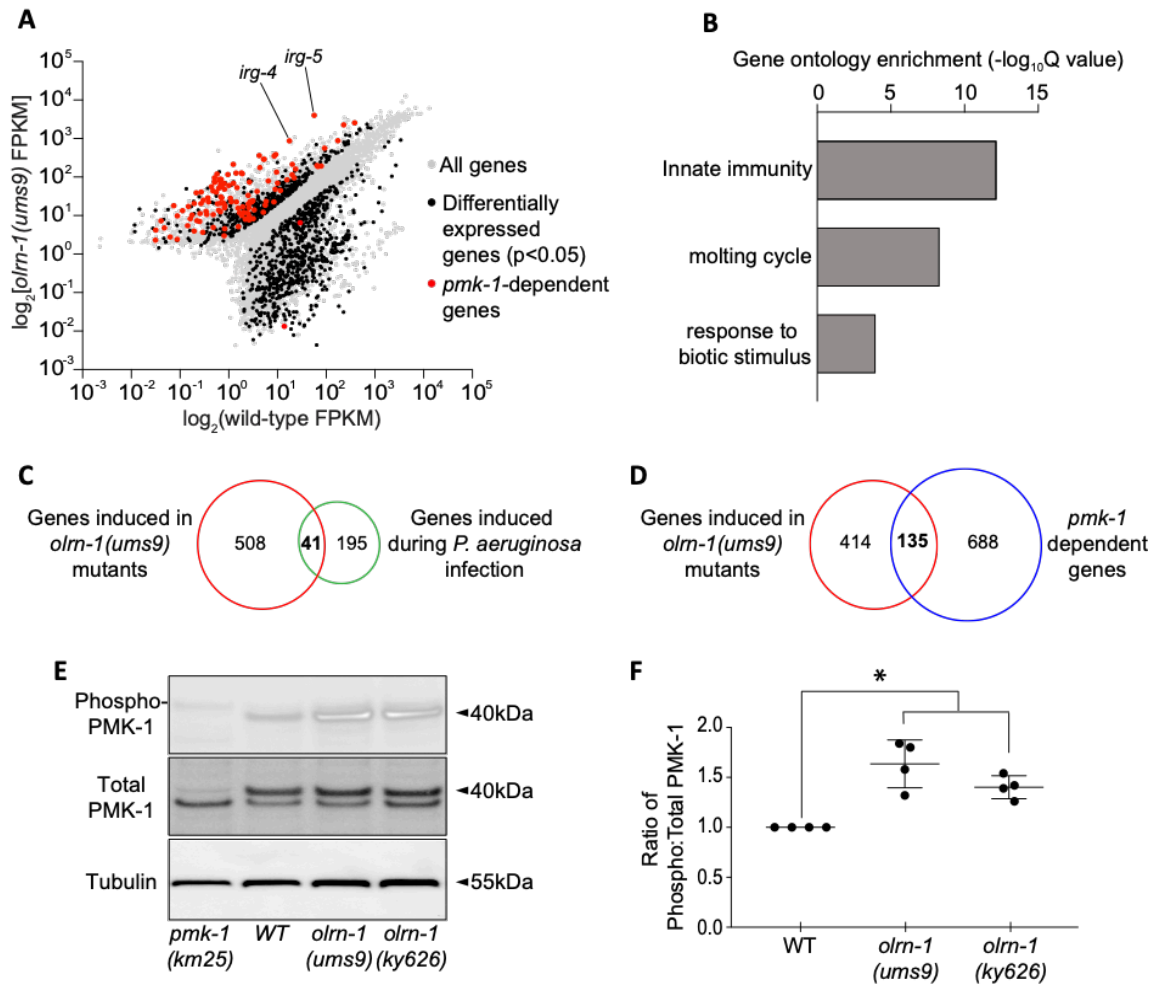
Figure 2.4 *olrn-1* suppresses the p38 MAPK PMK-1 innate immune pathway.

(A) Data from an mRNA-seq experiment comparing gene expression in *olrn-1(ums9)* mutants with wild-type animals are shown. All genes are shown in gray. Genes that are differentially expressed in *olrn-1(ums9)* mutants compared to wild-type animals are shown in black (Fold change>2, p<0.05). Genes that are known targets of the p38 MAPK *pmk-1* pathway are highlighted in red. The location of the representative genes *irg-4* and *irg-5* whose expression is examined throughout this manuscript are shown. **(B)** Gene ontology enrichment analysis for the 549 genes whose transcription were significantly upregulated in *olrn-1(ums9)* mutants compared to wild-type is shown. The three most significantly-enriched categories are shown, reported as the -log$_{10}$ transformation of the Q value for the enrichment of each category. Venn Diagrams show the overlap of the 549 genes upregulated in *olrn-1* mutants with genes that are known to be induced during *P. aeruginosa* infection **(C)** and are targets of the p38 MAPK PMK-1 pathway **(D)**. Hypergeometric p-values for the overlap in C and D are 3.68e-22 and 4.67e-69, respectively. **(E)** An immunoblot analysis of lysates from animals of the indicated genotype using antibodies that recognize the doubly-phosphorylated TGY motif of PMK-1 (Phospho-PMK-1), the total PMK-1 protein (Total PMK-1) and tubulin (Tubulin) is shown. PMK-1 is a 40 kDa protein and tubulin is a 55 kDa protein. **(F)** The band intensities of four biological replicates of the Western blot shown in **(E)** were quantified. The ratio of active to total PMK-1 is shown for

each genotype and is presented relative to the ratio in wild-type animals for each replicate. * equals p<0.05 by one-way ANOVA for the indicated comparison.

Consistent with these data, loss-of-function mutations in p38 MAPK PMK-1 pathway components, *pmk-1(km25)* and *tir-1(qd4),* suppressed the pathogen-resistance phenotype of the *olrn-1(ums9)* mutants **(Figure 2.5A)**. In addition, both *tir-1(qd4)* **(Figure 2.5B)** and *sek-1(km4)* **(Figure 2.7A)** suppressed the hyperactivation of P*irg-4::GFP* in the intestinal epithelial cells of the *olrn-1(ums9)* mutant. Moreover, *tir-1(qd4)* and *pmk-1(km25)* mutations each suppressed the constitutive activation of the immune effectors *irg-4* **(Figure 2.5C)** and *irg-5* **(Figure 2.5D)** in the *olrn-1(ums9)* background.

The bZIP transcription factor ZIP-2 and the G protein-coupled receptor FSHR-1 each function in parallel to the p38 MAPK PMK-1 pathway to promote host defense during an intestinal infection with *P. aeruginosa* (Estes et al., 2010; Powell et al., 2009; Kirthi C. Reddy et al., 2016). Loss-of-function mutants of *zip-2* and *fshr-1* are hypersusceptible to killing by *P. aeruginosa* and are unable to upregulate a suite of PMK-1-independent immune effectors (Estes et al., 2010; Powell et al., 2009; Kirthi C. Reddy et al., 2016). We examined the genes that are transcriptionally upregulated in the *olrn-1(ums9)* mutants to determine if *olrn-1* also suppresses the ZIP-2 or the FSHR-1 pathway. However, the overlap of *zip-2*-regulated genes **(Figure 2.5E)** or *fshr-1*-regulated genes **(Figure 2.5F)** with the genes that were upregulated in the *olrn-1(ums9)* mutant was not significant. In addition, we also found that targets of the FOXO transcription factor DAF-16 were not significantly over-represented among *olrn-1*-regulated genes **(Figure 2.5G).**

Together, these data demonstrate that OLRN-1 targets the p38 MAPK PMK-1 immune pathway to suppress immune effector expression in the intestine and modulate host susceptibility to bacterial infection.
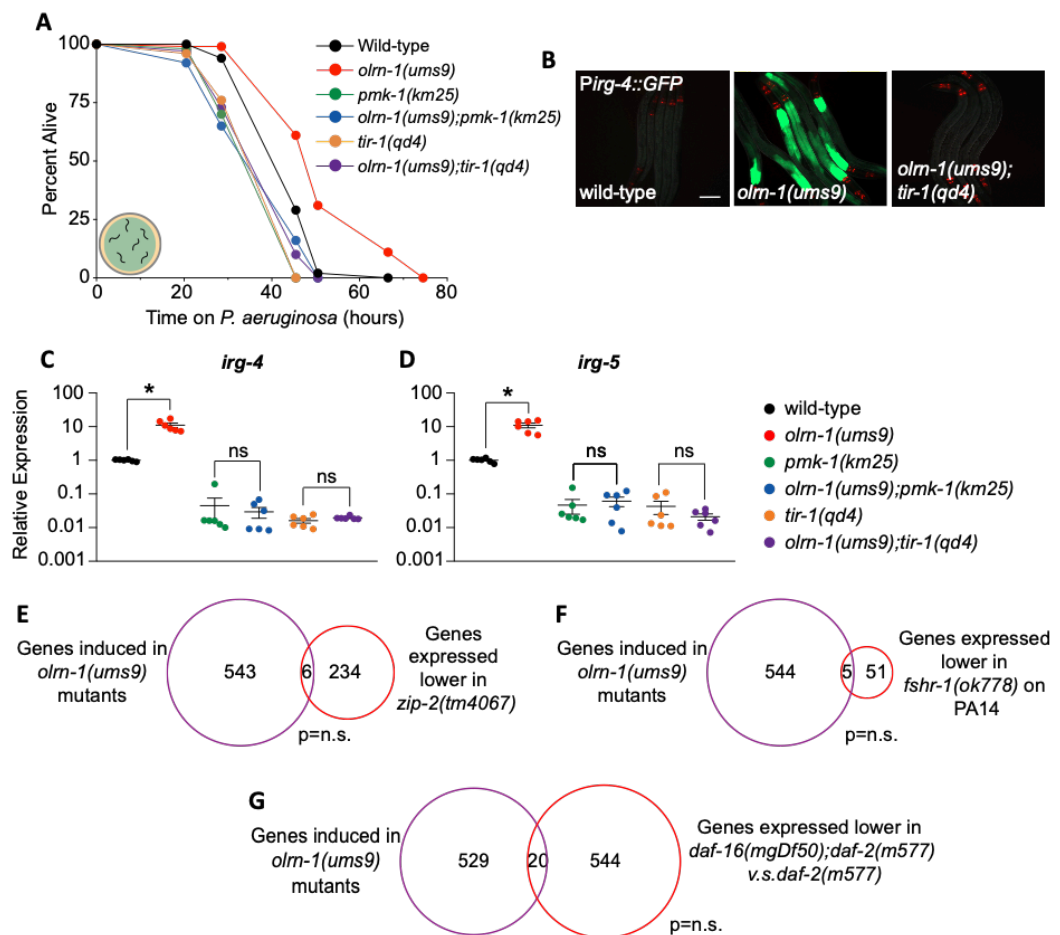
Figure 2.5 *olrn-1* suppresses the p38 MAPK PMK-1-depedent innate immune effectors.

(A) *C. elegans* pathogenesis assay conducted with a large lawn of *P. aeruginosa* and *C. elegans* of indicated genotypes at the L4 larval stage is shown. Data are representative of three trials. The Kaplan-Meier method was used to estimate the survival curves for each group, and the log rank test was used for all statistical comparisons. Sample sizes, mean lifespan and p-values for all trials are shown in Table 2.2. **(B)** Images of *olrn-1(ums9)* mutants and *olrn-1(ums9);tir-1(qd4)* double mutants are shown. Red pharyngeal expression is the P*myo-2::mCherry* co-injection marker, which confirms the presence of the P*irg-4::GFP* transgene. Scale bar is 100 μm. qRT-PCR data of *irg-4* **(C)** and *irg-5* **(D)** expression in the indicated genotypes. Data are the average of six independent replicates, each normalized to a control gene with error bars representing SEM. Data are presented as the value relative to the average expression from all replicates of the indicated gene in

wild-type animals. * equals p<0.05 by one-way ANOVA for the indicated comparison. 'ns' denotes that the difference between the indicated comparison was not statistically significant. Venn diagrams show the overlap of genes induced in *olrn-1(ums9)* mutants with targets of **(E)** the bZIP transcription factor *zip-2*, **(F)** the G protein-coupled receptor *fshr-1*, and **(G)** the FOXO transcription factor *daf-16*. In **(E)**, **(F)** and **(G)**, the hypergeometric p value for the overlap between these datasets was not significant (n.s.).

2.3.3 Promotion of intestinal immune homeostasis by *olrn-1* is required to ensure reproduction and development

We previously observed that aberrant activation of immune defenses in the intestine by a gain-of-function mutation in the p38 MAPKKK *nsy-1* or by exogenous treatment with an immunostimulatory small molecule slows nematode development (Cheesman et al., 2016). Like *nys-1(ums8)* mutants, *olrn-1(ums9)* mutants take a longer time to reach adulthood than wild-type animals **(Figures 2.6A and 2.6B)**. Re-introduction of *olrn-1* under the control of its own promoter restored wild-type developmental rates to the *olrn-1(ums9)* mutant **(Figures 2.6A and 2.6B)**.

To determine if the developmental delay in the *olrn-1(ums9)* mutant is a consequence of de-repression of the p38 MAPK PMK-1 pathway, we compared the developmental rates of the *pmk-1(km25)*, *tir-1(qd4)*, *atf-7(qd22 qd130)* and *olrn-1(ums9)* single mutants to the *olrn-1(ums9); pmk-1(km25)*, the *olrn-1(ums9); tir-1(qd4)*, and the *olrn-1(ums9);atf-7(qd22 qd130)* double mutants **(Figures 2.6G-I)**. ATF-7 is the transcription factor that functions downstream of p38 MAPK PMK-1 to control the basal expression of immune effectors (Shivers et al., 2010). The *pmk-1(km25)*, *tir-1(qd4)* and *atf-7(qd22 qd130)* null mutants each fully suppressed the developmental delay of the *olrn-1(ums9)* mutant **(Figures 2.6G-I)**. In addition, the brood sizes of both the *nsy-1(ums8)* gain-of-function mutants and *olrn-1(ums9)* mutants is significantly smaller than that of

wild-type animals **(Figure 2.6J)**. Consistent with our observations in the *C. elegans* development experiments, both the *pmk-1(km25)* and *tir-1(qd4)* mutation fully suppressed the small brood size of *olrn-1(ums9)* mutants **(Figure 2.6J)**. Thus, neuronal o*lrn-1* prevents the deleterious effects of aberrant immune activation on nematode development and reproductive fitness.
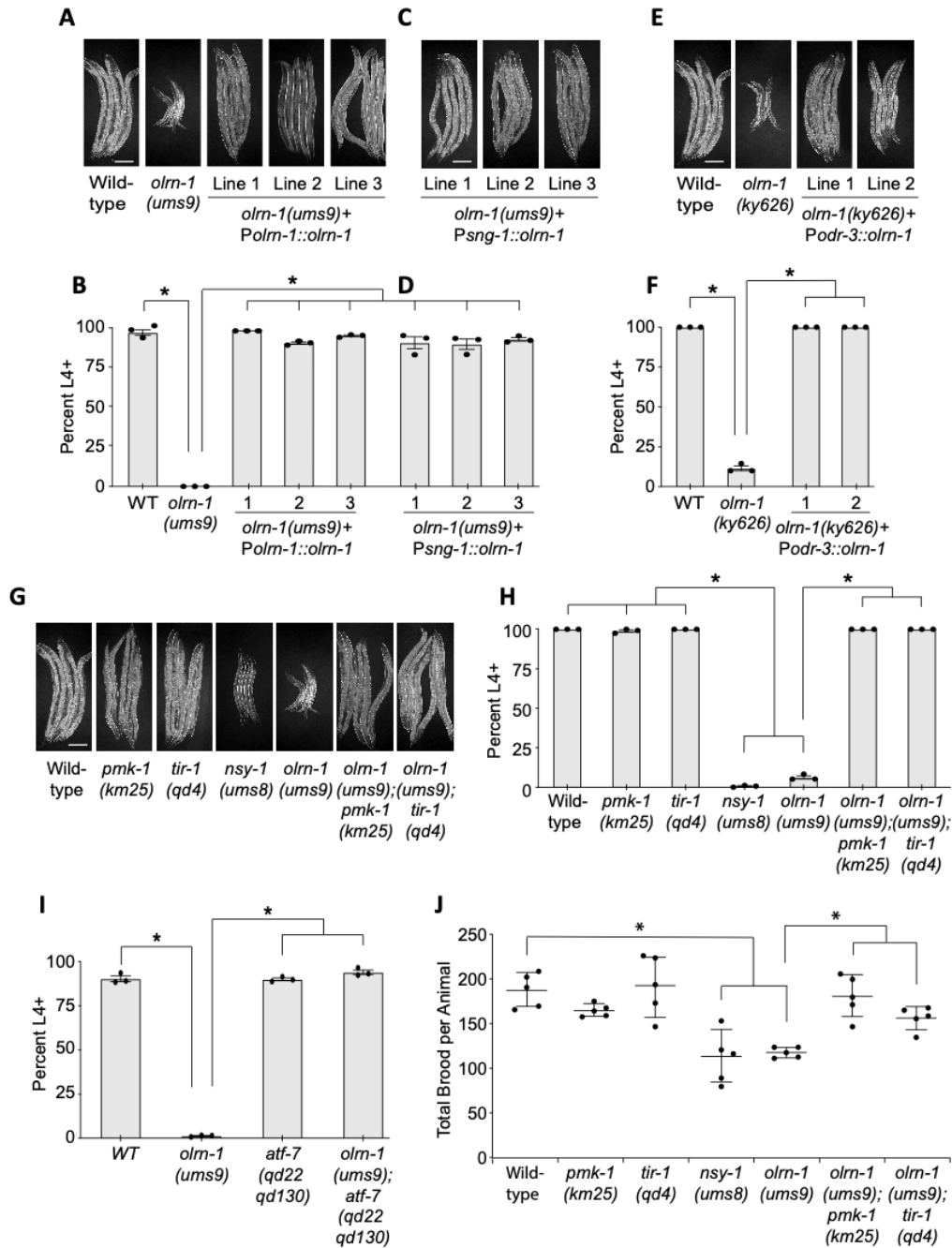
Figure 2.6 Promotion of intestinal immune homeostasis by *olrn-1* is required to ensure reproduction and development.

(A-I) Development assays were performed with the indicated genotypes. The stage of the animals was recorded at the same timepoint, approximately 72 hours after eggs from *C. elegans* of the indicated genotypes were laid. In (**B**), (**D**), (**F**), (**H**), and (**I**) data are presented as the average number of animals for each genotype that were at the L4 stage or older (Percent L4+) from three independent replicates with error bars representing SEM. * equals $p<0.05$ by one-way ANOVA. (**J**) Brood sizes from animals of the

indicated genotypes were quantified. Each data point is the average brood size from two animals. * equals p<0.05 by one-way ANOVA for the indicated comparison.

2.3.4 Expression of *olrn-1* in chemosensory neurons is sufficient to regulate innate immunity in the intestinal epithelium

OLRN-1 is expressed in AWC chemosensory neurons where it acts cell autonomously to promote olfactory receptor expression during nematode development (Huang et al., 2007). However, OLRN-1 is not expressed in the intestinal epithelium (Huang et al., 2007) where the p38 MAPK PMK-1 pathway coordinates the tissue autonomous expression of immune effectors and resistance to pathogen infection (Shivers et al., 2009). Therefore, we hypothesized that OLRN-1 acts in sensory neurons to control p38 MAPK PMK-1 transcriptional responses in the intestine.

We introduced an extrachromosomal array containing *olrn-1* under the control of a pan-neuronal promoter (P*sng-1::olrn-1*) into the *olrn-1(ums9)* mutant. Neuronal expression of *olrn-1* in three independent lines rescued the constitutive expression of P*irg-4::GFP* in the intestine of *olrn-1(ums9)* mutants **(Figure 2.7A).** We confirmed that neuronal expression of *olrn-1* was sufficient to suppress the constitutive activation of endogenous *irg-4* **(Figure 2.7B)** and *irg-5* **(Figure 2.7C)** in the *olrn-1(ums9)* mutant. Consistent with these gene expression data, neuronal expression of *olrn-1* in three independent lines suppressed the pathogen-resistance phenotype of the *olrn-1(ums9)* mutant **(Figure 2.7D).**

We also expressed *olrn-1* in the *olrn-1(ums9)* mutant under the *odr-3* promotor (P*odr-3::olrn-1*), which drives gene expression in a specific subset of chemosensory

neurons (Roayaie et al., 1998). A P*odr-3::GFP* transcription reporter is expressed strongly in AWC neurons, and weakly or inconsistently in AWB, AWA, ASH and ADF neurons (Roayaie et al., 1998). Historically, the *odr-3* promoter has been a useful tool to characterize AWC-dependent mechanisms (Huang et al., 2007). As observed in our experiments with the P*sng-1::olrn-1* constructs **(Figure 2.7D)**, expression of *olrn-1* under the *odr-3* promoter fully suppressed the pathogen-resistance phenotype of the *olrn-1(ky626)* mutant **(Figure 2.7E)**. Importantly, this experiment, which utilizes a second heterologous promoter to direct *olrn-1* expression in neurons, confirms that *olrn-1* activity in neurons is necessary to modulate resistance to a bacterial pathogen. Interestingly, multi-copy expression of *olrn-1* in a wild-type background, both under its own promoter and specifically in neurons, rendered *C. elegans* more susceptible to killing by *P. aeruginosa* **(Figure 2.7F)**.

In addition, expression of *olrn-1* only in neurons (under the *sng-1* promoter) **(Figures 2.6C and 2.6D)** or in chemosensory neurons (using the *odr-3* promoter) **(Figures 2.6E and 2.6F)** was sufficient to rescue the developmental delay of *olrn-1* mutants, as assessed in multiple independent lines carrying these rescue constructs. In summary, neuronal *olrn-1* is necessary and sufficient to control pathogen resistance and promote intestinal immune homeostasis. In addition, we show that expression of *olrn-1* in chemosensory neurons is sufficient to regulate innate immunity in the *C. elegans* intestinal epithelium.
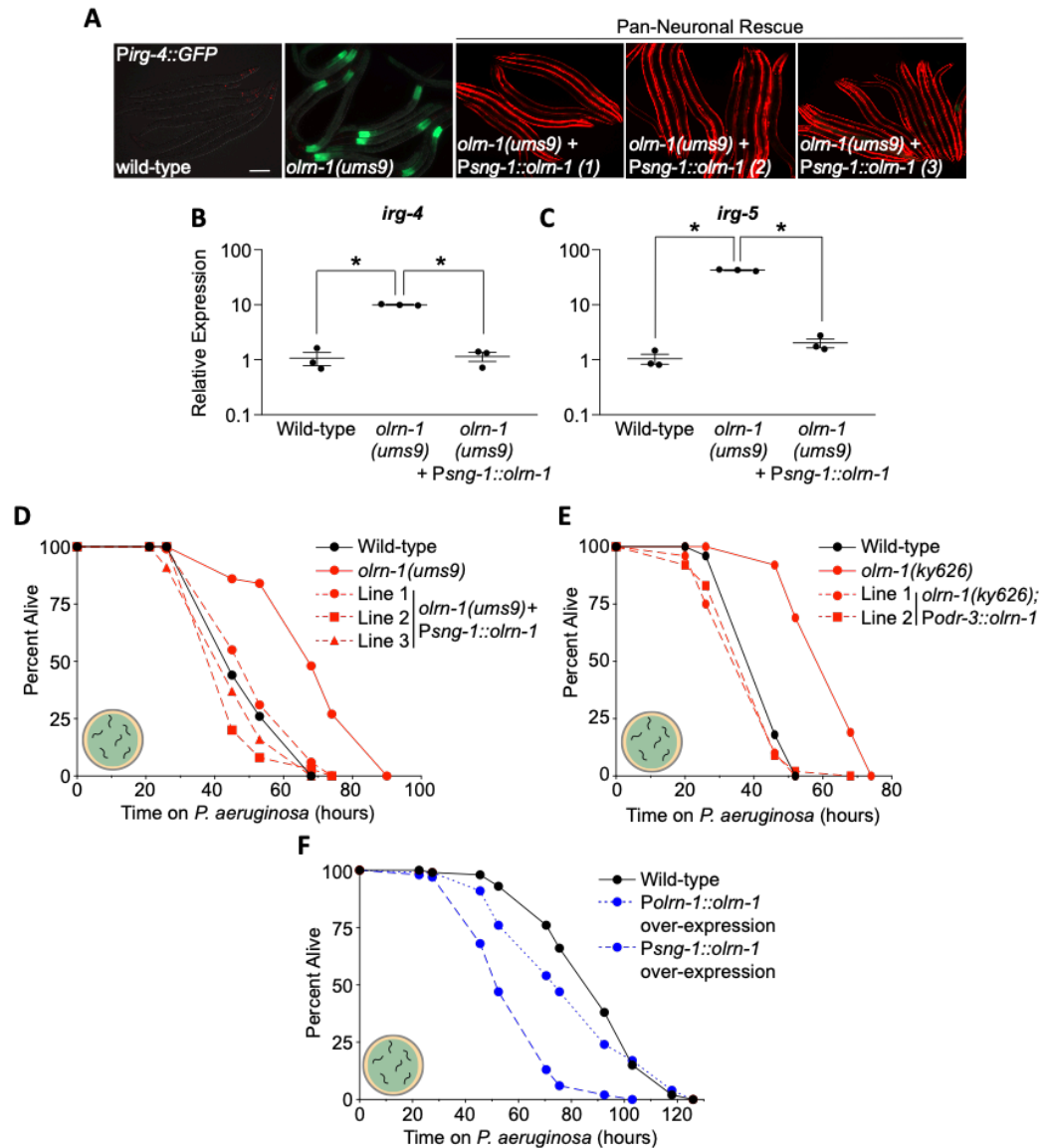
Figure 2.7 Expression of *olrn-1* in Chemosensory Neurons Is Sufficient to Regulate Innate Immunity in the Intestinal Epithelium

(A) Three independent lines of *olrn-1* under the control of a pan-neuronal promoter (*sng-1*) in the *olrn-1(ums9)* mutant along with the *olrn-1(ums9)* mutant are shown. P*myo-3::mCherry* expression indicates the presence of an extrachromosomal array that contains the P*sng-1::olrn-1* construct. Scale bar is 100 μm. qRT-PCR data showing *irg-4* **(B)** and *irg-5* **(C)** expression in animals of the indicated genotypes is shown. Data are the average of three independent replicates, each normalized to a control gene with error bars representing SEM, and are presented as the value relative to the average expression from all replicates of the indicated gene in wild-type animals. * equals p<0.05 by one-way ANOVA for the indicated comparison. **(D, E, F)** *C. elegans* pathogenesis assay conducted with a large lawn of *P. aeruginosa* and *C. elegans* of indicated genotypes at the L4 larval stage is shown. Data are representative of three trials.

2.3.5 Immune effectors regulated by neuronal *olrn-1* are dynamically expressed during nematode development

During *C. elegans* development, *olrn-1* suppresses the TIR-1/ NSY-1/ SEK-1 cassette in AWC neurons, which utilizes either the PMK-1 or PMK-2 p38 MAP kinases to promote left-right asymmetry of the odorant receptors *str-2* and *srsx-3* in AWC neurons (Chuang & Bargmann, 2005; Huang et al., 2007; Pagano et al., 2015a; Torayama et al., 2007; Troemel et al., 1999). Differentiation of odorant receptors in AWC neurons is a required developmental step for *C. elegans* to sense and move toward diverse attractive stimuli (Wes & Bargmann, 2001). Adult *C. elegans* have one AWC neuron that expresses *str-2*, called AWC^{ON} by convention, and one AWC neuron that expresses the *srsx-3* chemoreceptor instead (AWC^{OFF}). Forward genetic screens for mutants with two AWC^{ON} or two AWC^{OFF} neurons defined the genetic pathway that controls olfactory receptor development in AWC neurons. This work revealed that low *olrn-1* activity causes activation (de-repression) of the TIR-1/ NSY-1/ SEK-1/(PMK-1 or PMK-2) signaling cassette in AWC^{OFF} neurons (Huang et al., 2007; Troemel et al., 1997, 1999).

Given that the TIR-1/ NSY-1/ SEK-1/ PMK-1 pathway is required both in neurons for the development of odorant receptors and in the intestine for innate immunity, we determined the tissues where this signaling cassette is sufficient for the promotion of immune homeostasis by neuronal *olrn-1*. A P*ges-1::sek-1::GFP* construct, which directs *sek-1* expression in intestinal epithelial cells (Shivers et al., 2009), was introduced into the *olrn-1(ums9);sek-1(km4)* double mutant. Reconstitution of the p38 MAPKK *sek-1* in the intestine restored P*irg-4::GFP* expression in the *olrn-1(ums9);sek-1(km4)* double mutant

(**Figure 2.8A**). To confirm our results with the P*ges-1::sek-1::GFP* construct using a different heterologous promoter, we introduced a P*vha-6::pmk-1* construct (Bolz et al., 2010) into the *olrn-1(ums9);pmk-1(km25)* double mutant. Like P*ges-1*, P*vha-6* directs gene expression specifically in intestinal epithelial cells (McGhee et al., 1990; Oka et al., 2001). Consistent with our observations with the P*ges-1::sek-1* construct (**Figure 2.8A**), intestinal expression of *pmk-1* was sufficient to completely restore the pathogen resistance phenotype of the *olrn-1(ums9)* mutant to the *olrn-1(ums9);pmk-1(km25)* double mutant (**Figure 2.8B**). Expression of *sek-1* under the control of a neuronal-specific promoter (P*unc-119::sek-1*) (Shivers et al., 2009) in the *olrn-1(ums9);sek-1(km4)* double mutant, however, did not restore constitutive activation of P*irg-4::GFP* in the *olrn-1(ums9)* mutant background (**Figure 2.8A**). Thus, the p38 MAPK PMK-1 pathway in intestinal epithelial cells, but not in neurons, is sufficient for the modulation of immune effector expression and resistance to *P. aeruginosa* infection by neuronal *olrn-1*.

The function of the innexin gene *nsy-5* and the claudin/ calcium channel γ subunit gene *nsy-4* in promoting AWC neuron differentiation, as defined in genetic studies, is similar to *olrn-1* (Chuang et al., 2007; Huang et al., 2007; VanHoven et al., 2006). Like *olrn-1* mutants, both *nsy-4(ky616)* and *nsy-5(ky634)* loss-of-function mutants have two AWC[OFF] neurons, one of which never differentiates into an AWC[ON] neuron (Bauer Huang et al., 2007). Interestingly, the immune effectors *irg-4* (**Figure 2.8C**) and *irg-5* (**Figure 2.8D**) are not constitutively induced in *nsy-4(ky616)* and *nsy-5(ky634)* loss-of-function mutants, as they are in the *olrn-1* mutants. These data indicate that *olrn-1* has distinct roles

in regulating immune effector expression in the intestine and promoting olfactory receptor development in AWC neurons.

Considering the role of *olrn-1* in controlling olfactory receptor development in AWC neurons, we asked if *olrn-1*-depedent immune effectors are differentially expressed during larval development. We compared the RNA-seq transcriptome profiles of wild-type *C. elegans* at each larval stage, and identified 707 genes, 580 genes, 717 genes, 602 genes and 100 genes that were expressed at significantly higher levels in wild-type animals at the first larval stage (L1), the second larval stage (L2), the third larval stage (L3), the fourth larval stage (L4) and the young adult stage (YA) compared to adult animals, respectively (p<0.05, greater than 2-fold change). Interestingly, genes that are expressed at higher levels in *olrn-1(ums9)* mutants are significantly enriched among the genes that are developmentally-regulated in wild-type animals, including a significant number of the genes identified in Figure 2.4D that are targets of the *olrn-1*–p38 MAPK *pmk-1* signaling axis **(Figures 2.8C - 2.8E)**. In particular, innate immune genes were enriched among the genes expressed higher in L3 animals compared to adults (p value for GO term enrichment 4.8x10^{-5}), as were genes induced during *P. aeruginosa* infection (hypergeometric p value 7.9e-10). Additionally, we identified 100 genes that were expressed higher in young adult compared to adult animals, but neither *olrn-1*-regulated genes nor immune effectors in general were enriched in this dataset **(Figure 2.9F)**. Using qRT-PCR, we confirmed that the *olrn-1*-dependent immune effectors, *irg-4* **(Figure 2.9G)** and *irg-5* **(Figure 2.9H)** were expressed at higher levels in animals at the L2/L3 larval stage compared with young adult animals. Low activity of OLRN-1 leads to de-repression of the p38 MAPK pathway in

AWC neurons (Huang et al., 2007). Together, the data in this manuscript suggest that low levels of *olrn-1*, as recapitulated in multiple loss-of-function mutant alleles, also de-represses the p38 MAPK PMK-1 pathway in intestine to promote pathogen resistance during *C. elegans* development.

F

G *irg-4*

H *irg-5*
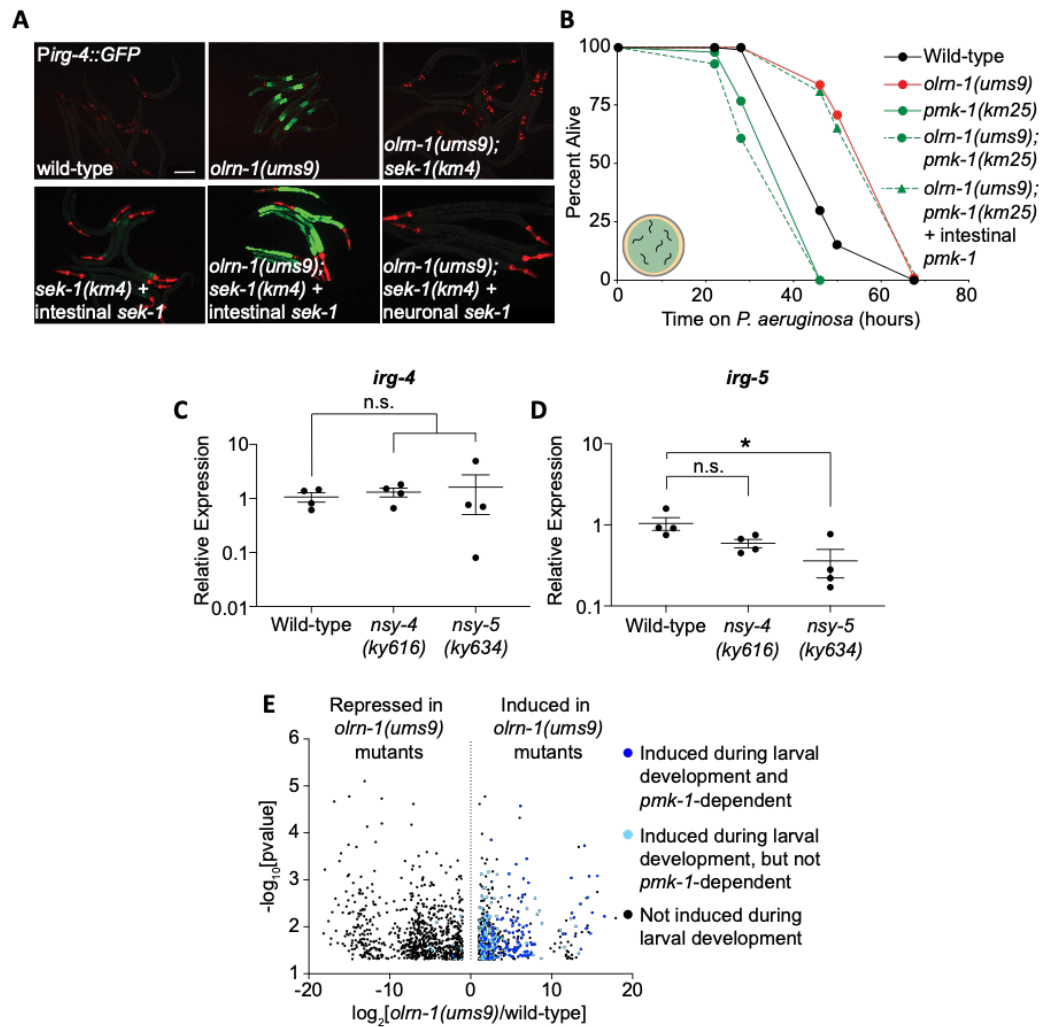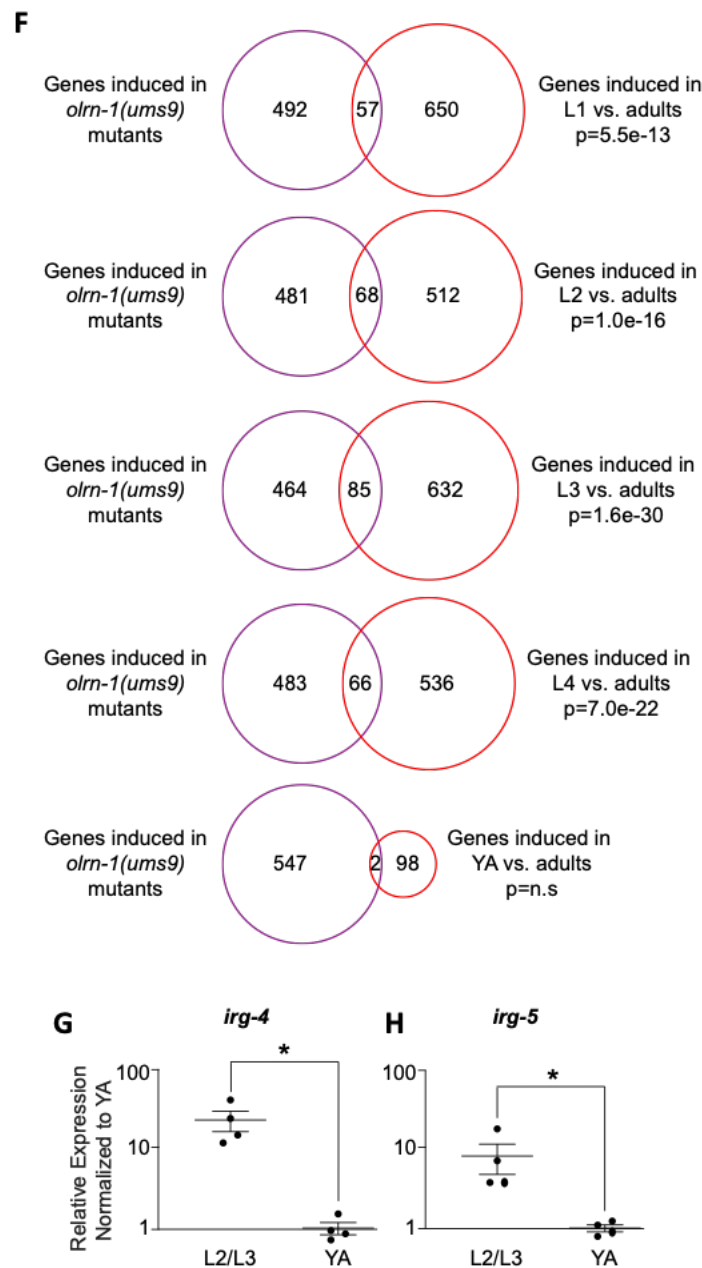
Figure 2.8 Neuronal *olrn*-1 regulates p38 MAPK PMK-1-dependent immune effector expression during nematode development

 (A) Representative images of animals with the indicated genotypes carrying an integrated P*irg-4::GFP* reporter. Red pharyngeal expression is the P*myo-2::mCherry* co-injection marker, which confirms the presence of the P*irg-4::GFP* transgene. Bright red pharyngeal expression in *C. elegans* with intestinal *sek-1* (P*ges-1::sek-1::GFP)* and neuronal *sek-1* (P*unc-119::sek-1::GFP)* is the P*myo-2:mStrawberry* co-injection marker. Presence of P*irg-4::GFP* reporter was confirmed in these animals by P*myo-2::mCherry* expression

in siblings that did not contain the indicated extrachromosomal arrays. Scale bar is 100 μm. **(B)** *C. elegans* pathogenesis assay conducted with a large lawn of *P. aeruginosa* and *C. elegans* of indicated genotypes at the L4 larval stage is shown. Data are representative of three trials. Sample sizes, mean lifespan and p-values for all trials are shown in Table 2.2. "intestinal *pmk-1*" indicates that these animals have the P*vha-6::pmk-1* extrachromosomal array. qRT-PCR data of irg-4 **(C)** and irg-5 **(D)** in wild-type, nsy-4(ky616) and nsy-5(ky634) animals is presented. Data are the average of three independent replicates, each normalized to a control gene with error bars representing SEM, and are presented as the value relative to the average expression from all replicates of the indicated gene in wild-type animals. "n.s." equals not significant for the p value and * equals p<0.05 by one-way ANOVA for the indicated comparison. **(E)** A volcano plot of the mRNA-seq transcriptome profiling analysis shows all genes that were differentially expressed in *olrn-1(ums9)* mutants compared to wild-type animals (Fold change>2, p<0.05), as described in Figure 2.4A. Highlighted in dark blue are the genes whose transcription are: *(i)* dependent in on the p38 MAPK *pmk-1* (from the overlap in Figure 2.4D), and *(ii)* also induced in wild-type animals at the L1, L2, L3 or L4 stage compared to wild-type young adult animals. Highlighted in light blue are the genes that are induced in L1, L2, L3 or L4 stage wild-type nematodes compared to adult animals, but whose transcription are not dependent on p38 MAPK *pmk-1*. Venn diagrams showing the overlap of genes that are induced at each larval stage compared to genes that are induced in *olrn-1(ums9)* mutants are shown. **(F)** Venn diagrams show the overlap of genes induced in olrn-1(ums9) mutants with genes that are upregulated at each larval stage in wild-type animals compared to wild-type adult animals. The hypergeometric p value for the overlap of each dataset is given in the Figure. "n.s." equals not significant. qRT-PCR data of irg-4 **(G)** and irg-5 **(H)** in wild-type animals at the second or third larval stage (L2/L3), and the young adult (YA) stage are shown. Data are the average of four independent replicates, each normalized to a control gene with error bars representing SEM, and are presented relative to the average expression from all replicates of the indicated gene in animals at the young adult stage. * equals p<0.05 by one-way ANOVA for the indicated comparison.

2.4 Materials and Methods

2.4.1 Forward genetic screen

Ethyl methanesulfonate (EMS) mutagenesis was performed on strain *agIs44* as previously described (Cheesman et al., 2016). Synchronized F2 progeny representing approximately 40,000 haploid genomes were screened for animals that constitutively express *agIs44* GFP fluorescence. Three alleles were identified (*ums9, ums10* and *ums11*). To identify the causative mutations, pooled genomes from 52 recombinants for *ums9* and 3 recombinants for *ums11* following a 2X outcross to N2 were sequenced along with the *agIs44* parent strain. All recombinants constitutively expressed *agIs44* GFP. Homozygous variants from WS220 (ce10) *C. elegans* reference genome that were present in the 2X

outcrossed samples, but not in *agIs44*, were identified using Cloud Map (Minevich et al., 2012). We were unable to identify the causative mutation in *ums10*.

2.4.2 *C. elegans* Bacterial Infection and Other Assays

"Slow killing" *P. aeruginosa* infection experiments were performed as previously described (Foster, McEwan, et al., 2020; Tan et al., 1999). The wild-type control for these assays is *agIs44*. In brief, a single colony of *P. aeruginosa* PA14 was inoculated into 5 ml of Luria-Bertani (LB) medium, and allowed to incubate at 37° for 15 hr. 10 µl of this culture was spread onto 35-mm tissue culture plates containing 4 ml of slow kill agar (0.35% peptone, 0.3% sodium chloride, 1.7% agar, 5 µg/ml cholesterol, 25 mM potassium phosphate, 1 mM magnesium sulfate, 1 mM calcium chloride). Plates were incubated for 24 hours at 37°C, and approximately 24 hours at 25°C. Approximately one hour before the start of the assay, 0.1 mg/ml 5-fluorodeoxyuridine (FUDR) was added to the medium to prevent progeny from hatching. For all pathogenesis assays that studied *C. elegans* with extrachromosomal arrays, control genotypes, which did not express the array, were obtained from siblings isolated from the same plates as nematodes that contained the array. *C. elegans* lifespan assays were conducted with animals grown on nematode growth media agar at 20ºC in the presence of 40 µg/mL 5-fluoro-2'-deoxyuridine. All pathogenesis and lifespan assays were conducted with nematodes at the L4 larval stage. To obtain stage-matched animals at the L4 larval stage for the pathogenesis and lifespan assays, *olrn-1* mutant animals at the L1 larval stage were added to growth plates (NGM with *E. coli* OP50) approximately 24 hours before wild-type L1 larval stage animals were added to growth

plates. Three trials of each pathogenesis assay were performed. Sample sizes, mean lifespan, and p-values for all trials are shown in Table 2.2.

The propensity of *C. elegans* to avoid a small lawn (10 μL) of *P. aeruginosa* was determined by counting the number of *C. elegans* on or off the lawn at 4, 8, 16, 24 and 30 hours after synchronized L4 were placed on the bacteria (Foster, McEwan, et al., 2020). *C. elegans* development assays were performed as previously described (Cheesman et al., 2016; Foster et al., 2020). Brood sizes were quantified from five independent plates, each with two animals per plate. Animals were transferred to new plates each day to facilitate scoring of the progeny. Data for all replicates of the development and brood size assays are shown in Table 2.2.

Colony forming units of *P. aeruginosa* were quantified in the intestine of *C. elegans* as previously described with some modifications (Foster, McEwan, et al., 2020; J. Singh & Aballay, 2019). Briefly, *C. elegans* animals were exposed to *P. aeruginosa* for 24 hours. Animals were then picked to NGM plates lacking bacteria and incubated for 10 minutes to remove external *P. aeruginosa*. Animals were then transferred to a second NGM plate after which 10-11 animals per replicate were collected, washed with M9 buffer containing 25 mM levamisole and 0.01% Triton X-100, and ground with 1.0 mm silicon carbide beads. CFUs were quantified from serial dilutions of the lysate.

2.4.3 Generation of transgenic *C. elegans* strains

To generate *olrn-1* rescue lines, primers 5'-CAG AAC CAG ATT CTC GGA ATG A-3' and 5'-AGA GGA AGA GAG ACA GGA TGA A-3' were used to amplify the entire

olrn-1 locus. The resulting PCR product (30 ng/l), the P*myo-3::mCherry* co-injection marker (15 ng/l) and pBluescript SK (-) vector (155 ng/l) were microinjected into *olrn-1(ums9);agIs44* animals to generate the arrays *umsEx4*, *umsEx6* and *umsEx7*.

The *olrn-1* neuron-specific rescue construct was generated using Gibson assembly to fuse 2kb of the *sng-1* promoter (amplified using primers 5'-CCC CCC CTC GAG GTC GAC GGT ATC GAT AAG CTT GAT ATC GTT GAG CAG CGA CTA ACA AAA-3' and 5'-ACC TGA CAC TAA TTT CTC TTG GCG CTG AAC ATC TAG TCA TGC TAA AAT AAA AGA AAT ATA-3') with 2960 bp of *olrn-1b* coding region + 667bp 3' UTR (amplified using primers 5'-ATGACTAGATGTTCAGCGCC-3' and 5'- GGC GGC CGC TCT AGA ACT AGT GGA TCC CCC GGG CTG CAG GTT TCA TAT ATC TTA TGC CGT -3') in pBluescript vector linearized with *Eco*R1 (Gibson et al., 2009). The plasmid (30 ng/l), the P*myo-3::mCherry* co-injection marker (15 ng/l) and pBluescript SK (-) vector (155 ng/l) were microinjected into *olrn-1(ums9);agIs44* animals to generate the arrays *umsEx20*, *umsEx21* and *umsEx23*.

2.3.4 Gene expression analyses and bioinformatics

For the RNA-seq experiment of olrn-1(ums9) and wild-type animals, synchronized L1 stage *C. elegans* were grown to the L4/young adult stage. RNA was isolated using TriReagent (Sigma-Aldrich), purified on a column (Qiagen), and analyzed by mRNA-seq using the BGISEQ-500 platform (BGI Americas Corp). The quality of raw sequencing data was evaluated by FastQC (version 0.11.8) and Multiqc (version 1.7) (Ewels et al., 2016; Wingett & Andrews, 2018). Low-quality reads were trimmed using Trimmomatic (version

0.36) (Bolger et al., 2014). The trimmed reads were mapped to the *C. elegans* reference genome, WS220/ce11 [University of California Santa Cruz (UCSC) genome browser] using HISAT2 (version 2.1.0)(D. Kim et al., 2015; Pertea et al., 2016). The sequence alignment map (SAM) files were then converted to sorted BAM files using Samtools (Version 1.3.1)(Li, 2011; Li et al., 2009). The general transfer format (GTF) annotation file (WS220/ce11) was downloaded from the UCSC genome website, and the assembled GTF file was generated for each sample using Stringtie (version 1.3.4)(Pertea et al., 2015, 2016). Stringtie was then used to compare each sample against the merged assembly, estimate transcript abundance, and to generate a count table for Ballgown analysis (Pertea et al., 2016). The Ballgown package from the Bioconductor software suite (version 3.8) was used to run a custom R script in R console (R Version 3.5) to analyze the differential gene expression, visualize the data, and perform statistical tests for differential expression with multiple test correction. A gene was considered to be differentially regulated if its fold change versus wild-type was greater than two, the adjusted p-value was less than 0.05, and its RPKM was greater than one.

To examine genes that are differentially expressed during *C. elegans* development, raw base-called fastq files were downloaded from the European Nucleotide Archive (accession number PRJEB31791). For each sample, reads were aligned to the WS220/ce11 on UCSC genome website using minimap2 (version 2.14-r883)(Li, 2018). Genomic alignments were run with the following parameters: -ax splice -k14 -uf -secondary=no -G 25000 -t 24. The resulting sam files were converted to bam format using samtools view with parameters: -b –F 2048 (Li et al., 2009). Read filtering and splice isoform

identification were analyzed as described (Roach et al., 2019). The GTF (WS220/ce11) annotation file was downloaded from UCSC genome website and the assembled GTF file was generated for each sample using Stringtie (version 1.3.4). Stringtie was used to compare each sample against the merged assembly, to estimate transcript abundance, and to generate a count table for Ballgown analysis. The Ballgown package from the Bioconductor software suite (version 3.8) was used to run a custom R script in R console (R Version is 3.5) to analyze differential gene expression, visualize the data and perform statistical tests for differential expression with multiple test correction. Differential gene expression was defined as a fold change (FC) versus wild-type greater than 2, adjusted P value less than 0.05 and RPKM greater than one.

For the qRT-PCR studies, RNA was reverse transcribed to cDNA using the RETROscript Kit (Life Technologies) and analyzed using a CFX1000 machine (Bio-Rad) using previously published primers (Cheesman et al., 2016; Peterson et al., 2019; Troemel et al., 2006). All values were normalized against the control gene snb-1. Fold change was calculated using the Pfaffl method (Pfaffl, 2001). The analysis of irg-4 and irg-5 expression using nanoString was performed as previously described (Anderson et al., 2019; Cheesman et al., 2016; Pukkila-Worley et al., 2014). Counts from each gene in wild-type and olrn-1(ums9) animals were normalized to three control genes: snb-1, ama-1 and act-1.

2.3.5 Immunoblot Analyses

Protein lysates from stage-matched *C. elegans* grown to the young L4 larval stage on *E. coli* OP50 on NGM agar were prepared as previously described (Cheesman et al.,

2016; Peterson et al., 2019). Harvested animals were washed twice with M9 buffer, incubated in a roller at room temperature for 15 minutes to allow the nematode intestine to clear of bacteria, washed an additional time and flash frozen in RIPA Buffer (Cell Signaling Technology, Inc.) using an ethanol and dry ice bath. Samples were lysed by sonication and centrifuged. Protein was quantified from the supernatant of each sample using Bradford Reagent (Bio-Rad Laboratories, Inc.). Laemmli buffer (Bio-Rad Laboratories, Inc.) was added to a concentration of 1X and the total protein from each sample was resolved on NuPage 4-12% gels (Life Technologies), transferred to nitrocellulose membranes (Life Technologies), blocked with 5% BSA in TBST and probed with a 1:1000 dilution of an antibody that recognizes the doubly-phosphorylated TGY motif of PMK-1 (Cell Signaling Technology), a previously characterized total PMK-1 antibody (Peterson et al., 2019) or a monoclonal anti-tubulin antibody (Sigma-Aldrich, Clone B-5-1-2). Horseradish peroxidase (HRP)-conjugated anti-rabbit (Cell Signaling Technology) and anti-mouse IgG secondary antibodies (Abcam) were used at a dilution of 1:10,000 to detect the primary antibodies following the addition of ECL reagents (Thermo Fisher Scientific), which were visualized using a ChemiDoc MP Imaging System (BioRad). The band intensities were quantified using Image Lab software version 6.0.1 (BioRad), and the ratio of active phosphorylated PMK-1 to total PMK-1 was calculated with all samples normalized to the ratio of wild-type control animals.

2.3.6 Microscopy

Nematodes were mounted onto agar pads, paralyzed with 10 mM levamisole (Sigma) and photographed using a Zeiss AXIO Imager Z2 microscope with a Zeiss Axiocam 506 mono camera and Zen 2.3 (Zeiss) software.

2.3.7 Quantification and Statistical Analysis

Differences in survival of *C. elegans* in the *P. aeruginosa* pathogenesis assays were determined with the log-rank test after survival curves were estimated for each group with the Kaplan-Meier method. OASIS 2 was used for these statistical analyses (Han et al., 2016). qRT-PCR studies, lawn occupancy studies, intestinal CFU quantification, western blot band intensity quantification, and developmental assays are presented as the mean ± standard error. p values were calculated using one-way ANOVA in Prism 8 (GraphPad Software), unless otherwise indicated in the Figure legend. Sample sizes, mean lifespan, and p-values for all trials are shown in Table 2.2.

Chapter 3: Discussion

3.1 Introduction

This study demonstrates that innate immunity in *C. elegans* intestinal epithelial cells and the development of AWC neurons are linked by a single neuronal protein. Neuronal *olrn-1* functions cell autonomously in AWC neurons to ensure olfactory receptor expression and cell non-autonomously to suppress the p38 MAPK PMK-1 immune pathway in the intestine. These findings have the following important implications: 1) Food preference and chemotaxis is coupled to innate immune regulation, 2) Suppression of the p38-PMK-1 pathway by OLRN-1 is required for development and evolutionary fitness, and 3) Neuronal regulation of immune defenses in evolutionarily ancient and 4) Triggering toxic immune hyperactivation in human pathogenic nematodes may provide a novel treatment strategy to combat the growing threat of helminthic resistance.

3.2 Food preference and chemotaxis may be coupled to innate immune regulation

The work described in this thesis supports the existence of an immune regulatory network by which neuronally expressed OLRN-1 in Amphid Wing C (AWC) controls the induction of PMK-1-dependent immune effectors in the intestinal epithelium of *C. elegans*. Why might such a mechanisms exist and what survival advantage might this provide? Olfactory neurons are key transducers of environmental conditions, providing the critical input necessary for worms to make important decisions pertaining to food acquisition and pathogen avoidance. The availability and quality of food has drastic effects on *C. elegans* locomotion, suggesting that sensory information is broadly integrated with many core physiological processes.

AWC olfactory neurons are required for chemoattraction towards a diverse set of volatile stimuli, including butanone, benzaldehyde, butanone, isoamylalcohol, 2,3 pentanedione and 2,4,5 trimethylthiazole. Many of these compounds are natural byproducts created when organic matter decomposes and are therefore attractive signals for *C. elegans*, which feeds on bacteria found in such microenvironments. When feeding on bacteria that promotes development, it is necessary to ensure that physiological stressors (i.e. immune responses) are not aberrantly initiated, as these processes could jeopardize immune homeostasis and have could have deleterious consequences on organismal fitness. To ensure this careful balance be maintained, chemoattraction and immune suppression may be inherently linked biological processes. Our data suggests that *C. elegans* may rely on a signaling axis by which OLRN-1 functions in AWC chemosensory neurons to repress PMK-1-dependent immune responses, a process which in the presence of attractive stimuli such nutritious food sources, may prevent unnecessary activation of immune defenses (Figure 3.1).
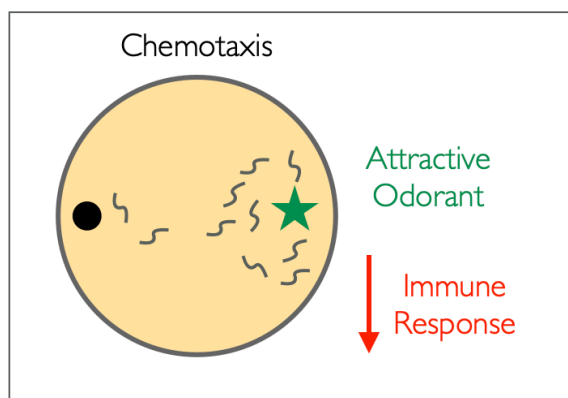
Figure 3.1 Chemotaxis may be linked to immune regulatory mechanisms

Numerous other chemosensory neurons have been linked to immune regulation, suggesting that input from many chemosensory neurons may influence not only behavioral responses, but also regulate key biological processes like immune regulation in order to promote healthspan. Previous work by Aballay et al. characterized two separate mechanisms by which sensory neurons function to modulate immunity in *C. elegans*. Mechanosensory CEP neurons responsible for regulating the "basal slowing response" necessary for maximizing the time animals spend in the presence of nutritious food, and gustatory ASG sensory neurons, have also been shown to modulate PMK-1-dependent immune responses via dopaminergic signaling (Cao & Aballay, 2016). Likewise, ASH and ASI neurons expressing the octopamine receptor OCTR-1, have been implicated in the regulation of both microbial killing pathways and pathogen avoidance behavior (Cao et al., 2017; Liu et al., 2016; Sellegounder et al., 2018; J Sun et al., 2011). Thus, chemosensation and immune regulation may not be independent protective processes. Rather, they very well may be two intrinsically associated processes that function cooperatively to ensure that worms are 1) able to locate and assess the quality of food 2) suppress protective immune defenses on bacteria that is determined not to pose a threat to organismal health.

Further evidence suggesting that OLRN-1-expressing AWC neurons might regulate immunity through a mechanism similar to the mechanisms described by Aballay et al. can be found upon close examination of the *C. elegans* connectome. In general, sensory neurons can be thought of as the first link in a long chain of signaling cascades that ultimately turns an input into an appropriate biological response. Interestingly, AWC, CEP, ASG, ASI and ASH neurons all function within the same neuronal circuit, whereby

chemosensory information is relayed to downstream AIY and AIA interneurons (Cook et al., 2019). Thus, as AWC neurons synapse with and communicate through the same set of downstream interneurons, it is feasible that AWC neurons function to regulate many of the same core biological processes (Figure 3.2).
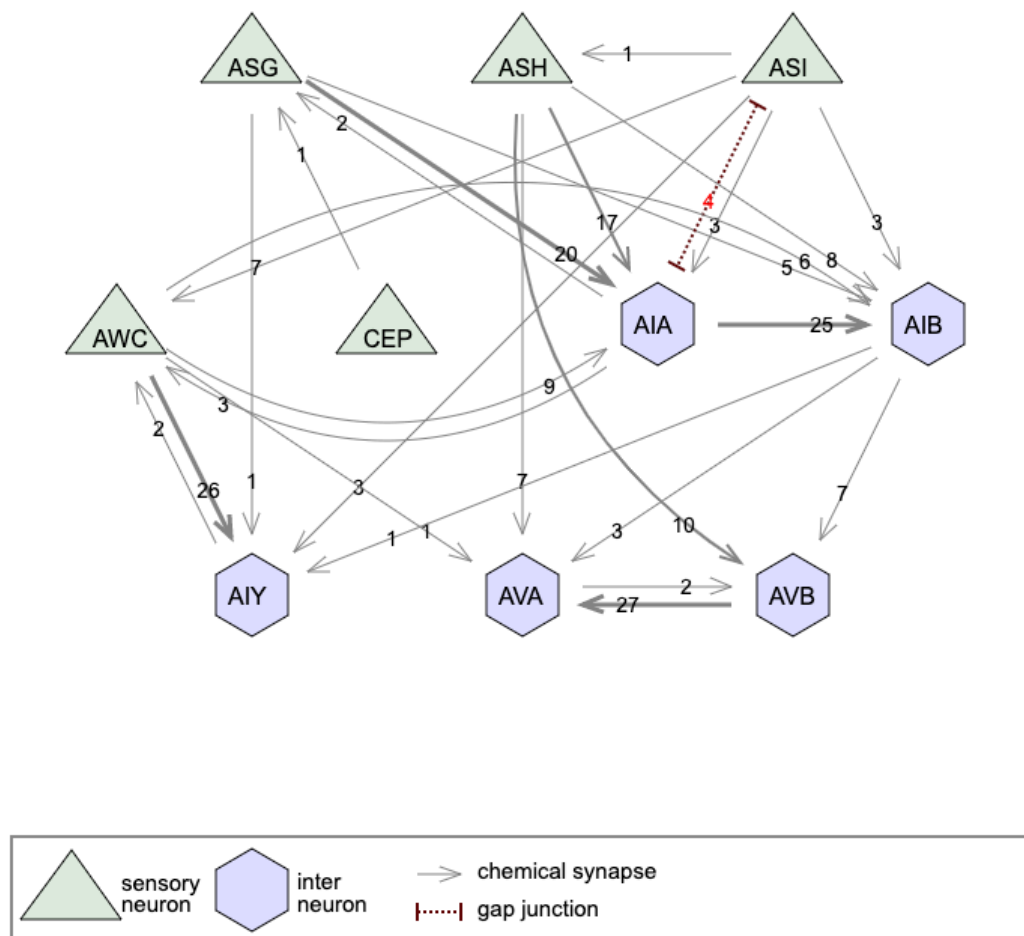
Figure 3.2 AIY, AIA, and AIB interneurons function as signaling hubs for AWC, ASG, CEP, ASH and ASI sensory neurons

3.3 Suppression of the p38-PMK-1 pathway by OLRN-1 is required for development and evolutionary fitness

While changes in environmental conditions have been known to effect growth and development of *C. elegans* for many years, recently it has become clear that immunological stressors can also have dire consequences on organismal fitness. Immune activation in the context of a pathogenic infection is crucial in order to ensure longevity. However, the initiation of protective immune mechanisms is an extraordinarily resource intensive process that puts significant stress on an organism. Following a forward genetic screen for novel immune regulators, Cheesman et al. identified a gain-of-function allele in the MAPKKK gene *nsy-1*, that resulted in hyperphosphorylation of PMK-1, resulting in the constitutive induction of immune effectors previously characterized to respond robustly to pathogen infection (Cheesman et al., 2016). Mutants harboring the *nsy-1(gf)* allele were notably resistant to pseudomonal infection relative to wild-type animals. While this immune activation provided protection against pathogenic microbes, the constant production of immune effectors put a significant amount of stress on the organism and was found to be toxic to developing nematodes. The immune toxicity observed in *nsy-1(gf)* animals resulted in severe developmental stunting and significantly reduced brood sizes, suggesting that while protective defenses are required to adequately defend nematodes against microbial threats, uncontrolled activation of these protective responses can result in toxicity that can even numerous core biological processes (Cheesman et al., 2016).

As it is evolutionarily advantageous for immune and stress responses to be carefully controlled to avoid the detrimental effects immune toxicity, numerous mechanisms have

been discovered to fine tune these responses in order to promote nematode development and healthspan. Richardson et al. characterized one of the first immune regulatory mechanisms that appeared to promote development by protecting against immune activation (Richardson et al., 2010). Their findings indicated that the unfolded protein response, which works to restore protein folding homeostasis in the ER, also has an essential role at limiting PMK-1-dependent toxic immune activation during normal growth and development. Animals lacking key elements of the UPR machinery, such as XBP-1 and PEK-1, displayed a decrease in stress resistance that often led to larval lethality phenotypes, thus suggesting the requirement of the UPR to maintain ER homeostasis in *C. elegans* under physiological conditions (Richardson et al., 2010). Follow up work aiming to better understand the relationship between immune control and development has resulted in the discovery of several other immune regulators that are critically important for productive nematode development. NIPI-3, a tribbles-family pseudokinase has been shown to negatively regulate the p38 PMK-1 signaling cascade in multiple tissues via the CCAAT/enhancer-binding protein homolog CEBP-1, in order to promote growth and development (K. W. Kim et al., 2016). Likewise, work by Amrit et al. demonstrated a similar phenomenon whereby TCER-1, the *C. elegans* homolog of the human transcription elongation and splicing factor TCERG, promoted longevity by suppressing the transcriptions of p38 PMK-1-depemndent genes, but also appeared to regulate the expression key intermediates involved in the UPR^{mt}, suggesting that TCER-1 may be playing a more general role in suppressing immune and stress response in order to promote organismal viability and development (Amrit et al., 2019). The functional redundancy of

mechanisms that work to limit toxic immune activation, reflects the key requirement to protect organisms against unnecessary or aberrantly activate immune responses.

In this recent study, I have shown that OLRN-1 is an important upstream neuronal regulator of the PMK-1 pathway in intestinal epithelial cells. Loss-of-function mutants *ums9*, *ums11* and *ky626* each displayed severe growth stunting and reproductive fitness defects. This observation suggests that immune suppression by OLRN-1 is yet another requirement to protect against potentially toxic immune activation necessary to ensure productive development and organismal fitness. Additionally, I discovered that a significant subset of genes under the control of *olrn-1* are also differentially expressed throughout nematode development. This interesting observation suggests that immune regulatory mechanisms may be inherently linked to genes involved in developmental processes, and that the two processes may be co-regulated to some degree in order to maintain a homeostatic relationship.

3.4 Neuronal regulation of immune defenses are evolutionarily ancient

The ability to mount protective defenses against pathogenic microbes has been an evolutionary requirement for millennia, thus many core innate immune signaling pathways are highly conserved in all metazoans. The requirement to maintain immune homeostasis suggests that regulatory mechanisms that function to fine tune these immune responses have also been carefully selected for. For nearly three decades it has been known that various components of the mammalian nervous system are tightly integrated with the immune system, especially within the gastrointestinal tract where a fine balance between

protective and tolerogenic responses must be maintained. Understanding the complexities of neuro-immune interactions within the intestine has been challenging however, and as a result progress in this field has been hindered. Recent discoveries suggesting that mechanisms of neuro-immune regulation are conserved in ancient organisms provides researchers with new tools that can be used to dissect the foundational principles underlying interactions between the nervous system and immune systems (Figure 3.3) (Foster, Cheesman, et al., 2020; Styer et al., 2008; J Sun et al., 2011).
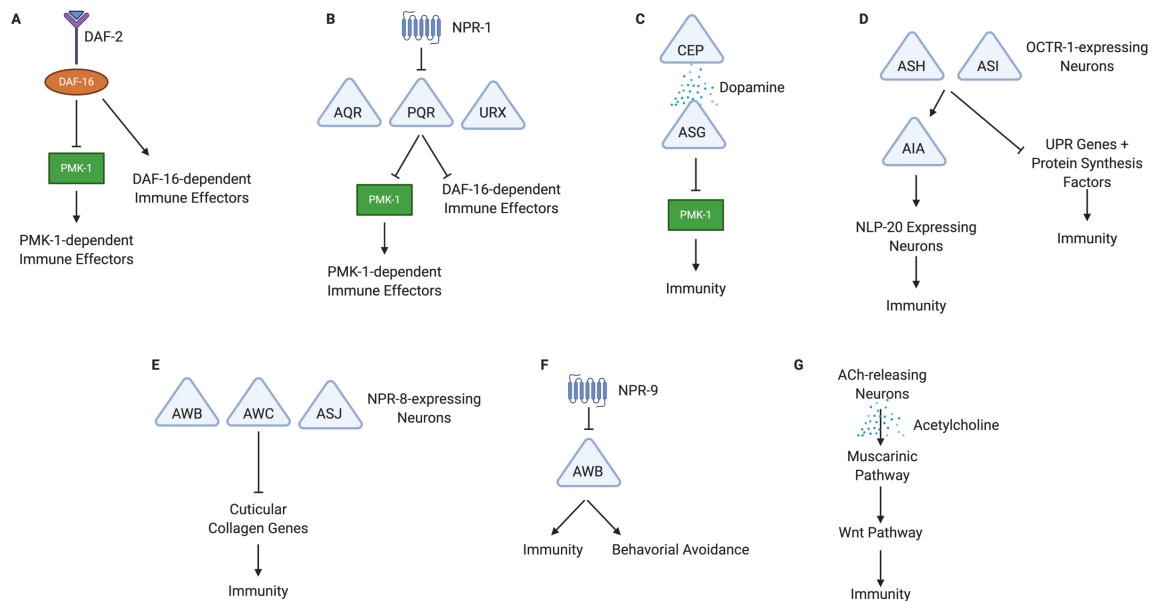
Figure 13 Previously described mechanisms of immune regulation by the nervous system in *C. elegans*

A) Insulin Signaling Pathway described in section 1.4.5.1 **B)** The NPR-1 Pathway described in section 1.4.5.2 **C)** Dopaminergic Signaling described in 1.4.5.6 **D)** The octopaminergic immunoregulatory axis 1.4.5.3 **E)** NPR-8 and cuticular collagens described in 1.4.5.4 **F)** NPR-9 Pathway described in and 1.4.5.5 and **G)** The ACh-Wnt Pathway as described in section 1.4.5.7.

Even though OLRN-1 is not widely conserved outside of invertebrates, the core idea that immune system function is heavily regulated by input received from the nervous system can be broadly applied. Interestingly, a structurally related protein expressed in *Drosophila melanogaster*, RAW, has been found to inhibit JNK MAPK signaling during development in order to promote the dorsal closure of the fly embryo (Byars et al., 1999; Luong et al., 2018). The JNK pathway is one of three signaling subfamilies of the MAP kinase signaling pathway in flies, the others being the extracellular signal-related kinase (ERK) pathway, and the p38 pathway. As both OLRN-1 and the related RAW proteins function to regulate MAPK signaling, it is likely that these proteins may utilize similar mechanisms to suppress signal transduction.

In humans, the liver, spleen, bone marrow, thymus, lymph nodes, and gastrointestinal system are all densely innervated by both the autonomic nervous and sympathetic nerve fibers (McCorry, 2007; Wehrwein et al., 2011). Secretion of numerous chemical messengers, including small molecules, neuroendocrine peptides, cytokines, and growth factors allow for complex bi-directional communication between the nervous system and the immune system. Thus, the immune system should no longer be regarded as an autonomously functioning entity, but rather it is quite clear that the immune system receives significant regulatory input from neuronal systems.

Modulation of pro-inflammatory responses by the nervous system is thought to be one of the primary drivers of immuno-tolerance mechanisms critical for maintaining a healthy balance of immune activation within the intestinal tract (Costantini & Baird, 2016; Lakhan & Kirchgessner, 2010; Nemati et al., 2017). Here, billions of microbial species co-

exist, requiring the immune system to distinguish commensal bacterial species from pathogenic ones in order prevent aberrant immune activation against beneficial microbes. Numerous chronic inflammatory diseases of the digestive tract, such as Crohn's disease and ulcerative colitis are believed to result in part from dysregulated immune suppression by the nervous system (Costantini & Baird, 2016; Lakhan & Kirchgessner, 2010; Mogilevski et al., 2019; Nemati et al., 2017). To date, the ability of the mammalian immune system to differentiate between microbial species remains poorly understood and continues to be an area of active research. As the nervous system is proving to play a critical role in this process, more research is needed to understand the precise integrations that are occurring between the nervous system, immune system and resident microbial communities. For these reasons, *C. elegans* has emerged as an important model to better define the neuronal circuitry that exists to modulate immunity within the intestine.

3.4 Next Steps

I have described a mechanism whereby neuronal OLRN-1 coordinates the expression of numerous PMK-1/p38 dependent immune effectors within the intestine. The details of the precise mechanism by which this occurs however, remain unclear. A critical gap in knowledge that remains is understanding the precise physiological function of OLRN-1 in AWC neurons. AWC neurons detect volatile odorants and promote chemotaxis towards the stimuli. To date, the attractive odorants AWC neurons have been implicated in detecting include benzaldehyde, butanone, isoamylalcohol, 2,3 pentanedione and 2,4,5 trimethylthiazole. One exciting hypothesis is that in addition to the odorants, AWC neurons

may also be able to detect specific bacterial secondary metabolites common among nutritious food sources and promote chemotaxis towards microbe rich environments. Previous studies have implicated sensory neurons in the detection of numerous bacterial secondary metabolites such as phenazine-1-carbox-amide and pyochelin, both of which activate a G-protein-signaling pathway in the ASJ chemosensory neuron pair to promote avoidance behavior when exposed to pathogens (Meisel & Kim, 2014). As both behavioral and microbial immunity are both important in the context of bacterial infection, it is possible the AWC neurons, and OLRN-1 in particular, utilize sensory information to coordinate both behavioral chemotactic responses and microbial defense mechanisms, thus promoting chemotaxis toward nutritious bacteria, while at the same time, suppressing deleterious immune responses.

Another critical gap in our understanding is the precise mechanism by which AWC neurons communicate with the intestine. Previous studies have determined that sensory neurons can communicate with the gut via the secretion of soluble neuromodulators. Inhibition of dopamine signaling between CEP and ASG neurons has been shown to protect *C. elegans* against bacterial infection by inducing expression of numerous PMK-1/p38 (Cao & Aballay, 2016). Likewise, a neuronal circuit involving ASH neurons and the neuropeptide NLP-20 has also been implicated in mediating protective defense mechanisms in *C. elegans* (Cao et al., 2017). Therefore, OLRN-1-expressing AWC sensory neurons may be similarly be signaling to the intestine via a secreted neurotransmitter or neuropeptide. As AWC neurons are glutamatergic and have also been shown to express the neuropeptide NLP-1, either of these molecules may be involved in this signaling axis.

Additionally, transcriptome analysis of OLRN-1 mutants showed differential expression of five neuropeptide-like proteins. Many of these neuropeptides are uncharacterized, and thus their expression patterns remain unknown, therefore it is possible that one or multiple of these molecules plays an important role in the AWC signaling axis.

Post-synaptic output from AWC neurons is received by AIY interneurons, where sensory cues from many sources are integrated. As AIY neurons can be thought of as a sensory hub where chemosensation, mechanosensation and olfactory cues are processed, it is possible that OLRN-1-expressing AWC neurons communicate through AIY neurons in order to relay sensory data to distal tissues such as the intestine. The idea that interneurons may function as linkers between sensory neurons and downstream tissues is not novel. The AIA interneuron pair, which integrates sensory information from ASH sensory neurons has been found to be involved in the aforementioned NLP-20-dependent regulation of intestinal immunity (Cao et al., 2017). Further research must be conducted in order to determine the precise neuronal circuitry involved in the AWC-dependent immune regulatory pathway we have characterized.

The *C. elegans* intestine is not directly innervated, therefore, in order to completely elucidate the mechanism by which sensory cues can illicit transcriptional changes within the intestine, it must be understood precisely how the nervous system relays signals to intestinal epithelial cells. One hypothesis is that specific surface receptors on intestinal epithelial cells are able to bind to neuro-modulatory molecules and subsequently initiate downstream immune signaling pathways. Numerous GPCRs have been observed as having

neuropeptide and/or neurotransmitter binding capabilities (Hartenstein, 2006; Janssen et al., 2010; Jee et al., 2012; Keating et al., 2003; Rual et al., 2004). Interestingly, the initial forward genetic screen seeking to identify novel immune regulators that was conducted at the onset of this thesis also resulted in the identification of an intestinally expressed putative neuroendocrine receptor, GNRR-3. Mutants harboring a loss-of-function mutations in *gnrr-3* constitutively induced numerous PMK-1-dependent immune effectors, were resistant to pathogen, and displayed hyperphosphorylation of PMK-1 in a manner virtually identical to that of OLRN-1 mutants. It is quite possible that GNRR-3 is a downstream target of a neuro-immune signaling axis and may even be one of the downstream targets of the OLRN-1, functioning as the key surface receptor linking the nervous system to the intestine. Further research needs to be conducted in order to determine if these hypothesis have merit. Performing additional targeted GPCR knockdown screens in *olrn-1(lf)* mutants may assist in the identification of other involved downstream gut-specific neuron-endocrine receptors that allow for further characterization of the OLRN-1 signaling axis.

3.5 Potential Clinical Applications of Toxic Immune Hyper-activation in Human Pathogenic Nematodes

In alignment with previous studies, this study has demonstrated the importance of maintaining immune homeostasis within the intestine, as mis-regulated defense responses have severe deleterious effects of development and reproductive fitness. OLRN-1 was found to be a necessary negative regulator of immune defenses in nematodes in order to

prevent severe developmental and reproductive fitness defects. Interestingly, OLRN-1 is conserved in many nematodes that are pathogenic to humans, but it is not present in humans. This lack of conservation combined with its role in modulating potentially toxic immune responses, may allow OLRN-1 to be used a nematode-specific therapeutic target in order to combat worm infections that pose serious health risks to mammals.

Soil-transmitted helminths (STHs) are parasitic nematodes that are estimated to chronically infect over one-fifth of the world's population and are one of the most prevalent health afflictions of the developing world (Mascarini-Serra, 2011). The most common soil-transmitted helminths are *Ascaris lumbricoides*, whipworm (*Trichuris trichiura*), and hookworm (*Anclostoma duodenale* and *Necator americanus*). Chronically infected patients often present with anemia, gastrointestinal distress, severe growth stunting and cognitive retardation. As infections are most common within developing nations, poor sanitation, lack of infrastructure and inaccessible medical care are major contributors to the epidemic.

Even though parasitic nematodes chronically infect over a billion people worldwide, there remains a significant unmet medical need to develop efficacious broad-spectrum treatments to combat this health crisis. The current standard of care treatments prescribed for chronically infected individuals includes albendazole, ivermectin, and praziquantel. Ivermectin and praziquantel are both neurotoxic, and lead to rapid paralysis of exposed helminths, causing them to detach from their sites of action after which they can be either excreted or destroyed by host immune responses. Albendazole on the other

hand inhibits microtubule polymerization and subsequently leads a host of deleterious physiological consequences such as impaired glucose uptake, sterility, and reduced ATP production. While these drugs are generally effective, resistance to these widely distributed and commonly used medications is making it much more difficult to adequately treat patients in areas where reinfection is likely. Thus, it is important reevaluate treatment strategies and develop novel broad-spectrum therapeutics in order to meet the current unmet medical needs of patients suffering from the debilitating consequences of chronic helminth infection.

In the context of a pathogenic nematode infection, the fitness defects caused by uncontrolled immune activation, could be harnessed to develop novel targeted treatment strategies. Interestingly, OLRN-1 contains two putative transmembrane domains, suggesting that it is a membrane bound surface receptor, making it a promising candidate drug target. If the immuno-regulatory role of OLRN-1 is in fact ligand-dependent as structural analyses suggest, it may be possible to pharmacologically inhibit OLRN-1 in parasitic nematodes in order to induce aberrant immune hyperactivation. Fitness defects caused by OLRN-1-dependent immune mis-regulation would most likely severely reduce intestinal worm burdens and fecal egg counts in infected hosts, thus increasing the chance that chronic infections can be properly cleared. As helminth infections continue to be a major public health emergency in many developing nations, continuing to take advantage of the genetic tractability of *C. elegans* to identify novel nematode-specific drug targets such as OLRN-1, will provide patients with an increase in alternative treatment option

3.6 Conclusion

The work presented in this thesis enhances our understanding of how the nervous system plays a key role in the modulation of immune defenses within the intestine, and demonstrates that food preference, chemotaxis, development and immune regulation in the nematode *Caenorhabditis elegans* are co-regulated processes that function together to ensure organismal survival. These findings demonstrate how simplistic model organisms can be utilized to tease apart important biological systems that have direct relevance to human health. The mechanism of immune regulation that I have described contributes to a growing body of evidence that suggests the nervous system plays a vital role in the maintenance of immune homeostasis.

Appendix I: The nuclear hormone receptor NHR-86 controls anti-pathogen responses in *C. elegans*

Attributions

The work presented in Appendix I is the result of a collaborative effort among all authors of the publication listed below:

Peterson, N., Cheesman, H., Liu, P., Anderson, S., Foster, K., Chhaya, R., Perrat, P., Thekkiniath, J., Yang, Q., Haynes, C., Pukkila-Worley, R. (2019). The nuclear hormone receptor NHR-86 controls anti-pathogen responses in *C. elegans*. PLoS genetics 15(1), e1007935.

I was responsible for performing initial and follow-up RNAi screens, during which I knocked down 1032 transcription factors in *irg-4*::GFP reporter animals in search for immune regulators of *irg-4*. After preforming multiple rounds of screening, and validating potential hits, we ultimately identified NHR-86 as a transcriptional regulator of genes required for pathogen defense in *C. elegans*

The resulting characterization of NHR-86 and data analysis that followed the initial discovery was performed collaboratively by Nicholas Peterson, Hilary Cheesman, Pengpeng Liu, Sarah Anderson, Richa Chhaya, Paula Perrat, Jose Thekkiniath, and Qiyuan Yang.

Abstract

Nuclear hormone receptors (NHRs) are ligand-gated transcription factors that control adaptive host responses following recognition of specific endogenous or exogenous ligands. Although NHRs have expanded dramatically in *C. elegans* compared to other metazoans, the biological function of only a few of these genes has been characterized in detail. Here, we demonstrate that an NHR can activate an anti-pathogen transcriptional program. Using genetic epistasis experiments, transcriptome profiling analyses and chromatin immunoprecipitation-sequencing, we show that, in the presence of an immunostimulatory small molecule, NHR-86 binds to the promoters of immune effectors to activate their transcription. NHR-86 is not required for resistance to the bacterial pathogen *Pseudomonas aeruginosa* at baseline, but activation of NHR-86 by this compound drives a transcriptional program that provides protection against this pathogen. Interestingly, NHR-86 targets immune effectors whose basal regulation requires the canonical p38 MAPK PMK-1 immune pathway. However, NHR-86 functions independently of PMK-1 and modulates the transcription of these infection response genes directly. These findings characterize a new transcriptional regulator in *C. elegans* that can induce a protective host response towards a bacterial pathogen.

Introduction

Nuclear hormone receptors (NHRs) are transcription factors that regulate a number of key biological processes following recognition of specific exogenous or endogenous ligands. Interestingly, the genomes of *Caenorhabditis* species contain a large number of

NHRs compared to other metazoans (Sluder et al., 1999). 284 NHRs are present in *C. elegans*, whereas *Drosophila* and humans have only 21 and 48, respectively (Taubert et al., 2011). The marked expansion of NHRs suggests that these proteins play particularly important roles in nematode physiology (Arda et al., 2010; Taubert et al., 2011); however, only a very small minority of *C. elegans* NHRs have been characterized in detail (Taubert et al., 2011). Like other metazoans, *C. elegans* rely on inducible host defense mechanisms during infection with bacterial pathogens (Cohen & Troemel, 2015; Ewbank & Pujol, 2016; Peterson & Pukkila-Worley, 2018; Pukkila-Worley & Ausubel, 2012b). The mechanisms that engage these immune defenses are not completely understood. Considering their roles as intracellular sensors of specific ligands, we hypothesized that NHRs function in innate immune activation in *C. elegans*. However, forward genetic screens did not previously identify an NHR that is necessary for pathogen resistance (D. H. Kim et al., 2002; Shivers et al., 2010). We, therefore, designed a genetic screen to determine if an NHR could activate protective immune defenses in *C. elegans*.

Utilizing a potent immunostimulatory small molecule as a chemical probe, we identified NHR-86 and showed that it drives a transcriptional response that protects *C. elegans* from infection with the bacterial pathogen *Pseudomonas aeruginosa*. NHR-86 is a homolog of mammalian hepatocyte nuclear factor 4 (HNF4), an NHR that has been implicated in the pathogenesis of inflammatory bowel disease (Ahn et al., 2008; Consortium et al., 2009; Sommeren et al., 2010). We show that, in the presence of an immunostimulatory small molecule, NHR-86 induces innate immune defenses by binding to the promoters of immune effectors, in a manner that does not require the canonical p38

MAPK PMK-1 pathway. In this context, PMK-1 sets the basal expression of innate immune response genes, but is dispensable for their induction by NHR-86. These data demonstrate a new mechanism by which immune defenses are engaged to protect the worm and raise the possibility that the expansion of the NHR family in *C. elegans* may have been fueled, at least in part, by the roles of these proteins in the activation of host defense responses.

Results

An RNAi screen identifies a role for the nuclear hormone receptor nhr-86 in the induction of *C. elegans* immune effectors

To determine if an NHR can induce protective immune responses, 258 of the 284 NHR genes in the *C. elegans* genome were screened by RNAi using the *C. elegans Pirg-4*(F08G5.6)::*GFP* transcriptional immune reporter and the immunostimulatory xenobiotic R24 (MacNeil et al., 2015). R24 (also referred to as RPW-24) was originally identified in a screen of 37,214 small molecules for new anti-infective compounds(Moy et al., 2009). This molecule robustly activates innate immune defenses and protects nematodes infected with bacterial pathogens (Cheesman et al., 2016; Peterson & Pukkila-Worley, 2018; Pukkila-Worley et al., 2012, 2014). For this screen, the *Pirg-4*::*GFP* transcriptional reporter was chosen as a convenient readout of immune activation. IRG-4 (infection response gene-4) contains a CUB-like domain, a group of secreted proteins that are postulated to play a role in host defense (Troemel et al., 2006). Basal levels of *irg-*

4 transcription are controlled by the p38 MAPK PMK-1 pathway (Troemel et al., 2006). This gene is induced during infection by multiple bacterial pathogens, including *P. aeruginosa,* and by the small molecule R24 (Bolz et al., 2010; Cheesman et al., 2016; Engelmann et al., 2011; S.-H. Lee et al., 2013; Pukkila-Worley et al., 2012, 2014; Troemel et al., 2006; Wong et al., 2007). RNAi-mediated knockdown of ten NHRs partially affected the R24-mediated induction of *Pirg-4*::*GFP* by R24 (S1 Table), but only one NHR (*nhr-86*) completely abrogated the upregulation of this immune reporter (Figure 1A).
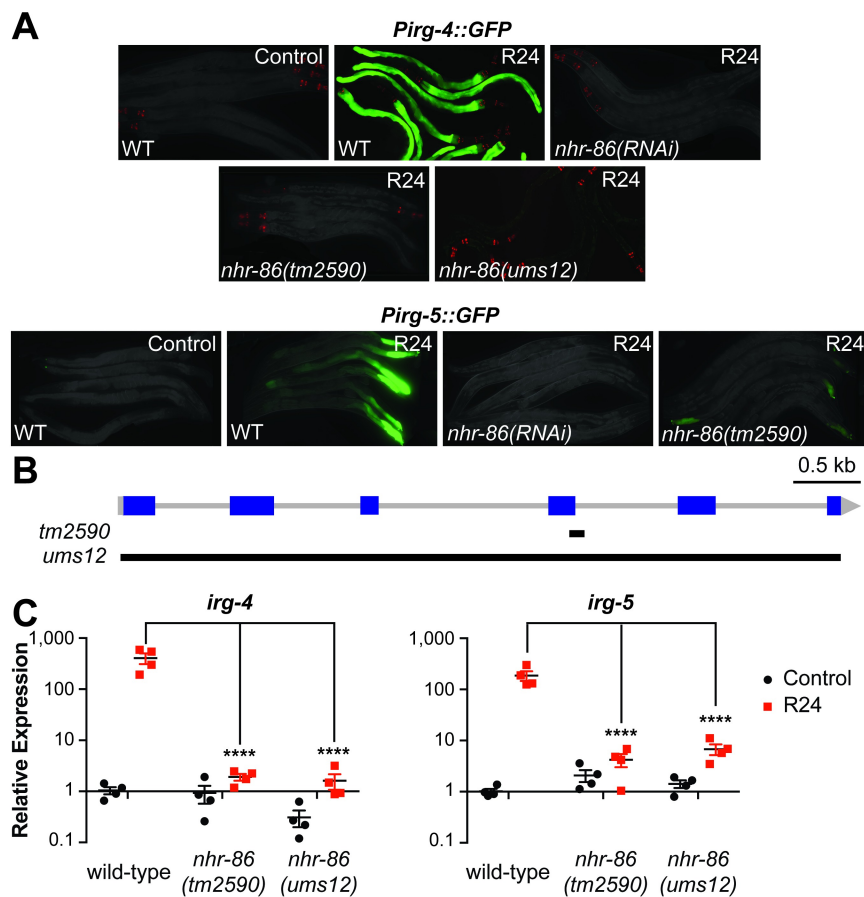
Figure 1. An RNAi screen identifies a role for the nuclear hormone receptor *nhr-86* in the induction of *C. elegans* immune effectors. (A) *C. elegans* carrying either the *Pirg-4*(F08G5.6)::*GFP* or the *Pirg-5*(F35E12.5)::*GFP* immune reporter of the indicated genotypes were transferred at the L4 stage to media supplemented with either R24 or the solvent control (1% DMSO) for approximately 18 hours. Red pharyngeal expression is the *Pmyo-2*::*mCherry* co-injection marker, which confirms the presence of the *Pirg-4*::*GFP* transgene. Presence of the *Pirg-5*::*GFP* transgene was confirmed by assaying for the Rol phenotype. Photographs were acquired using the same imaging conditions for each immune reporter. **(B)** Model of the *nhr-86* gene. Blue squares are exons. Black lines show the locations of the deletions in each of the *nhr-86* mutants. **(C)** The expression of the *C. elegans* immune effector genes *irg-4*, *irg-5* and *irg-6* (C32H11.1) were analyzed by qRT-PCR in wild-type animals and in two different *nhr-86* loss-of-function mutants (*tm2590* and *ums12*), each exposed to either R24 or control for approximately 18 hours. Data for *irg-6* is shown in S1B Fig. Data are the average of four independent replicates, each normalized to a control gene with error bars representing SEM. Data are presented as the value relative to the average expression from all replicates of the indicated gene in the baseline condition (wild-type animals exposed to control). The difference in induction of *irg-4*, *irg-5* and *irg-6* by R24 in wild-type animals compared to each of the two *nhr-86* mutant strains is significant (**** $p<0.0001$ by 2-way ANOVA with Bonferroni multiple comparisons test).

We confirmed the results of the *nhr-86(RNAi)* experiment using several approaches. The previously characterized null allele *nhr-86(tm2590)*, which contains a 172 bp deletion that removes 33 bp in exon 4 of *nhr-86*, suppressed *Pirg-4*::*GFP* induct(Arda et al., 2010)1A and 1C) (Arda et al., 2010). CRISPR-Cas9 was used to generate a clean deletion of *nhr-86 [nhr-86(ums12)]* (Figure 1B). *ums12* is a 5.5 kb deletion that removes nearly all of the *nhr-86* coding region, which caused a marked reduction in the *nhr-86* transcript (S1A Figure). The *nhr-86(ums12)* mutation fully suppressed the induction of *Pirg-4*::*GFP* by R24 (Figure 1A and 1C).

In addition to *irg-4*, *nhr-86* is required for the R24-dependent transcriptional upregulation of two additional immune effectors that contain CUB-like domains, *irg-5* (F35E12.5) and *irg-6* (C32H11.1) (Figures 1 and S1B). Like *irg-4*, *irg-5* and *irg-6* are induced by several different bacterial pathogens, require the p38 MAPK PMK-1 pathway

for their basal transcriptional levels, and are induced in accordance with the virulence potential of the pathogen (Bolz et al., 2010; Engelmann et al., 2011; Gravato-Nobre et al., 2005; S.-H. Lee et al., 2013; Pukkila-Worley et al., 2014; Troemel et al., 2006; Wong et al., 2007). R24-mediated induction of the *Pirg-5::GFP* transgene was abrogated by *nhr-86(RNAi)* and in the *nhr-86(tm2590)* background (Figure 1A). In addition, qRT-PCR of *irg-5* and *irg-6* showed that *nhr-86* loss-of-function mutations suppress induction by R24 (Figures 1C and S1B).

Interestingly, RNAi-mediated knockdown of *irg-4* renders worms hyper-susceptible to killing by *P. aeruginosa* (Nandakumar & Tan, 2008; Shapira et al., 2006). Importantly, *irg-4* knockdown does not shorten the lifespan of nematodes growing on *E. coli* OP50, the normal laboratory food source, nor does its knockdown cause susceptibility to other stressors (Nandakumar & Tan, 2008; Shapira et al., 2006). We confirmed these observations and also found that *irg-5(RNAi)* and *irg-6(RNAi)* animals are more susceptible to killing by *P. aeruginosa* (S1C Figure). As with *irg-4(RNAi)*, knockdown of *irg-5* or *irg-6* did not shorten the lifespan of *C. elegans* growing on *E. coli* OP50 (S1D Figure). Thus, *nhr-86* drives the induction of at least three innate immune effectors that confer resistance to *P. aeruginosa* infection.

nhr-86 activates the transcription of innate immune response genes

To define the genes that are dependent on *nhr-86* for their transcription, we performed mRNA-sequencing. We compared the mRNA expression profiles of wild-type animals and two different *nhr-86* loss-of-function alleles (*tm2590* and *ums12*), each

exposed to the immunostimulatory molecule R24 or mock treatment. Exposure to R24 caused the induction of 391 genes, which (as in previous studies) were enriched for innate immune response and xenobiotic detoxification genes (Cheesman et al., 2016; Pukkila-Worley et al., 2012, 2014). The upregulation of 147 of these genes in the *nhr-86*(*tm2590)* mutants and 205 genes in the *nhr-86(ums12)* mutants were significantly attenuated (Figure 2A). Importantly, the mRNA expression patterns of both *nhr-86* loss-of-function mutants were tightly correlated (Figure 2B) with 142 misregulated genes in common between these two datasets (S2 Table). Analysis of these 142 *nhr-86*-dependent genes revealed a significant enrichment of innate immune genes and those involved in the defense response to bacterial pathogens (Figure 2A and 2C). Included among these *nhr-86*-dependent genes are the representative immune effectors *irg-4*, *irg-5*, *irg-6*, *mul-1*(F49F1.6) and *drd-50*(F49F1.1) (Fig 2A). *mul-1* and *drd-50* are induced during infection with multiple bacterial pathogens, including *P. aeruginosa* (Pukkila-Worley:2014,Troemel:2006,Wong:2007,Bolz:2010,Engelmann:2011,Lee:2013,Gravato-Nobre:2005)
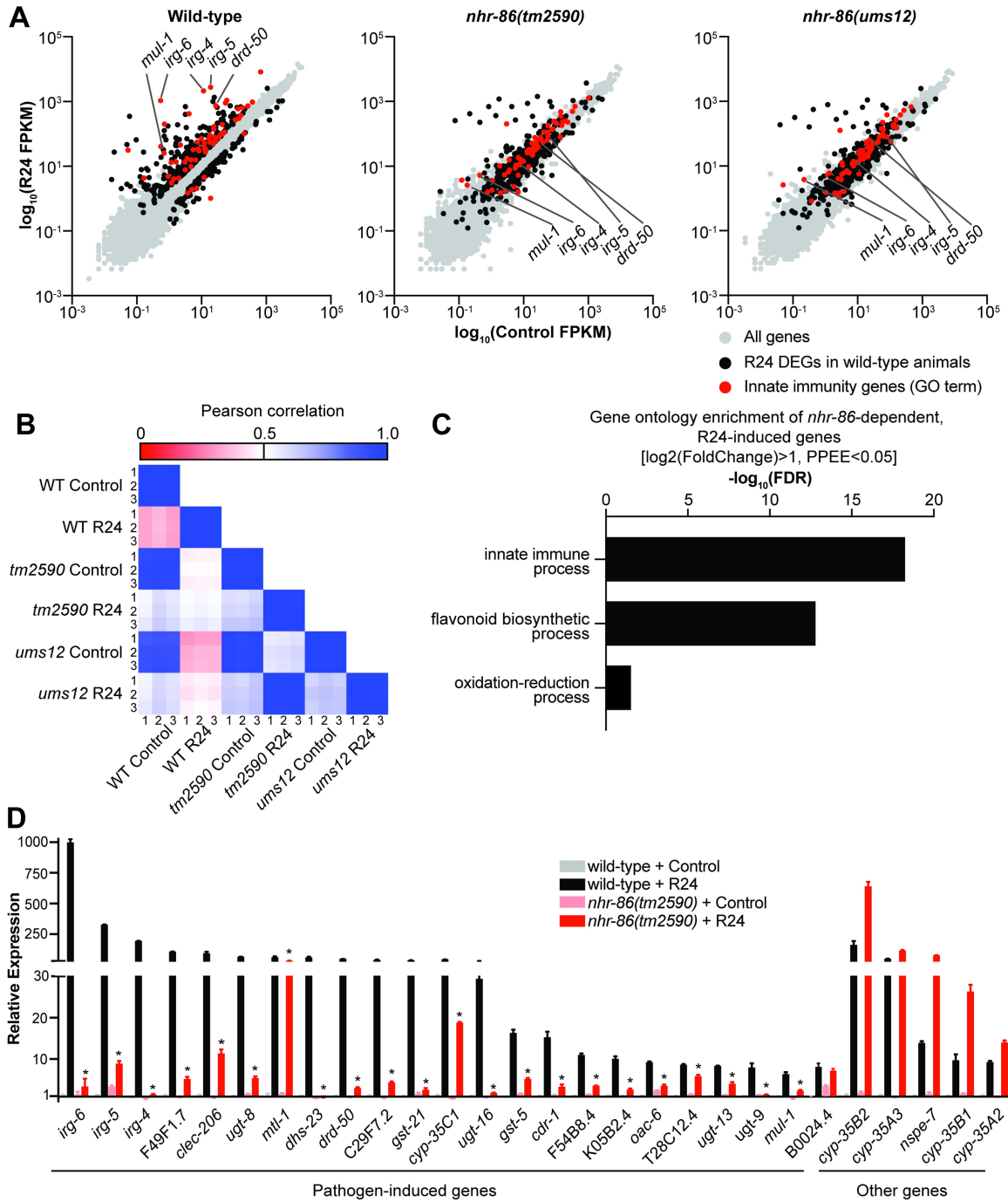
Figure 2. *nhr-86* activates the transcription of innate immune response genes. (A) All data from the mRNA-seq experiment are presented on scatter plots. Genes that were differentially regulated upon R24 treatment in wild-type animals are shown in black (Fold change> 2, PPEE<0.05). These same genes are also highlighted in black in the *nhr-86(tm2590)* and *nhr-86(ums12)* scatter plots. Genes involved in innate immunity by Gene Ontology (GO) term are highlighted in red. **(B)** Pearson correlation coefficients are

presented for all samples in the mRNA-seq experiment. **(C)** Gene ontology enrichment of the *nhr-86*-dependent, R24-induced genes identified in the mRNA-seq experiment are shown. **(D)** Results of NanoString nCounter gene expression analysis for 118 *C. elegans* genes performed on wild-type and *nhr-86(tm2590)* animals exposed to either R24 or control. The 28 genes that were induced 5-fold or greater in wild-type animals by R24 are presented. Data are the average of three replicates, each of which was normalized to three control genes, with error bars representing standard deviation and are presented as the value relative to the average expression from the replicates of the indicated gene in the baseline condition (wild-type animals exposed to control). * p<0.05 by student's t-test for the comparison of the R24-induced conditions.

To confirm the results of our mRNA-seq data, we used a NanoString codeset to examine the expression of 118 innate immune and stress response genes in biological replicate RNA samples from wild-type and *nhr-86(tm2590)* animals (Figure 2D). From the NanoString codeset, we identified 28 genes induced by R24, 23 of which were pathogen-response genes. Of the 23 pathogen-response genes, we identified 22 that are dependent on *nhr-86* for their induction. The NanoString experiment also confirmed the observation in the mRNA-seq experiment that *nhr-86* is not required for the induction of all R24-induced genes (Figure 2A and 2D). Interestingly, many of these genes that are upregulated by R24 in a manner independent of *nhr-86* are cytochrome P450s, which are involved in the detoxification of xenobiotics (Figure 2D and S2 Table). Thus, *nhr-86* is required for the upregulation of only a specific subset of the R24-induced genes, a group that is strongly enriched for innate immune effectors (Figure 2C).

Interestingly, examination of the mRNA-seq profiles of *C. elegans* that were not exposed to compound (*i.e.*, normal growth conditions or basal expression) revealed that the expression of 302 genes were significantly lower in the *nhr-86* loss-of-function mutants compared to wild-type animals (>2-fold change, PPEE<0.05) and only 11 of these genes were differentially regulated more than 4-fold (PPEE<0.05). Only 6 of these genes were

among the 142 genes that required *nhr-86* for their induction by R24. Comparison of the basal expression of *irg-4*, *irg-5* and *irg-6* in the two *nhr-86* loss-of-function alleles with wild-type animals by qRT-PCR confirmed this observation (Figure 1C and S1B Figure). Thus, while *nhr-86* is necessary for the transcriptional induction of genes and innate immune effectors in particular, it is largely dispensable for their basal regulation.

NHR-86 binds to the promoters of innate immune genes to drive their transcription

To determine the direct targets of NHR-86 during R24 exposure, we performed chromatin immunoprecipitation-sequencing (ChIP-seq). Of the 142 genes that are induced by R24 in an *nhr-86*-dependent manner, NHR-86 bound to the promoters of 32 of these genes following treatment with R24 compared to control (Figure 3A and S3 Table). All but one of these 32 genes are induced during infection with at least one bacterial pathogen, including 14 genes that are upregulated during infection with *P. aeruginosa* (S3 Table). Among the immune effectors whose transcription is directly regulated by NHR-86 are *irg-4* (Figure 3B), *irg-5* (Figure 3C), *mul-1* (Figure 3D), *drd-50* (Figure 3E) and *irg-6* (S3 Table). The ChIP-seq experiment was performed with a strain containing a GFP-tagged NHR-86 protein (NHR-86::GFP) that has been previously characterized (Arda et al., 2010). The induction of *irg-4* by R24 was restored in *nhr-86(tm2590)* mutants, which contained this NHR-86::GFP construct (S2A Figure).
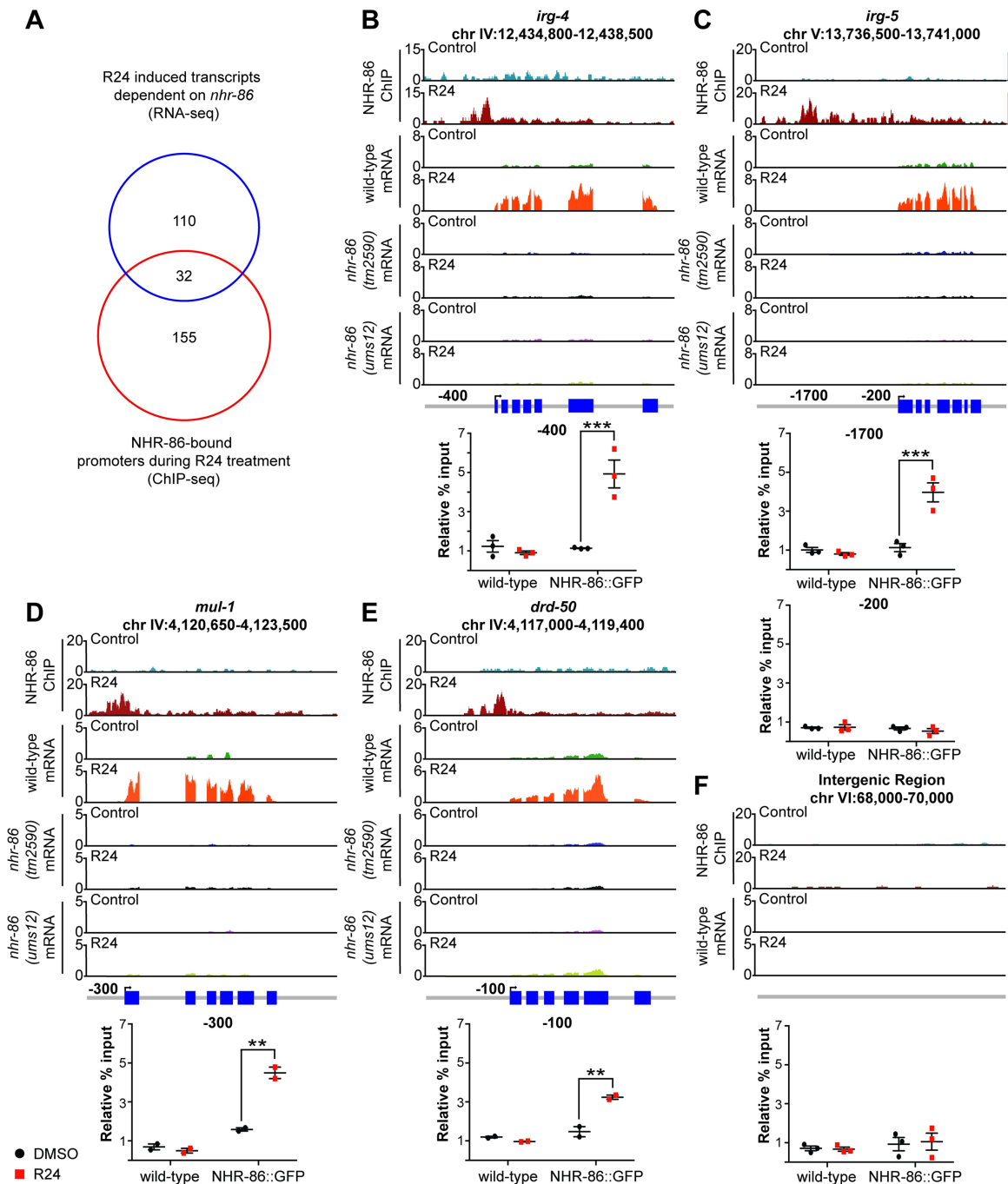
Figure 3. NHR-86 binds to the promoters of innate immune genes to drive their transcription. (A) Venn diagram showing the number of *nhr-86*-dependent, R24-induced genes in the mRNA-seq experiment, the genes whose promoters were bound by NHR-86 following R24 treatment in the ChIP-seq experiment, and the overlap between these datasets. The overlap between these datasets is significantly more than is expected by chance alone (1.1 gene overlap expected by chance, hypergeometric p-value = 2x10^{-39}). ChIP-seq profiles, mRNA-seq profiles and confirmatory ChIP-PCR are presented for the representative immune effectors *irg-*

4 **(B),** *irg-5* **(C),** *mul-1* (F49F1.6) **(D)** and *drd-50* (F49F1.1) **(E)** in animals of the indicated genotype exposed to R24 or the control. The y-axis is the number of reads (log$_2$). A gene model shows the location of the exons (blue) of the indicated genes. ChIP was performed with an anti-GFP antibody in *C. elegans* wild-type and transgenic NHR-86::GFP animals. Final set of peaks were called if the difference in intensity values of samples had a significance level of p-value < 0.025 (see S3 Table) for the indicated comparison. In the ChIP-PCR data, the percent input for each condition was normalized to the abundance of a random intergenic region of chromosome four. ** $p<0.01$ and *** $p<0.001$ by 2-way ANOVA with Bonferroni multiple comparisons test for the indicated comparison. A region 200 bp upstream of *irg-5* **(C)** and a random intergenic region on chromosome six **(F)** were not enriched by control or R24 treatment. Each data point in the ChIP-qPCR data is from an independent biological replicate.

ChIP followed by qPCR (ChIP-qPCR) was used to confirm that NHR-86 binds to the promoters of innate immune effectors following R24 treatment. Promoter regions associated with *irg-4* (Figure 3B), *irg-5* (Figure 3C), *mul-1* (Figure 3D) and *drd-50* (Figure 3E) were significantly enriched following R24 treatment, but not in samples exposed to the solvent control. In addition, these promoter regions were not enriched in either control or R24-exposed wild-type animals, which do not express NHR-86::GFP that was used to immunoprecipitate promoter fragments. Binding of NHR-86 to the promoters of immune response genes upon R24 treatment was associated with a corresponding increase in mRNA transcript levels of these genes, which was entirely abrogated in both *nhr-86* loss-of-function mutants (Figure 3B–3E). Importantly, a control region within the *irg-5* promoter (Figure 3C) and a random intergenic region on chromosome VI (Figure 3F) were not enriched in the ChIP-qPCR or ChIP-seq experiments. In addition, 110 genes were induced by R24 in an *nhr-86*-dependent manner, but NHR-86 did not bind to their promoters. Of note, NHR-86 is expressed in the nuclei of *C. elegans* intestinal epithelial cells (Arda et al., 2010) and promotes the induction of the innate immune effectors *irg-*

4::*GFP* and *irg-5*::*GFP* in the intestine (Figure 1A), the tissue that directly interfaces with ingested pathogens.

A motif analysis was performed on the promoters bound by NHR-86::GFP to identify putative regulatory sequences. A single 15 bp sequence was strongly enriched in these promoters (E-value: 1.7e-003, S2C Figure). 15 of the 32 genes whose transcription were directly regulated by NHR-86 in the presence of R24 contain this 15 bp element in their promoters, including *irg-4*, *irg-5* and *mul-1* (S3 Table). However, only 3 of 172 genes that are induced by R24 independent of NHR-86 contain this 15 bp element. These data suggest that this 15 bp sequence may be a potential binding site for NHR-86.

Together, the mRNA-seq and ChIP-seq data demonstrate that, in the presence of an immunostimulatory molecule, NHR-86 engages the promoters of innate immune effector genes to drive their transcription. Under normal growth conditions, *nhr-86* does not bind to the promoters of immune effectors (*e.g.*, *irg-4*, *irg-5*, *mul-1* and *drd-50*) and does not affect their basal expression. These data are the first demonstration of direct immune effector regulation by a nuclear hormone receptor in *C. elegans*.

The immune response induced by *nhr-86* protect a *C. elegans* from P. aeruginosa infection

To determine if *nhr-86* induces a physiologically relevant transcriptional response, we compared the susceptibility of the *nhr-86* loss-of-function mutants to *P. aeruginosa* infection following exposure to R24. R24 protects wild-type *C. elegans* during *P. aeruginosa* infection (Cheesman et al., 2016; Pukkila-Worley et al.,

2012, 2014). Consistent with the key role of *nhr-86* in driving the induction of innate immune defenses, *nhr-86* loss-of-function mutants (*tm2590* and *ums12*) significantly suppressed the pathogen-resistance phenotype of R24-exposed wild-type worms (Figure 4A). Together, these data demonstrate that the defense response induced by *nhr-86* promotes host resistance to bacterial infection.
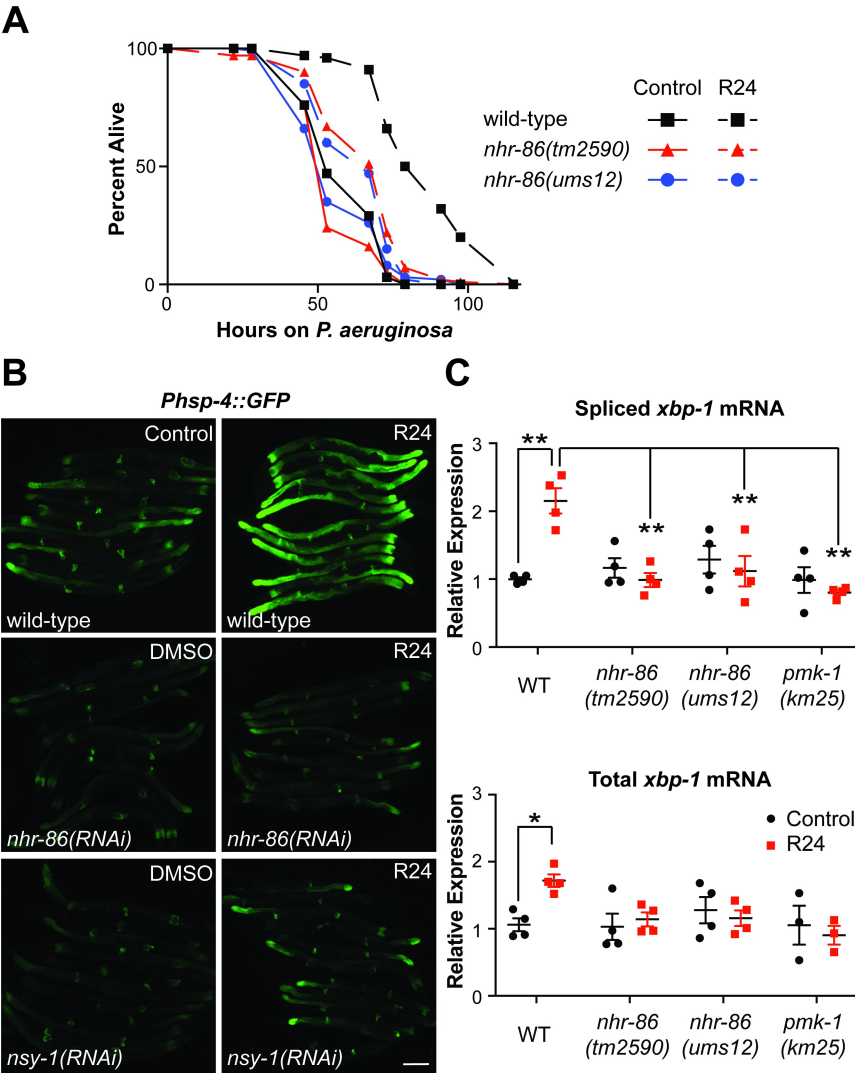
Figure 4. The immune response induced by *nhr-86* protects *C. elegans* from *P. aeruginosa* infection.
(A) *P. aeruginosa* infection assays of *C. elegans* wild-type, *nhr-86(tm2590)* and *nhr-86(ums12)* treated with R24 or 1% DMSO (control) are shown. The difference in susceptibility to *P. aeruginosa* between R24-exposed wild-type and each of the mutant animals is significant ($p<0.001$ by the log-rank test). Data are representative of three trials. Sample sizes, mean lifespan, % lifespan extension conferred by R24 treatment in each background and p values for all trials are shown in S4A Table. Significance was determined using Kaplan-Meier survival curves and log-rank tests. **(B)** *C. elegans* carrying the *Phsp-4::GFP* reporter were exposed to the indicated RNAi bacteria and transferred at the L4 stage to media supplemented with either R24 or control for approximately 18 hours. Scale bar equals 100 μm. **(C)** qRT-PCR was used to measure the spliced (active) and total *xbp-1* mRNA in animals of the indicated genotype exposed to R24 or control. Comparisons were calculated using 2-way ANOVA with Bonferroni multiple comparisons test and * $p<0.05$ and ** $p<0.0001$. Data are the average of four independent replicates, each normalized to a control gene with error bars representing SEM. Data are presented as the value relative to the average expression from all replicates of the indicated gene in the baseline condition (wild-type animals exposed to control).

An alternate method of examining the physiological relevance of immune effector induction in *C. elegans* involves studying the effect of induced transcriptional responses on stress in the endoplasmic reticulum (ER). The induction of host immune effectors in *C. elegans* requires compensatory activation of the unfolded protein response (UPR) in the ER, presumably to handle the increase in proteins trafficking through this organelle (Richardson et al., 2010, 2011). Accordingly, R24 exposure caused the induction of *Phsp-4::GFP*, a transcriptional reporter for the BiP/GRP78 homolog in *C. elegans*, which indicates UPR activation (Figure 4B). *hsp-4* transcription is regulated by the transcription factor XBP-1, which is activated by the ER-transmembrane protein IRE-1 when unfolded proteins accumulate in the ER. IRE-1 has RNase activity, which upon activation, cleaves *xbp-1* mRNA to change its reading frame and encode the active XBP-1 protein (Ron & Walter, 2007). We found that exposure to R24 increased the active, spliced form of *xbp-1* (Figure 4C). Total *xbp-1* mRNA was also increased following R24 treatment (Figure 4C). Interestingly, knockdown of *nhr-86* suppressed *Phsp-4::GFP* induction (Figure 4B) and the accumulation of active *xbp-1* (Figure 4C) following exposure to the

xenobiotic R24. In addition, animals deficient in *nsy-1*, the MAPKKK upstream of the p38 MAPK *pmk-1* (Figure 4B), and *pmk-1* (S3A Figure), failed to induce the *Phsp-4*::*GFP* following exposure to R24. *pmk-1(km25)* mutants abrogated the cleaving of *xbp-1* into its active form (Figure 4C). Thus, R24-mediated immune induction activates the UPR, in a manner dependent on *nhr-86* and the p38 MAP *pmk-1* pathway.

We considered the possibility that R24 is a direct poison of the ER. However, tunicamycin, a potent inducer of ER stress and the UPR, did not activate the immune reporter *Pirg-4*::*GFP* (S3B Figure). In addition, RNAi-mediated knockdown of *nhr-86* did not suppress *Phsp-4*::*GFP* induction by tunicamycin (S3C Figure). Thus, ER stress itself does not lead to the induction of *nhr-86*-dependent innate immune responses, but rather occurs as a consequence of mobilizing this protective host response. These data are consistent with prior reports, which demonstrate that activation of the p38 MAPK *pmk-1* pathway is not dependent on IRE-1/XBP-1 (Richardson et al., 2010, 2011). Together, these data demonstrate that the immune response induced by *nhr-86* following exposure to R24 is a physiologically relevant source of ER stress and provide further support for the conclusion that *nhr-86* activates a pathogen-defense response involving secreted proteins.

In the absence of R24, *C. elegans* nhr-86 mutants are not more susceptible to P. aeruginosa infection than wild-type animals (Figure 4A). In addition, the induction of the innate immune effectors irg-5, irg-6 and irg-1 during P. aeruginosa infection is not attenuated in the nhr-86(ums12) mutant; however, the induction of irg-4 is significantly lower (S4 Figure). Given the marked expansion of the NHR family in *C. elegans*, NHRs, or potentially another mechanism, may function redundantly with NHR-86 to activate host

defense genes during P. aeruginosa infection. It is also possible that P. aeruginosa does not produce the ligand sensed by NHR-86.

nhr-86 induces innate immune defenses independent of the p38 MAPK *pmk-1*

The immunostimulatory molecule R24 upregulates innate immune effectors whose basal expression requires the p38 MAPK *pmk-*1 (Pukkila-Worley et al., 2012), a key signaling mediator in a pathway that is critically important for host defense against bacterial pathogens (D. H. Kim et al., 2002; Troemel et al., 2006). To determine if *nhr-86* and *pmk-1* function in the same or distinct pathways in the transcriptional modulation of innate immune effector genes, we compared gene expression (Figures 5A and S5A) and pathogen resistance (Figure 5B) phenotypes of the *pmk-1(km25)* and *nhr-86(tm2590)* single mutants with the *pmk-1(km25); nhr-86(tm2590)* double mutant. We previously observed that R24 can extend the lifespan of *pmk-1(km25)* mutant animals that are infected with *P. aeruginosa* [(Pukkila-Worley et al., 2012) and Figure 5B]. In addition, we found that *pmk-1* is dispensable for the induction of a group of innate immune effectors, including *irg-4*, *irg-5*, *mul-1* and *drd-50* [(Pukkila-Worley et al., 2012), see also Figures 5A and S5A]. However, because the basal level of expression of these four effectors is decreased in the *pmk-1(km25)* mutant, the absolute level of immune effector expression following exposure to R24 is markedly lower compared to controls (Figures 5A and S5A). The deficiency in the basal regulation of immune effectors in the *pmk-1(km25)* mutant contributes to the enhanced susceptibility of this mutant to *P. aeruginosa* infection in both naive and R24-treated animals (D. H. Kim et

al., 2002; Troemel et al., 2006) (Figure 5B). These data indicate that R24 drives the induction of a protective immune response independent of *pmk-1*. Consistent with this observation, exposure to R24 does not cause an increase in the percentage of active (phosphorylated) PMK-1 relative to total PMK-1 in wild-type or *nhr-86(ums12)* animals (Figure 5C and 5D).

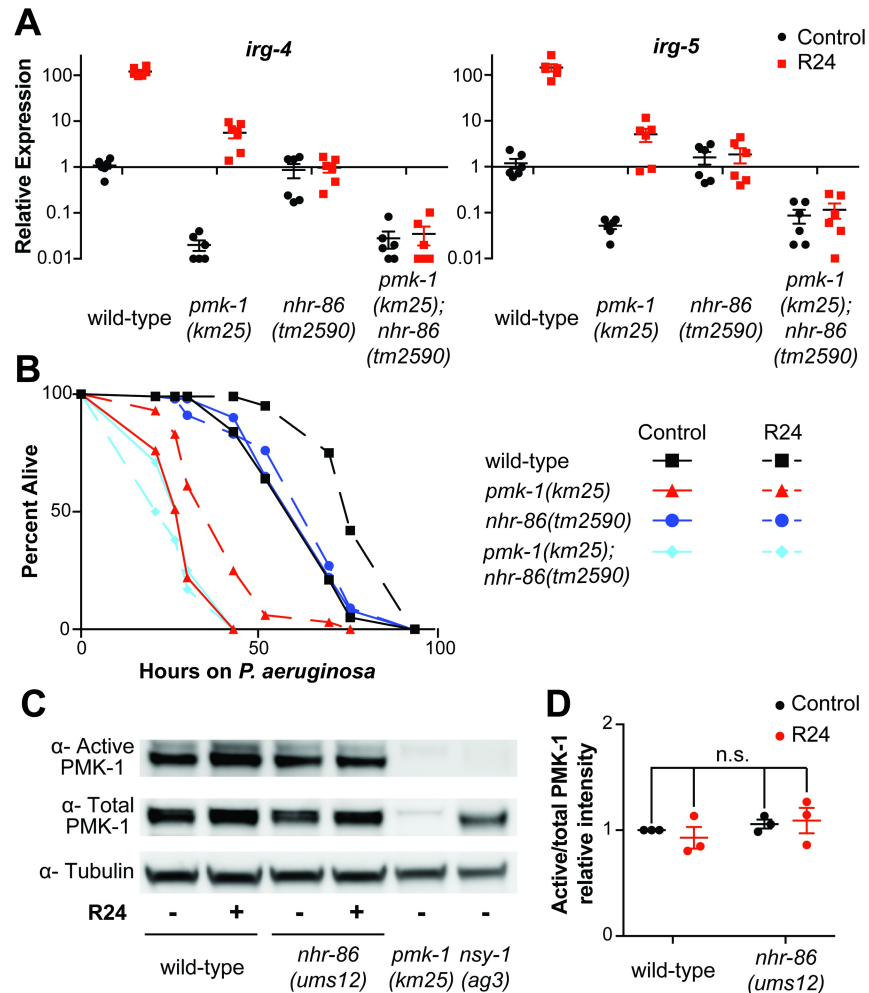**Figure 5. *nhr-86* induces innate immune defenses independent of the p38 MAPK *pmk-1*.**
(**A**) The expression of the *C. elegans* immune effector genes *irg-4*, *irg-5*, *drd-50*, *mul-1* and *irg-6* were analyzed by qRT-PCR in wild-type animals, *pmk-1(km25)*, *nhr-86(tm2590)*, and *pmk-1(km25); nhr-86(tm2590)* double mutants, each exposed to either R24 or the control for approximately 18 hours. Data

for *drd-50*, *mul-1* and *irg-6* are shown in S5A Figure. Data are the average of six independent replicates, each normalized to a control gene with error bars representing SEM. Data are presented as the value relative to the average expression from all replicates of the indicated gene in the baseline condition (wild-type animals exposed to control). The difference in induction of *irg-4*, *irg-5*, *drd-50*, *mul-1* and *irg-6* by R24 in wild-type animals compared to each of the mutant strains is significant ($p<0.0001$ by 2-way ANOVA with Bonferroni multiple comparisons test). There is no significant difference between the expression of these genes in *pmk-1(km25)* animals exposed to control compared to either condition in the *pmk-1(km25); nhr-86(tm2590)*. **(B)** *P. aeruginosa* infection assays of *C. elegans* wild-type, *pmk-1(km25)*, *nhr-86(tm2590)*, and *pmk-1(km25); nhr-86(tm2590)*, each exposed to control or R24, are shown. The difference in susceptibility to *P. aeruginosa* between control and R24-exposed wild-type and *pmk-1(km25)* animals is significant ($p<0.001$). There is no significant difference between control and R24-exposed *nhr-86(tm2590)* and *pmk-1(km25); nhr-86(tm2590)* animals. Data are representative of three trials. Sample sizes, mean lifespan, % lifespan extension conferred by R24 treatment in each background and p values for all trials are shown in S4B Table. Significance was determined using Kaplan-Meier survival curves and log-rank tests. **(C)** Immunoblot analysis of lysates from L4 stage animals of the indicated genotype using antibodies that recognize the doubly phosphorylated TGY motif of PMK-1 (α-Active PMK-1), the total PMK-1 protein (α-Total PMK-1) and tubulin (α-Tubulin). The total PMK-1 antibody detects total, but not active (phosphorylated) PMK-1. **(D)** The relative intensity of active PMK-1 and total PMK-1 was quantified from three biological replicates and is expressed as the average ratio of active to total PMK-1, relative to wild-type control. Error bars report SEM. There is no significant difference (n.s.) between these conditions (2-way ANOVA with Bonferroni multiple comparisons test).

The susceptibility of the *pmk-1(km25); nhr-86(tm2590)* double mutant to *P. aeruginosa* infection in the absence of R24 is identical to the *pmk-1(km25)* mutant, further suggesting that NHR-86 functions in an R24-dependent manner (Figure 5B). Importantly, the *nhr-86(tm2590)* allele suppressed the R24-mediated enhanced longevity in the *pmk-1(km25)* background (Figure 5B). Accordingly, the basal expression of *irg-4*, *irg-5*, *mul-1*, *drd-50* and *irg-6* is reduced in the *pmk-1(km25); nhr-86(tm2590)* double mutant to the same level as the *pmk-1(km25)* mutant (Figures 5A and S5A). Importantly, the R24-mediated induction of these immune effectors in the *pmk-1(km25)* background is blocked by the *nhr-86(tm2590)* mutation (Figures 5A and S5A).

Of note, the induction of at least two cytochrome P450 xenobiotic detoxification genes by R24 is not dependent on either *nhr-86* or *pmk-1* (S5B Figure). These data further

support that *nhr-86* is required for only a specific subset of the R24-induced genes (Figure 2).

In summary, these genetic epistasis experiments support the model that, upon activation, NHR-86 traffics to the promoters of immune effectors to mount a protective immune response in a manner independent of the p38 MAPK *pmk-1* pathway (Figure 6). In this context, a principal role of the p38 MAPK *pmk-1* is to ensure basal resistance to pathogens by controlling the tonic expression of innate immune effectors, such as *irg-4*, *irg-5*, *mul-1* and *drd-50*.
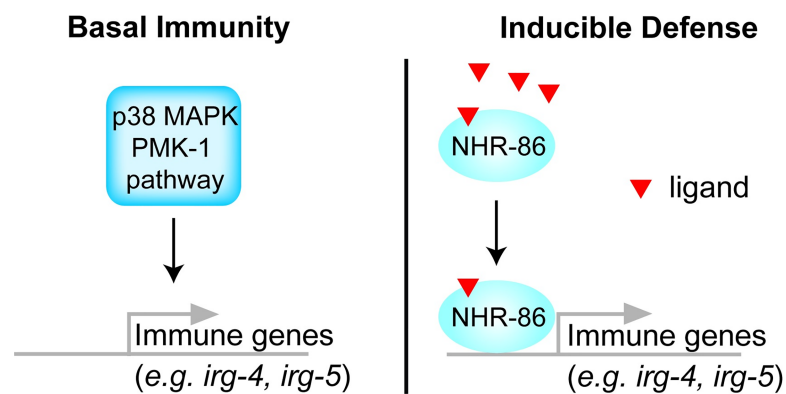
Figure 6. Model of NHR-86-mediated immune regulation in *C. elegans*. The basal expression of immune effectors such as *irg-4*, *irg-5*, *mul-1* and *drd-50* are ensured by p38 MAPK PMK-1. Activated NHR-86 traffics to the promoters of these and other immune effectors to drive their induction and provide protection from bacterial infection.

Discussion

This study extends the known functions of *C. elegans* NHRs to include the activation of anti-pathogen transcriptional responses. Following treatment with an immunostimulatory small molecule, NHR-86 directly activates innate immune effector transcription in a manner that promotes resistance to bacterial infection. ChIP-seq and

mRNA-seq revealed an enrichment for innate immune effectors among the transcriptional targets of NHR-86, including at least three genes, *irg-4*, *irg-5* and *irg-6*, that are each required for normal resistance to *P. aeruginosa* infection. Consistent with this model, the induction of protective immune defenses by NHR-86 occurs independently of the p38 MAPK *pmk-1*. In addition, in the absence of an immunostimulatory molecule, NHR-86 is not required for the basal regulation and is not at the promoters of immune effectors. Arda *et al*. proposed that NHRs, and NHR-86 in particular, organize modular gene regulatory networks to facilitate the rapid coordination of adaptive responses to intracellular ligands (Arda et al., 2010). Our data show that an anti-pathogen transcriptional response is one such adaptive response.

We previously demonstrated that a conserved component of the Mediator transcriptional regulatory complex, MDT-15/MED15, links detoxification and innate immune defenses in *C. elegans* (Pukkila-Worley et al., 2014). The Mediator complex is conserved from yeasts to humans and regulates transcription by physically interacting with both transcriptional regulators and RNA polymerase II (Conaway & Conaway, 2011; Malik & Roeder, 2010). Individual mediator subunits, particularly those like MDT-15, which are in the tail region of the complex, dictate the physical interactions with transcriptional regulators and play important roles in modulating specific transcriptional outputs (Conaway & Conaway, 2011; Malik & Roeder, 2010; Taubert et al., 2006, 2008). Like *nhr-86*, *mdt-15* is required for the induction of immune effectors whose basal expression is dependent on the p38 MAPK PMK-1 pathway (Pukkila-Worley et al., 2014). In addition, MDT-15 functions downstream of the PMK-1 cascade to control the

expression of immune effectors (Pukkila-Worley et al., 2014). Notably, a subset of the immune effectors in *mdt-15*-deficient animals, including *irg-4*, *irg-5*, and *drd-50* have reduced basal levels of expression [as in *pmk-1(km25)* mutants] and cannot be induced by the small molecule R24 (as in *nhr-86* loss-of-function mutants). Importantly, NHR-86 is known to physically interact with MDT-15 (Arda et al., 2010). Thus, we hypothesize that MDT-15 and NHR-86 function together to drive the transcription of immune response genes, such as *irg-4*, *irg-5* and *drd-50*.

The ligand that activates NHR-86 is not known. Indeed, it is possible that R24 or a metabolite derived from this compound is an activating ligand of NHR-86. However, it is important to note that not all R24-induced genes are dependent on *nhr-86* for their upregulation. Alternatively, NHR-86 may detect a host-derived ligand that is associated with the toxic effects of R24 on nematode cells. R24 induces xenobiotic detoxification genes and shortens the lifespan of nematodes growing in standard laboratory conditions (Pukkila-Worley et al., 2012). *C. elegans* activates immune defenses following toxin-mediated disruption of cellular homeostasis (Pukkila-Worley, 2016a). Thus, NHR-86 may function as part of a similar cellular surveillance mechanism, although this is not known. Notably, *nhr-86* loss-of-function mutants are not more susceptible to *P. aeruginosa* infection at baseline. While *nhr-86* is required for the induction of the immune effectors *irg-5* and *irg-6* by the immunostimulatory xenobiotic R24, it is dispensable for their induction during *P. aeruginosa* infection. Thus, it is possible that *P. aeruginosa* infection does not produce a ligand that is sensed by NHR-86 or there are redundant mechanisms engaged to activate *C. elegans* defenses during pseudomonal

infection. In either case, our data demonstrate that a *C. elegans* NHR can drive a protective transcriptional response towards a bacterial pathogen. These findings raise the possibility that NHRs provide a facile and evolutionarily adaptable mechanism to activate protective immune defenses in response to diverse ligands.

Material and Methods

C. elegans and bacterial strains

C. elegans strains were maintained on standard nematode growth media plates with *E. coli* OP50 as a food source, as described (Brenner, 1974). The previously published *C. elegans* strains used in this study were: N2 Bristol, KU25 *pmk-1(km25)*, AU306 *agIs44* [P*irg-4*::GFP::*unc-54-3'UTR;Pmyo-2::mCherry*], AY101 *acIs101* [p*DB09.1(Pirg-5::gfp)*; p*RF4(rol-6(su1006)]* (Bolz et al., 2010), SJ405 *zcIs4 (Phsp-4*::*gfp)*(Calfon et al., 2002), VL491 *nhr-86(tm2590)* (Arda et al., 2010), and VL648 *unc-119(ed3)*; *wwIs22 [Pnhr-86::nhr-86ORF::GFP unc-119(+)]* (Arda et al., 2010)The strains developed in this study were: RPW137 *nhr-86(ums12)*, RPW119 *pmk-1(km25);nhr-86(tm2590)*, RPW99 *nhr-86(tm2590); agIs44*, RPW106 *nhr-86(tm2590); acIs101*, and RPW165 *nhr-86(ums12); agIs44*. *Pseudomonas aeruginosa* strain PA14 was used for all studies (Rahme et al., 1995).

C. elegans strain construction

CRISPR/Cas9 was used to generate *nhr-86(ums12)* as described (Arribere et al., 2014). Target sequences were selected on exons 1 and 6 of *nhr-86*. Forward and reverse oligonucleotides were designed to contain the target sequence and overhangs compatible with *Bsa*I sites in plasmid pPP13, a modified version of pRB1017 (Arribere et al., 2014; J. D. Ward, 2014). Forward and reverse oligonucleotides were annealed and ligated into pPP13 cut with *Bsa*I to create the gRNA plasmids. Plasmids were confirmed by sequencing. A DNA mixture of pDD162 (50 ng/L), the gRNA plasmids (25 ng/L each), pJA58 (50 ng/L) and the ssODN repair template for *dpy-10(cn64)* (20 ng/L) was prepared in injection buffer (20 mM potassium phosphate, 3 mM potassium citrate, 2% PEG, pH 7.5) and injected into N2 worms. Mutations in the *dpy-10* gene were used as a CRISPR co-conversion marker. The F1 progeny were screened for Rol and Dpy phenotypes 3–4 days after injection and then for deletions in the *nhr-86* coding region using PCR. The *nhr-86(ums12)* mutant contains a 5539 bp deletion that spans from 17 bp upstream of the ATG to 30 bp before the stop codon with an insertion of 6 bp at the breakpoint. Primer sequences used for genotyping are listed in S5 Table.

Feeding RNAi screen

A previously described library containing RNAi clones corresponding to 258 of the 284 NHRs in the *C. elegans* genome was used for this study (MacNeil et al., 2015). These

genes were screened for their ability to abrogate the induction of *agIs44* by 70 μM R24, as described (Pukkila-Worley et al., 2014)

C. elegans bacterial infection and other assays

"Slow killing" *P. aeruginosa* infection experiments were performed as previously described (Cheesman et al., 2016; Tan et al., 1999). In all of these assays, the final concentration of DMSO was 1% and 70 μM R24 was used. Wild-type is either N2 or *agIs44*. All pathogenesis and lifespan assays are representative of three biological replicates. Sample sizes, mean lifespan, % lifespan extension conferred by R24 treatment in each background (where applicable) and p values for all trials are shown in S4 Table.

mRNA-seq, NanoString ncounter gene expression analyses and qRT-PCR

Synchronized, L1 stage, hermaphrodites *C. elegans* of the indicated genotypes were grown to the L4/ young adult stage, transferred to assay plates, and incubated at 20°C overnight. 70 μM R24 or solvent control (DMSO, 1% final concentration) assay plates were prepared as described (Cheesman et al., 2016; Pukkila-Worley et al., 2012, 2014). RNA was isolated using TriReagent (Sigma-Aldrich), purified on a column (Qiagen), and analyzed by mRNA-seq using the BGISEQ-500 platform (BGI Americas Corp). mRNA-seq data analysis was performed by BGI Americas Corp. Biological replicate RNA samples were analyzed using NanoString nCounter Gene Expression Analysis (NanoString Technologies) with a "codeset" designed by NanoString that contained probes for 118 *C. elegans* genes. The codeset has been described previously (Cheesman et al., 2016; Pukkila-

Worley et al., 2014). Probe hybridization, data acquisition and analysis were performed according to instructions from NanoString with each RNA sample normalized to the control genes *snb-1*, *ama-1* and *act-1*. For the qRT-PCR studies, RNA was reverse transcribed to cDNA using the RETROscript Kit (Life Technologies) and analyzed using a CFX1000 machine (Bio-Rad). The sequences of primers that were designed for this study are presented in S5 Table. Other primers were previously published (Estes et al., 2010; Richardson et al., 2010; Taubert et al., 2005; Troemel et al., 2006). All values were normalized against the control gene *snb-1*. Fold change was calculated using the Pfaffl method (Pfaffl, 2001).

Immunoblot analyses

C. elegans were prepared as described above to ensure that stage-matched, hermaphrodite animals at the young L4 larval stage were studied in each condition. Protein lysates were prepared as previously described (Pukkila-Worley et al., 2014) and probed with a 1:1000 dilution of an antibody that recognizes the doubly-phosphorylated TGY motif of PMK-1 (Promega Corporation). Monoclonal anti-α-tubulin antibody was used at a dilution of 1:1,000 (Sigma-Aldrich). A polyclonal antibody against the total PMK-1 protein was raised using the peptide DFQKNVAFADEEEDEEKMES (PMK-1 amino acids 358 to 377) in a rabbit (Thermo Scientific Pierce Custom Antibody Services) and used at a dilution of 1:1000. We confirmed that the total PMK-1 antibody detects total, but not active (phosphorylated) PMK-1 (Figure 5C). Horseradish peroxidase (HRP)-conjugated anti-rabbit (Cell Signaling Technology) and anti-mouse IgG secondary

antibodies (Abcam) were diluted 1:10,000 and used to detect the primary antibodies following the addition of ECL reagents (Thermo Fisher Scientific, Inc.), which were visualized using a BioRad ChemiDoc MP Imaging System. The band intensities were quantified using BioRad Image Lab software version 5.2.1, and the ratio of active phosphorylated PMK-1 to total PMK-1 was calculated with all samples normalized to the ratio of wild-type control animals.

ChIP-qPCR, ChIP-seq and bioinformatics

Chromatin immunoprecipitation was performed with a strain containing a GFP-tagged NHR-86 protein (NHR-86::GFP) that has been previously characterized (Arda et al., 2010). *nhr-86* transcript levels are 2.7-fold elevated in the NHR-86::GFP strain compared to wild-type (S2B Figure). ChIP was performed as previously described (Ercan et al., 2007; Amrita M Nargund et al., 2015) with modifications. Briefly, L4 synchronized, hermaphrodite *C. elegans* (wild-type and transgenic NHR-86::GFP animals) were exposed to "slow killing" plates (Tan et al., 1999) containing either DMSO (1%) or 70 μM R24 for approximately 18 hours. Animals were then collected and washed with 4°C M9 and phosphate-buffered saline to remove bacteria. Cross-linking of protein and DNA was performed in 2% formaldehyde for 30 minutes at room temperature. Cross-linking was quenched with 100 mM glycine, animals were washed in M9, resuspended in lysis buffer (50 mM Hepes–KOH pH 7.5, 300 mM NaCl, 1 mM EDTA, 1% (v/v) Triton X-100, 0.1% (w/v) sodium deoxycholate, 0.5% (v/v) N-Lauroylsarcosine, and protease inhibitors) and lysed with a Teflon homogenizer. Lysates were then sonicated using a Bioruptor UCD-200

for 10 cycles (30 s on, 30 s off) to obtain 500–1000 bp DNA fragments. Sonicated lysates (2 mg) were pre-cleared with protein G Dynabeads (Invitrogen), 10% of lysate removed for input, and incubated with 5 µg anti-GFP antibody (Roche) overnight. Immune complexes were collected with protein G Dynabeads, washed, and eluted from beads. Cross-links were reversed at 65°C overnight and DNA fragments were purified with PCR purification columns (Qiagen). qPCR was performed on input and immunoprecipitated samples using primers designed around the transcription start site. All ChIP data are presented as percent input normalized to a random intragenic region on chromosome four. Primer sequences are available in S5 Table.

ChIP-seq was performed by BGI Americas Corp. The raw sequencing data were first clipped for adaptor sequences and then mapped to the *C. elegans* genome (ce10, UC Santa Cruz) by the Burrows-Wheeler Aligner algorithm (BWA MEM, BWA version 0.7.15). The output SAM files were processed and sorted with the Picard tools. The output mapping files (BAM files) were filtered with SAMtools to remove any read that had a mapping quality less than 10 (SAMtools view–b–q 10 input.bam > output.bam). Peaks were determined using MACS version 2.1 with the no-model parameter. The final set of peaks were called if the difference in intensity values of samples had a significance level of p-value < 0.025.

To identify candidate motifs for NHR-86 binding, ChIP peaks that were located in promoter regions of genes were examined using the MEME motif analysis platform [Parameters: minw = 8, maxw = 25, in two modes (zoops & anr), significance threshold (E-value > = 1e-01), http://meme.sdsc.edu]. A background model is used by MEME to

calculate the log likelihood ratio and statistical significance of the motif. We set the following requirements: the most significant motif should exist in 50% of input sequences, and the genes containing the motif should have the largest overlap between ChIP-Seq and RNA-seq datasets. A single 15 bp motif was identified that met these criteria (E-value: 1.7e-003, S2C Figure). 66 sites of 101 input sequences had this motif, including 15 of the 32 genes that overlapped in the ChIP-Seq and RNA-seq datasets.

Microscopy

Nematodes were mounted onto agar pads, paralyzed with 10 mM levamisole (Sigma) and photographed using a Zeiss AXIO Imager Z2 microscope with a Zeiss Axiocam 506mono camera and Zen 2.3 (Zeiss) software.

Statistical analyses

Differences in survival of *C. elegans* in the *P. aeruginosa* pathogenesis assays were determined with the log-rank test using OASIS 2 as previously described (Han et al., 2016). Data from one experiment that is representative of the replicates is shown. Other statistical tests, indicated in the Figure legends, were performed using Prism 7 (GraphPad Software).

Supplemental Figures
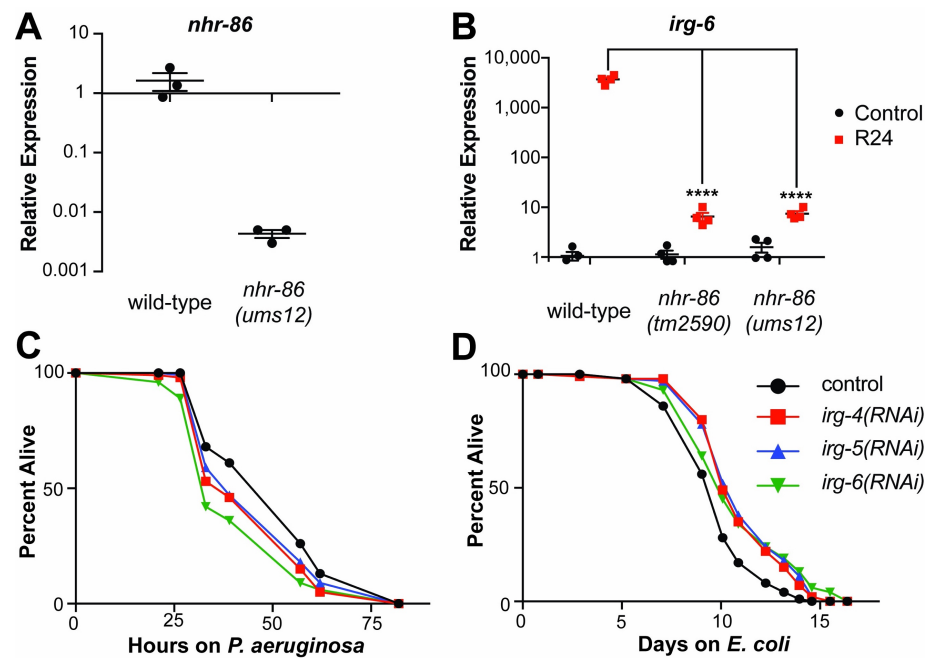
S1 Fig: An RNAi screen identifies a role for the nuclear hormone receptor *nhr-86* in the induction of *C. elegans* immune effectors.
(A) qRT-PCR data of *nhr-86* mRNA in the *nhr-86(ums12)* mutant. **(B)** qRT-PCR data of *irg-6* as described in Fig 1. In A and B, data are the average of three or four independent replicates, respectively, each normalized to a control gene with error bars representing SEM. Data are presented as the value relative to the average expression from all replicates of the indicated gene in the baseline condition (wild-type animals exposed to control). **(C)** *P. aeruginosa* pathogenesis assay and **(D)** lifespan on *E. coli* OP50 of animals exposed to the indicated RNAi bacteria. Data are representative of three trials. Sample sizes, mean lifespan and p values for all trials are shown in S4C and S4D Table. Significance was determined using Kaplan-Meier survival curves and log-rank tests.
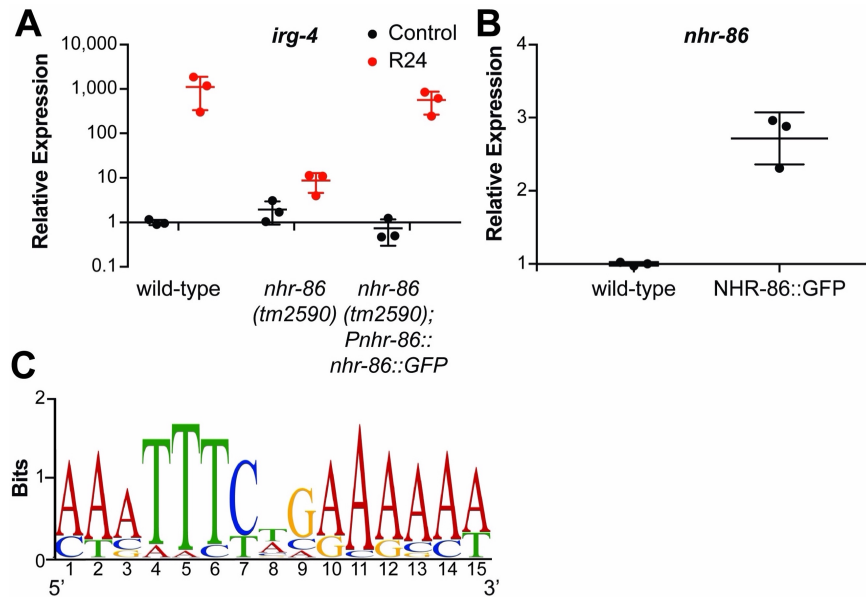
S2 Fig: NHR-86 binds to the promoters of innate immune genes to drive their transcription.
qRT-PCR was used to measure **(A)** *irg-4* and **(B)** *nhr-86* in animals of the indicated genotypes. Data are the average of three independent replicates, each normalized to a control gene with error bars representing SEM. Data are presented as the value relative to the average expression from all replicates of the indicated gene in the baseline condition (wild-type animals exposed to control in A and wild-type in B). **(C)** The 15-bp sequence that was enriched in the promoters that were bound by NHR-86::GFP.
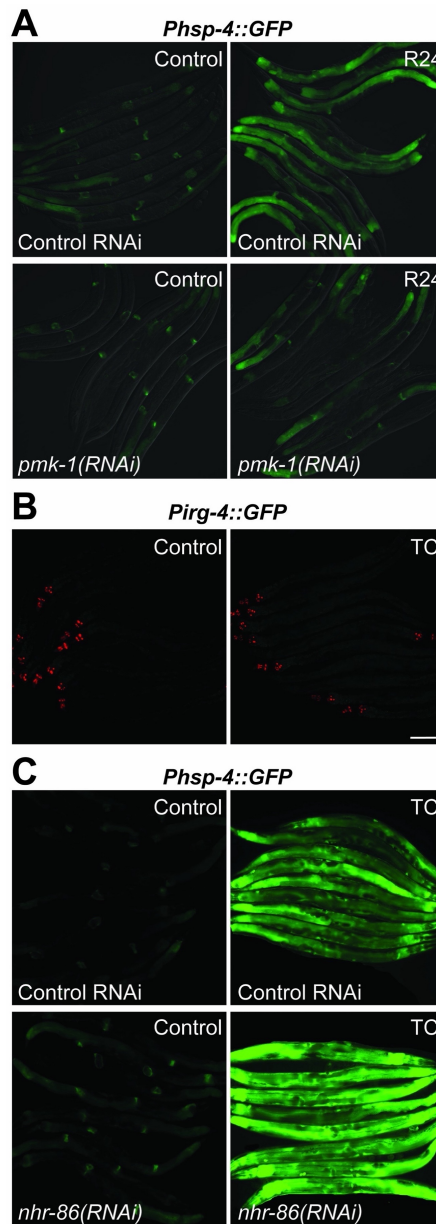
S3 Fig: The Immune response induced by *nhr-86* protects *C. elegans* against *P. aeruginosa* infection.
(**A**) *Phsp-4*::*GFP*, (**B**) *Pirg-4*::*GFP* and (**C**) *Phsp-4*::*GFP* animals were exposed to the indicated RNAi conditions and treated with DMSO (control) or 10 μg/mL tunicamycin (TC) overnight at 20°C and photographed. Red expression in *Pirg-4*::*GFP* animals is the *Pmyo-2*::*mCherry* co-injection marker. Scale bar equals 100 μm.
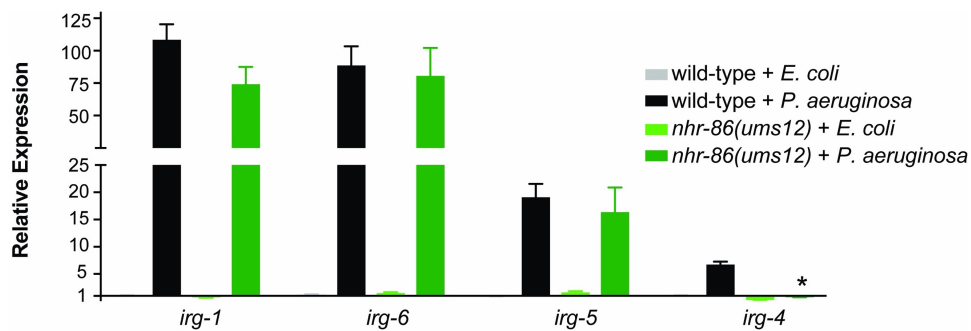
S4 Fig: ***nhr-86(ums12)* does not abrogate the induction of *irg-1*, *irg-5* or *irg-6* during**
***P. aeruginosa* infection**
qRT-PCR data of *irg-1*, *irg-4*, *irg-5* and *irg-6* in wild-type or *nhr-86(ums12)* animals
exposed to *E. coli* or *P. aeruginosa* for 6 hours. * equals p<0.05 for the difference in
expression of the indicated gene between wild-type and *nhr-86(ums12)* in
the *P. aeruginosa*-exposed condition. All other differences were not significant. Data are
presented relative to uninfected wild-type animals.
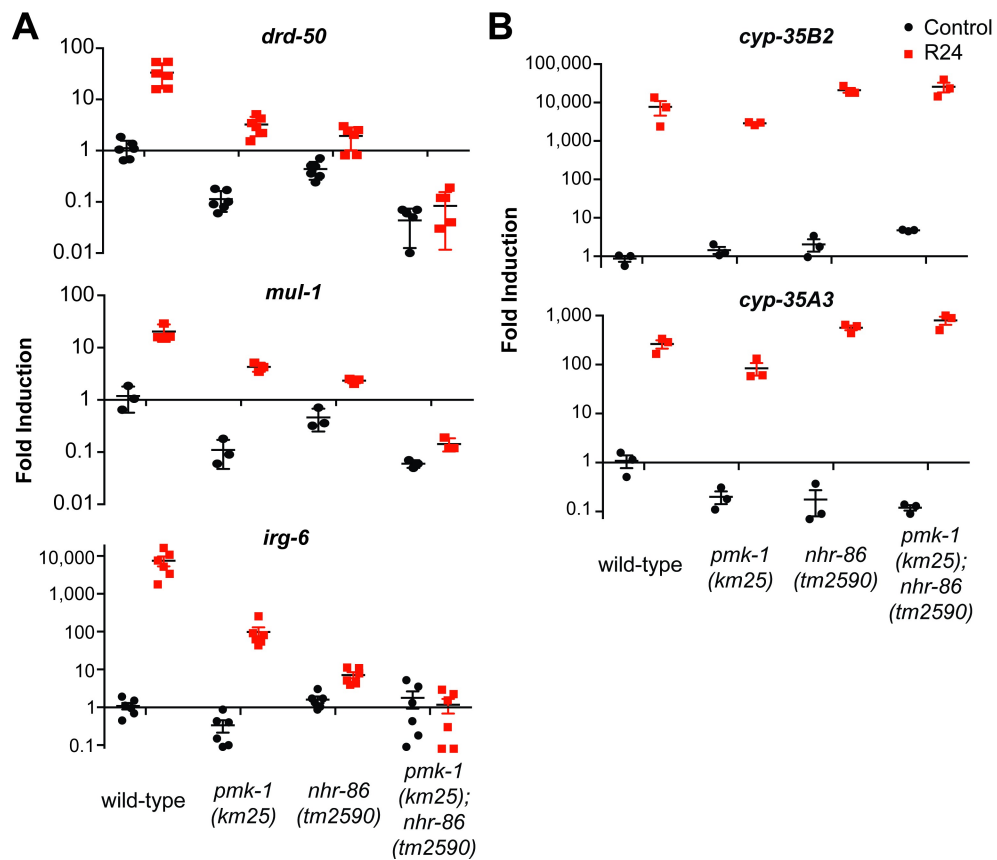
S5 Fig: *nhr-86* **induces innate immune defenses independent of the p38 MAPK** *pmk-1.*
qRT-PCR data of *drd-50*, *mul-1 and irg-6* (**A**)**,** and *cyp-35B2* and *cyp-35A3* (**B**) as
described in Fig 5A.

Supplemental Tables

Supplemental tables referenced in this manuscript can be found by following the included links to the publisher's website.

Table S1: Genes identified in an RNAi screen for NHRs that control the induction of *Pirg-4*::GFP by R24.
https://doi.org/10.1371/journal.pgen.1007935.s006

Table S2: *nhr-86*-dependent genes from the mRNA-seq experiment.
https://doi.org/10.1371/journal.pgen.1007935.s007

Table S3: ChIP-seq data showing the promoters that were bound by NHR-86.
https://doi.org/10.1371/journal.pgen.1007935.s008

Table S4: Sample sizes, mean lifespan, % lifespan extension conferred by R24 treatment in each background and p values for the *C. elegans* pathogenesis and lifespan assays.
(A) Data for Fig 4A. **(B)** Data for Fig 5B. **(C)** Data for S1C Fig. **(D)** Data for S1D Fig.
https://doi.org/10.1371/journal.pgen.1007935.s009

Table S5: Primer sequences that were designed for this study.
https://doi.org/10.1371/journal.pgen.1007935.s010

Appendix II: Measurements of Innate Immune Function in *C. elegans*

Attributions

The work presented in Appendix II is the result of a collaborative effort among all authors of the publication listed below:

Foster K.J., McEwan D.L., Pukkila-Worley R. (2020) Measurements of Innate Immune Function in C. elegans. In: Curran S. (eds) Aging. Methods in Molecular Biology, vol 2144. Humana, New York, NY.

I was responsible for the compiling of the included protocols, and in the writing and editing process of this methods review article. The tissue-specific RNAi data presented in Table 2 was generously provided by Deborah McEwan.

Abstract

The microscopic nematode *C. elegans* has emerged as a powerful system to characterize evolutionarily ancient mechanisms of pathogen sensing, innate immune activation and protective host responses. Experimentally, *C. elegans* can be infected with a wide variety of human pathogens, as well as with natural pathogens of worms that were isolated from wild-caught nematodes. Here, we focus on an experimental model of bacterial pathogenesis that utilizes the human opportunistic bacterial pathogen *Pseudomonas aeruginosa* and present an algorithm that can be used to study mechanisms of immune function in nematodes. An initial comparison of the susceptibility of a *C. elegans* mutant to *P. aeruginosa* infection with its normal lifespan permits an understanding of a mutant's effect on pathogen susceptibility in the context of potential pleotropic consequences on general worm fitness. Assessing the behavior of nematodes in the presence of *P. aeruginosa* can also help determine if a gene of interest modulates pathogen susceptibility by affecting the host's ability to avoid a pathogen. In addition, quantification of the pathogen load in the *C. elegans* intestine during infection, characterization of immune effector transcription that are regulated by host defense pathways and an initial assessment of tissue specificity of immune gene function can refine hypotheses about the mechanism of action of a gene of interest. Together, these protocols offer one approach to characterize novel host defense mechanisms in a simple metazoan host.

Introduction

In their natural habitats, the microscopic nematode *Caenorhabditis elegans* forage microorganisms within decomposing organic matter. As a result, their evolution has been shaped by interactions with pathogenic and nonpathogenic bacteria. For over two decades, researchers have exploited a wealth of genetic tools available in *C. elegans* to characterize the host defense mechanisms utilized by nematodes to survive challenge from pathogenic microbes. This effort has revealed that *C. elegans* mount inducible anti-pathogen defenses towards diverse pathogens, which involve the elaboration of secreted immune effectors, and also program behavioral avoidance responses to minimize exposure to pathogens (Cohen & Troemel, 2015; Ewbank & Pujol, 2016; D. H. Kim, 2018; Meisel & Kim, 2014; Pukkila-Worley & Ausubel, 2012b). Interestingly, detection of pathogens in these contexts involves surveillance of core host processes that are often disrupted during microbial infection (*e.g.* translation and mitochondrial respiration), monitoring for host damage associated with pathogen invasion, and sensory nervous system activation by microbial molecules (Aballay, 2009; Cao et al., 2017; Dunbar et al., 2012; Hoffman & Aballay, 2019; Labed et al., 2018; McEwan et al., 2012; Meisel et al., 2014; Melo & Ruvkun, 2012; Pukkila-Worley, 2016b; Kirthi C. Reddy et al., 2016; Zugasti et al., 2014). Moreover, anti-pathogen immune defenses are induced following physical damage to core cellular structures; as a host protective response after DNA damage and disruption of the ubiquitin proteasome system; and by a nuclear hormone receptor following activation by ligands in the chemical environment (Ermolaeva & Schumacher, 2014; Melo & Ruvkun, 2012; Peterson et al., 2019; Kirthi C. Reddy et al., 2016). These studies have revealed that

multiple biological processes are connected with pathogen defense mechanisms and have fueled interest in using genetic approaches in *C. elegans* to define new mechanisms of innate immune regulation. In this chapter, we aim to provide a framework for the experimental assessment of innate immune function in *C. elegans* by assimilating commonly-used protocols in the field.

In the laboratory, *C. elegans* can be infected with a variety of human pathogens, as well as with natural pathogens isolated from Pukkila-Worley & Ausubel 2012b; Tan et al. 1999; Troemel et al. 2008; Troemel 2011(Pukkila-Worley & Ausubel, 2012b; Tan et al., 1999; Troemel, 2011; Troemel et al., 2008). Here, we will focus on *C. elegans* experimental models that use the human opportunistic bacterial pathogen *Pseudomonas aeruginosa*, a widely-used assay that has been the subject of several published protocols (Conery et al., 2014; Kirienko et al., 2014; Powell & Ausubel, 2008). A *C. elegans – P. aeruginosa* pathogenesis assay can be used to determine if a gene of interest leads to enhanced susceptibility of *C. elegans* to bacterial infection when it is mutated or knocked down by RNAi (Tan et al., 1999; Troemel et al., 2006). Interpretation of a phenotype in *C. elegans – P. aeruginosa* pathogenesis assay should be made with an understanding of how the gene affects the longevity of *C. elegans* growing under standard laboratory conditions to assess pleiotropic effects of the mutant or gene knockdown on general nematode fitness.

An assessment of *C. elegans* behavior in the presence of pathogenic bacteria is an important next step to determine if a gene affects susceptibility to *P. aeruginosa* infection by modulating the ability of the host to avoid the pathogen or by modulating some aspect of the inducible immune response (Aballay, 2009; Cao et al., 2017; J Sun et al., 2011).

Upon exposure to pathogenic food sources or noxious compounds, neuronal receptors induce programmed behavioral avoidance responses to minimize exposure to the insult (Aballay, 2009; Kumar et al., 2019; K. Lee & Mylonakis, 2017; J. Singh & Aballay, 2019; Zhang et al., 2005). Avoidance behaviors are both innately programmed and learned as the result of prior exposure to toxic stimuli (Cao & Aballay, 2016; Hoffman & Aballay, 2019; Zhang et al., 2005). One way to determine if a gene of interest modifies the behavior of nematodes is to perform a lawn occupancy assay whereby *C. elegans* are exposed to a small lawn of a pathogenic bacteria and their bChang et al. 2011; Styer et al. 2008; Sun et al. 2011(Chang et al., 2011; Styer et al., 2008; J Sun et al., 2011).

Does a gene of interest affect intestinal colonization of the bacterial pathogen? Mutations in key immune defense pathways in *C. elegans* cause an increased burden of bacteria in the nematode intestine, presumably as a consequence of the failed immune response (D. H. Kim et al., 2002; Portal-Celhay et al., 2012). Alternatively, mutations can modify the ability of the host to tolerate infection or affect post-infection wound healing in a manner that does not modulate the burden of bacteria in the intestine (Cao et al., 2017; Head & Aballay, 2014). Measurements of bacterial colonization within the *C. elegans* intestine can help distinguish between these possibilities.

An important next step is to determine whether a gene of interest affects the function of known immune pathways. Multiple pathways operate in parallel in *C. elegans* to control protective host defenses during bacterial infection. Transgenic *C. elegans* strains that express green fluorescent protein under the control of a promoter for an innate immune effector, called transcriptional immune reporters, can provide a visual readout of host

defense activation (Cheesman et al., 2016; Estes et al., 2010; Irazoqui et al., 2010; Peterson et al., 2019; Pukkila-Worley et al., 2012). Assessing a panel of these immune reporters in a mutant background can help focus subsequent genetic epistasis analyses.

When it is established that a gene of interest affects host defense mechanisms towards *P. aeruginosa*, it is often useful to determine the tissues where gene function is necessary to modulate anti-pathogen defenses. Transgenic *C. elegans* strains in which the RNAi machinery has been reconstituted in specific tissues are available and can provide a useful starting point to assess the tissue-specific (Espelt et al., 2005; Melo & Ruvkun, 2012). We discuss the benefits and pitfalls of this method. Together, these protocols offer an approach to assess immune gene function in *C. elegans*.

Materials

- **Worm Pick:** Carefully break off the tip of a Pasteur pipette just below the neck. Over a flame, use forceps to slowly insert a 2 inch-long segment of 90% Platinum/10% Iridium wire into the fractured end of the Pasteur pipette. Heat until the Pasteur pipette melts around the platinum wire, securing it in place. Once cooled, the wire tip can be hammered flat or pressed with jewelry pliers in order to increase its surface area.

- **1-mm Silicon Carbide Beads**

- **Streptomycin (2.5% w/v):** Dissolve 1.25-gm streptomycin sulfate in 50-mL ddH$_2$O. Filter sterilize and store in the dark at 4C

- **Nystatin (50 x 10 mg/mL stocks):** Suspend 500-mg Nystatin in 50-mL 70% EtOH. Aliquot into 1-mL tubes and store at -20C. Nystatin will precipitate out of the ethanol. Resuspend prior to use.

- **M9W (1 L):** Dissolve 3-gm of KH_2PO_4, 6-gm of Na_2HPO_4, and 5-gm NaCl in 1-L of ddQ H_2O. Autoclave and cool in a 55C water bath. Once solution has cooled, add 1-mL of filter sterilized 1M $MgSO_4$.

- **5-Fluoro-2′-deoxyuridine [FUDR] (50 x 10 mg/mL stocks):** Dissolve 0.5-gm of 5-Fluoro-2′-deoxyuridine in 50-mL ddQ H_2O. Filter sterilize and aliquot into 1-mL tubes.

- **5 mg/mL Cholesterol in Ethanol (50-mL):** Dissolve 0.25-gm cholesterol in 50-mL of 99.5% EtOH. Filter sterilize.

- **1M Magnesium Sulfate (100-mL):** Dissolve 12.04-gm $MgSO_4$ in 100-mL of ddH2O. Autoclave.

- **1M Calcium Chloride (100-mL):** Dissolve 14.7-gm $CaCl_2$ in 100-mL of ddH2O. Autoclave.

- **2N NaOH (50-mL):** Dissolve 4-gm NaOH in 50-mL of ddH2O.

- **5M NaOH (50-mL):** Dissolve 14.6-gm NaOH in 50-mL of ddH2O.

- **LB Broth (1 L):** Dissolve 10-gm Bacto-Tryptone, 5-gm Bacto-Yeast extract, and 5-gm NaCl in 1 L of ddQ H_2O. Autoclave.

- **LB Agar Plate Media (1 L):** Dissolve 10-gm Bacto-Tryptone, 5-gm Bacto-Yeast Extract, 5-gm NaCl, 15-gm Bacto-Agar, and dispense 1.5-mL 2N NaOH in 1 L of ddQ H_2O. Autoclave. Place media in a 55C water bath for 30 minutes to cool before using.

- **"Slow Killing" Plate Media (1 L):** Dissolve 3-gm NaCl, 3.5-gm Bacto-Peptone, and 17-gm Bacto-Agar, in 1 L of ddH$_2$O. Autoclave. Place media in a 55C water bath for 30 minutes to cool. Once media is cool enough to be handled, add 1-mL 1M MgSO$_4$, 1-mL 1M CaCl$_2$, 1-mL 5 mg/mL cholesterol in EtOH, and 25-mL 1M KPO$_4$ buffer. Using a Unispense plate pourer or repeater pipette, pour media into the desired plates.

- **Nematode Growth Media Plates (1 L):** Dissolve 3-gm NaCl, 2.5-gm Bacto-Peptone, and 17-gm Bacto-Agar, in 1 L of ddH$_2$O. Autoclave. Place media in a 55C water bath for 30 min to cool. Once media is cool enough to be handled, add 1-mL 1M MgSO$_4$, 1-mL 1M CaCl$_2$, 1-mL 5 mg/mL cholesterol in EtOH, 25-mL 1M KPO$_4$ Buffer, 7.5-mL 2.5% (w/v) Streptomycin, and 1-mL 10 mg/mL Nystatin. Using a Unispense plate pourer or repeater pipette, pour media into the desired plates.

C. elegans Maintenance Plate Preparation

NGM-OP50 Plate Preparation

1. Inoculate a single colony of *E. coli* OP50 in LB broth + Streptomycin (10 ug/mL). Incubate the culture at 37C overnight while shaking continuously at 250 rpm.

2. Spin resulting bacterial culture at 3000 x g for 10 minutes at 4C and pour off the supernatant. Ensure that the bacterial pellet is not disturbed. Resuspend bacterial pellet in appropriate volume of M9W so that the resulting OP50 concentration is 10x. Less concentrated OP5O can be used; however, worms may exhaust the food source and starve.

3. Spread between 100-500-μL of 10x OP50 onto the surface of 6-cm or 10-cm petri dishes containing NGM media, ensuring that the bacterial lawn does not reach the sides of the plates. Allow plates to dry completely before using. Seeded plates can be stored for 1-2 weeks at 15C.

P. aeruginosa PA14 Pathogenesis Assay Plate Preparation

1. Inoculate one *P. aeruginosa*, strain PA14 colony in 5-mL LB broth. Incubate culture overnight (16 h maximum) at 37C while shaking at 250 rpm.

2. Dry the *P. aeruginosa* PA14 plates uncovered in a biologic hood for 10 minutes

3. Using a pipette, drop 10-μL of *P. aeruginosa* PA14 culture onto the center of Slow Kill (SK) plates. Carefully tip the plates from side to side in order to increase the surface area of the bacterial lawn, ensuring that the bacterial lawn does not reach the sides of the plates

4. Incubate seeded *P. aeruginosa* PA14 plates at 37C for 24 h and then 24 h at 25C.

C. elegans Maintenance and Synchronization

Carry out all centrifugation steps at 3100 rpm unless otherwise specified.

1. From NGM plates containing starved L1-stage *C. elegans*, remove a "chunk" of agar and place on a 6-cm or 10-cm NGM plate containing *E. coli* OP50, prepared as described above. Incubate plates at 20C until they reach the gravid adult stage (approximately three days).

2. Using a serological pipette, add 3-mL of M9W to each NGM plate and rinse worms off into 15-mL conical tubes (combine plates of the same condition into one tube).

3. Pellet worms by spinning down tubes at 3100 rpm for 30 seconds. Remove supernatant until 500-μL liquid remains.

4. Add 400-μL of ~8% bleach and 100-μL 5M NaOH into each tube and gently agitate by hand for 2-3 minutes. Check under a microscope to ensure that the carcasses have broken open and that eggs have been released. Do not expose eggs to concentrated bleach solution for more than 5 minutes. Quench the bleach by adding M9W up to 15-mL total volume.

5. Centrifuge for 30 seconds. Aspirate supernatant down to egg pellet.

6. Wash pellet with M9W 3-4 times.

7. Resuspend purified eggs in 5-mL of M9W and place on a rocker overnight at room temperature to allow the eggs to hatch and arrest at the L1 stage.

8. Drop approximately 200 L1-stage nematodes onto 6-cm NGM-OP50 plates and incubate at 20C until animals reach the L4 stage. Note: You may need to concentrate the egg isolation if the volume required to obtain 200 eggs is greater than 200 μL. Volumes of buffer added to plates larger than this may not dry completely.

Pseudomonas aeruginosa PA14 Pathogenesis and *C. elegans* Lifespan Assays

The *P. aeruginosa* PA14 pathogenesis assay described here is also referred to as the "slow killing" assay (Conery et al., 2014; Tan et al., 1999). In this assay, *P. aeruginosa* kills *C.*

elegans via an infection-like process that requires live bacteria and engages host defense mechanisms in the worm.

P. aeruginosa PA14 Pathogenesis Assay Setup

1. Prepare NGM-OP50 and *P. aeruginosa* PA14 pathogenesis assay plates as described in sections 3.1 and 3.2, respectively.

2. Obtain synchronized populations of strains to be assessed as described in section 3.

3. Spot the seeded *P. aeruginosa* PA14 plate with 4 10-μL drops of 10 mg/mL FUDR around the perimeter of the bacterial lawn (final concentration 40 μg/mL). Leave plates to dry at room temperature for 30 minutes to allow the FUDR to absorb into the plates. Adding FUDR prevents the hatching of progeny during the assay.

4. Pick 50 *C. elegans* at the L4 stage to each of three separate *P. aeruginosa* PA14-seeded plates. Be careful not to injure the worms during assay setup. After animals are transferred to assay plates, ensure that residual OP50 is removed from the *P. aeruginosa* PA14-seeded plates.

5. Incubate assay plates at 25C for the duration of the pathogenesis assay.

Assay Scoring and Statistical Analyses

1. Score assay twice daily, by counting the total number of live and dead animals on each assay plate. Animals may need to be prodded in order to determine whether they have succumbed to the infection. Remove all carcasses by picking them into a flame.

2. Calculate the cumulative number of dead worms at each time point for each condition. Subsequently determine the percent survival of each condition and plot this versus time.

3. Mean Lifespan, Kaplan-Meier Estimator, and Log-rank test calculations can be performed by inputting survival data into the Online Application for Survival Analysis (OASIS) (Han et al., 2016).

C. elegans Lifespan Assay Setup

1. Prepare NGM-OP50 as described in sections 3.1.

2. Obtain synchronized populations of strains to be assessed as described in section 3.3.

3. From synchronized NGM-OP50 plates, pick 50 synchronized L4 animals of each condition to 3 separate freshly seeded NGM-OP50 plates that contain 40μg/mL FUDR). Be careful not to injure the worms during assay setup. FUDR is used in the *C. elegans* lifespan assays to mirror the conditions in the *P. aeruginosa* PA14 pathogenesis assays.

4. Incubate assay plates at 20C for the duration of the lifespan assay. As lifespan assays typically take several weeks, it is advised to wrap assay plates in aluminum foil in order to limit contamination for the duration of the experiment.

C. elegans Lifespan Assay Scoring and Statistical Analyses

1. Score assay once daily by counting the total number of live and dead animals on each assay plate. Animals may need to be tapped on the head in order to determine whether they are alive. Remove all carcasses by picking them into a flame.

2. Data processing and statistical analyses can be performed as described in section 4.1.2.

Lawn Occupancy Assay

Assay Setup

1. Prepare NGM-OP50 and *P. aeruginosa* assay plates as described in sections 3.1 and 3.2, respectively.

2. Obtain synchronized populations of strains to be assessed as described in section 3.3

3. From synchronized OP50-NGM plates, pick 50 synchronized L4 animals of each strain to three separate *P. aeruginosa* assay plates. Be careful not to injure the worms during assay setup. After animals are transferred to assay plates, ensure that residual OP50 is removed from the *P. aeruginosa* assay plates.

4. Flip over assays plates and use a fine tip marker to carefully trace the perimeter of the pathogenic lawn.

5. Incubate plates at 25C for the duration of the assay.

Scoring and Statistical Analysis

1. Score assay at several time points by counting the total number of animals that reside off and on the bacterial lawn (Figure 1). Typically, scoring at 4h, 8h, 16h, 24h, and 30h allows you to record sufficient data to understand the dynamics of behavioral avoidance to *P. aeruginosa*.

Intestinal Pseudomonal CFU Quantification

Bacterial Isolation and Plating

1. Prepare NGM-OP50 and *P. aeruginosa* PA14 pathogenesis assay plates as described in sections 3.1 and 3.2, respectively.

2. Obtain synchronized populations of strains to be assessed as described in section 3.3.

3. From synchronized OP50-NGM plates, pick 50 synchronized L4 animals of each strain to three separate *P. aeruginosa* PA14 pathogenesis assay plates. After animals are transferred to assay plates, ensure that residual OP50 is removed from the *P. aeruginosa* PA14-seeded plates.

4. Incubate *P. aeruginosa* PA14-seeded plates at 25C overnight.

5. Make bacterial isolation buffer by adding 300-mg tetramisole hydrochloride to 50-mL M9W. Vortex. Add 50-μL of 10% Triton X-100.

6. Pick 10-20 L4 worms from *P. aeruginosa* PA14 plates to unseeded NGM plates (one plate per condition per replicate) and let them crawl around for 10 minutes to dislodge bacteria attached to cuticle.

7. After 10 minutes, pick worms to another unseeded NGM plates and let them crawl around for 10 more minutes.

8. Dispense 150-μL of bacterial isolation buffer into 1.5-mL tubes (1 tube per condition)

9. Pick at minimum 10 L4 animals of each condition from unseeded NGM plates into each 1.5-mL tube.

10. Important: Count the worms after transferring to ensure that you have an accurate worm count for each tube.

11. Spin down worms at 3000 rpm for 30 seconds. Remove supernatant down to 50-μL. Add 1-mL M9W. Repeat wash steps 5 times.

12. Perform one final wash. After last wash, transfer 200-μl of supernatant from each sample to clean Eppendorf tube before aspirating volume down to 100-μl. This aliquot will be used to assess the effectiveness of the wash steps at removing surface bacteria from the animals.

13. Count worms and record the final number present in each tube. Add 80-μL of bacterial isolation buffer + 20-μL of 10% Trition.

14. Add 400-mg (~ 0.5 mL mark) of 1.0-mm silicon carbide beads to 1.5-mL screw top Eppendorf tubes (1 tube per condition).

15. Transfer animals and liquid to bead-filled tubes by pipetting and vortex for 1 minute to homogenize worms. Hold the tube vertically while vortexing to limit foam formation.

16. Transfer foam and liquid to new tube. Try to remove as much liquid as possible to ensure all bacteria is collected.

17. Spin tubes at 8000 rpm for 2 minutes to reduce foam that formed during homogenization. Vortex solution briefly to resuspend bacterial pellet.

18. Perform three 1:5 serial dilutions of worm lysate for each sample in a 96 well plate. Dispense 60-μL of wash buffer (isolated form step 12) into row E and perform three 1:5 serial dilutions. Refer to plate diagram below (Figure 2).

19. Plate 10-μl liquid from all wells onto agar plates. Tilt the plate and let the liquid spread down the plate. Incubate plates at 25C overnight.

Intestinal CFU Calculations

1. Count the number of colonies for each dilution under a dissecting microscope.

2. Calculate CFUs/worm by multiplying the number of colonies for each lysate dilution by its respective dilution factor, followed by a factor of 20 (each plated well contained 10-μL of the total 200-μL lysate volume)

3. Divide the total CFU count by the number of worms counted in Step 13

4. Perform the calculations on wells containing the isolated wash buffer (Step 12) for each condition and subtract this result from the result obtained from plating the worm lysate. This step ensures that bacteria that may have been attached to the cuticle are not counted.

Utilizing Transcriptional Readouts to Examine Immune Pathway Function

Multiple pathways operate in parallel in *C. elegans* to promote host defense towards diverse pathogens. Understanding how putative immune regulators function together with these known host defense mechanisms can be challenging given the number of pathways that have been implicated. One approach to streamline this characterization is to examine the regulation of specific genes, which are known to be downstream of different host defense pathways in *C. elegans*. This approach can give an initial understanding of the mechanisms underlying immune misregulation in a particular mutant strain and can be accomplished using quantitative real time-PCR (qRT-PCR) to study the expression of these

genes upon pathogen exposure in mutant or RNAi-knockdown animals. Alternatively, transgenic, GFP-based transcriptional reporters, in which the promoter for an immune effector has been fused to GFP, can provide a visual readout of pathway regulation. In Table 1, we have included a list of genes and available transcriptional reporters that are regulated downstream of different pathways, which have been implicated in *C. elegans* immune defenses.

Pathway Implicated in *C. elegans* Immune Defense	Selected Genes Downstream of Indicated Pathway	Selected Transcriptional Immune Reporters	References
DBL-1/DAF-7 (TGFβ)	*clec-66, clec-67, lys-1*	P*clec-67::GFP* P*sma-6::GFP*	(Alper et al., 2007; Kerry et al., 2006; Liang et al., 2007; Mallo et al., 2002; Mochii et al., 1999; Pujol, Zugasti, et al., 2008; Roberts et al., 2010)
DAF-2/ DAF-16 (Insulin Signaling)	*lys-7, dod-22, nlp-31*	P*lys-7::GFP* P*dod-24::GFP* P*nlp-31::GFP*	(Evans, Kawli, et al., 2008; Murphy et al., 2003; Nathoo et al., 2001; Ookuma et al., 2003)
PMK-1 MAPK (basal regulation in the intestine)	*irg-4, irg-5, T24B8.5*	P*irg-4::GFP* P*irg-5::GFP* P*T24B8.5::GFP*	(Cheesman et al., 2016; Peterson et al., 2019; Pukkila-Worley et al., 2014; Troemel et al., 2006)
PMK-1 MAPK (hypodermis)	*nlp-29, sta-2, elt-3*	P*nlp-29::GFP* P*elt-3::GFP*	(Dierking et al., 2011; Pujol, Zugasti, et al., 2008)
Wnt/ β-catenin BAR-1	*ilys-3, lys-5, clec-60*	P*clec-60::GFP*	(Irazoqui et al., 2008; Labed et al., 2018)
ZIP-2	*irg-1, irg-2*	P*irg-1::GFP*	(Estes et al., 2010)
FSHR-1	*F01D5.5, clec-67, irg-5*	P*irg-5::GFP* P*clec-67::GFP*	(Miller et al., 2015; Powell et al., 2009)
HLH-30 (TFEB)	*ilys-2, lys-3 lys-5*	P*ilys-2::GFP* HLH-30::GFP	(Visvikis et al., 2014)
SKN-1 (Nrf1)	*gst-4, gcn-1*	P*gst-4::GFP*	(Hoeven et al., 2011; Miller et al., 2015)
ATFS-1 Mitochondrial Unfolded Protein Response (UPR^MT)	*hsp-6*	P*hsp-6::GFP*	(A M Nargund et al., 2012)
Endoplasmic Reticulum Protein Response (UPR^ER)	*xbp-1* (activated splice form), *hsp-4*	P*hsp-4::GFP*	(Richardson et al., 2010)

Table 1. Genes and transcriptional immune reporters that are regulated downstream of pathways that have been implicated in *C. elegans* host defense

It is important to note that this is not an exhaustive list of immune effectors or host defense pathways in *C. elegans*, and some of the listed genes are regulated by more than one pathway. In addition, depending on the context and pathogen used, the transcription of the listed putative immune effectors can be induced in other ways. For example, upon activation with a chemical ligand, the nuclear hormone receptor NHR-86 traffics to the promoters of genes whose basal expression is ensured by the p38 MAPK PMK-1 pathway. NHR-86 drives the induction of these genes in a manner independent of the PMK-1 immune pathway (Peterson et al., 2019). In addition, many of the genes listed in the table are not induced during infection with *P. aeruginosa*, but are upregulated during infection with other pathogens. For example, *clec-60* is important for defense against *Staphylococcus aureus* in a manner dependent on Wnt/ *β*-catenin BAR-1 signaling. (Irazoqui et al., 2008, 2010). Therefore, we suggest that this list should be employed as a hypothesis-generating tool and as a prelude to further characterization of a new immune regulator with classic epistasis experiments, biochemical analyses of pathway activation and whole genome transcriptome profiling studies.

An Initial Evaluation of Tissue Specificity in Immune Function

Innate immune defenses in *C. elegans* are controlled via tissue-autonomous mechanisms at sites of pathogen encounter, such as the intestine and hypodermis, and are also regulated tissue non-autonomously from neurons and the germline. One commonly-used method for the initial examination of tissue specificity of gene function is to use a panel of transgenic *C. elegans* strains in which the RNAi machinery has been re-constituted

only in specific tissues, thereby permitting tissue-specific gene knockdown; however, an important caveat with this approach is discussed below.

We examined the ability of a panel of *C. elegans* strains that were engineered for tissue specific RNAi-mediated gene knockdown to perform RNAi in different tissues. We exposed these strains to *E. coli* RNAi-feeding bacteria that target genes, which confer visible phenotypes that are scorable under a dissecting microscope: RNAi-mediated knockdown of *act-5*, a gene required for intestinal development, causes developmental arrest; *unc-22(RNAi),* a gene expressed in body wall muscle, causes a twitching phenotype in levamisole; knockdown of *bli-1* in the hypodermis causes blistering of the cuticle; and *pos-1(RNAi)*, a gene expressed in the germline, prevents eggs from hatching (Table 2). We found that *C. elegans* strain MGH167, in which machinery essential for RNAi was reconstituted only in the intestine, demonstrated excellent tissue specificity in RNAi-mediated gene knockdown with no detectable RNAi-mediated gene knockdown outside of the intestine (McEwan et al., 2016). In contrast, RNAi in *C. elegans* strain VP303, which also reports intestinal specificity, occurs efficiently in the intestine and not in body wall muscle or the germline; however, 36% of VP303 animals exposed to *bli-1(RNAi)* had cuticle blistering. Likewise, RNAi in the *C. elegans* strain JM43 is primarily restricted to hypodermal cells, although a subset of animals showed evidence of some RNAi-mediated gene knockdown in the intestine (33%) or body-wall muscle (13%). These data indicate that results with *C. elegans* JM43 and VP303 strains should be interpreted with caution. For these reasons, it can be useful to confirm results with tissue-restricted RNAi strains by

generating mosaic *C. elegans* with a tissue-specific mutation in a given gene (Besseling &

Bringmann, 2016)

	Percent of animals with the phenotype associated with the indicated RNAi strain (total n counted)			
	Strains			
	Wild-type N2	**MGH167** *sid-1(qt9); alxIs9 [Pvha-6p::sid-1::SL2::GFP]*	**VP303** *rde-1(ne219); kbIs7 [Pnhx2::rde1+ rol-6(su1006)]*	**JM43** *rde-1(ne219); Is [Pwrt-2::rde1; Pmyo-2::rfp]*
	Capable of RNAi in intestine, germline and hypodermis	Designed to perform RNAi only in intestine (Melo & Ruvkun, 2012)	Designed to perform RNAi only in intestine (Melo & Ruvkun, 2012)	Designed to perform RNAi only in hypodermis (Espelt et al., 2005)
L4440(RNAi) **Control vector**	0% (82)	0% (96)	0% (199)	0% (151)
act-5(RNAi) **Affected tissue in *act-5(RNAi)*: intestine** **Phenotype scored: developmental arrest**	100% (74)	99% (70)	100% (170)	No arrest: 67% (77) Intermediate Arrest: 16% (18) N2-Like arrest: 17% (20)
unc-22(RNAi) **Affected tissue in *unc-22(RNAi)*: body wall muscle** **Phenotype scored: twitching in 10mM levamisole**	100% (100)	0% (100)	0% (100)	13% (100)
bli-1(RNAi) **Affected tissue in *bli-1(RNAi)*: hypodermis** **Phenotype scored: blistered cuticle**	100% (97)	0% (168)	36% (168)	100% (214)
pos-1(RNAi) **Affected tissue in *pos-1(RNAi)*: germline** **Phenotype scored: >50 unhatched eggs**	100% (10)	0% (10)	0% (10)	20% (10)

Table 2. Assessing the specificity of transgenic *C. elegans* engineered for tissue-restricted RNAi.

Experiments with tissue-restricted RNAi can help determine if expression of a gene is necessary in a given tissue for a particular immune-related phenotype (*e.g.* resistance to pathogen infection or induction of an immune effector). It is also important to determine if gene expression in a particular tissue is sufficient for the phenotype by generating transgenic *C. elegans* strains in which the gene of interest is only expressed in a particular tissue. Most commonly, this is accomplished by introducing an extrachromosomal array, which expresses the gene of interest under the control of a tissue-specific promoter, into a loss-of-function mutant and assays for complementation of the immune-related phenotype.

Bibliography

Aballay, A. (2009). Neural regulation of immunity: Role of NPR-1 in pathogen avoidance and regulation of innate immunity. *Cell Cycle*, *8*(7), 966–969. https://doi.org/10.4161/cc.8.7.8074

Aballay, A. (2013). Role of the Nervous System in the Control of Proteostasis during Innate Immune Activation: Insights from *C. elegans*. *PLoS Pathogens*, *9*(8), e1003433. https://doi.org/10.1371/journal.ppat.1003433

Aballay, A., Drenkard, E., Hilbun, L. R., & Ausubel, F. M. (2003). Caenorhabditis elegans Innate Immune Response Triggered by Salmonella enterica Requires Intact LPS and Is Mediated by a MAPK Signaling Pathway. *Current Biology*, *13*(1), 47–52. https://doi.org/10.1016/s0960-9822(02)01396-9

Ahn, S.-H., Shah, Y. M., Inoue, J., Morimura, K., Kim, I., Yim, S., Lambert, G., Kurotani, R., Nagashima, K., Gonzalez, F. J., & Inoue, Y. (2008). Hepatocyte nuclear factor 4α in the intestinal epithelial cells protects against inflammatory bowel disease. *Inflammatory Bowel Diseases*, *14*(7), 908–920. https://doi.org/10.1002/ibd.20413

Alper, S., McBride, S. J., Lackford, B., Freedman, J. H., & Schwartz, D. A. (2007). Specificity and Complexity of the Caenorhabditis elegans Innate Immune Response. *Molecular and Cellular Biology*, *27*(15), 5544–5553. https://doi.org/10.1128/mcb.02070-06

Alspaugh, J. A., Pukkila-Worley, R., Harashima, T., Cavallo, L. M., Funnell, D., Cox, G. M., Perfect, J. R., Kronstad, J. W., & Heitman, J. (2002). Adenylyl Cyclase Functions Downstream of the Gα Protein Gpa1 and Controls Mating and Pathogenicity of Cryptococcus neoformans. *Eukaryotic Cell*, *1*(1), 75–84. https://doi.org/10.1128/ec.1.1.75-84.2002

Amrit, F. R. G., Naim, N., Ratnappan, R., Loose, J., Mason, C., Steenberge, L., McClendon, B. T., Wang, G., Driscoll, M., Yanowitz, J. L., & Ghazi, A. (2019). The longevity-promoting factor, TCER-1, widely represses stress resistance and innate immunity. *Nature Communications*, *10*(1), 3042. https://doi.org/10.1038/s41467-019-10759-z

Anderson, S. M., Cheesman, H. K., Peterson, N. D., Salisbury, J. E., Soukas, A. A., & Pukkila-Worley, R. (2019). The fatty acid oleate is required for innate immune

activation and pathogen defense in Caenorhabditis elegans. *PLOS Pathogens*, *15*(6), e1007893. https://doi.org/10.1371/journal.ppat.1007893

Arda, H. E., Taubert, S., MacNeil, L. T., Conine, C. C., Tsuda, B., Gilst, M. V., Sequerra, R., Doucette-Stamm, L., Yamamoto, K. R., & Walhout, A. J. M. (2010). Functional modularity of nuclear hormone receptors in a Caenorhabditis elegans metabolic gene regulatory network. *Molecular Systems Biology*, *6*(1), 367. https://doi.org/10.1038/msb.2010.23

Arribere, J. A., Bell, R. T., Fu, B. X. H., Artiles, K. L., Hartman, P. S., & Fire, A. Z. (2014). Efficient marker-free recovery of custom genetic modifications with CRISPR/Cas9 in Caenorhabditis elegans. *Genetics*, *198*(3), 837–846. https://doi.org/10.1534/genetics.114.169730

Arthur, J. S. C., & Ley, S. C. (2013). Mitogen-activated protein kinases in innate immunity. *Nature Reviews Immunology*, *13*(9), 679–692. https://doi.org/10.1038/nri3495

Ballestriero, F., Nappi, J., Zampi, G., Bazzicalupo, P., Schiavi, E. D., & Egan, S. (2016). Caenorhabditis elegans employs innate and learned aversion in response to bacterial toxic metabolites tambjamine and violacein. *Scientific Reports*, *6*(1), 29284. https://doi.org/10.1038/srep29284

Bargmann, C. (2006). Chemosensation in C. elegans. *WormBook*, 1–29. https://doi.org/10.1895/wormbook.1.123.1

Bargmann, C. I., Hartwieg, E., & Horvitz, H. R. (1993). Odorant-selective genes and neurons mediate olfaction in C. elegans. *Cell*, *74*(3), 515–527. https://doi.org/10.1016/0092-8674(93)80053-h

Belvin, M. P., & Anderson, K. V. (1996). A CONSERVED SIGNALING PATHWAY: TheDrosophilaToll-Dorsal Pathway. *Annual Review of Cell and Developmental Biology*, *12*(1), 393–416. https://doi.org/10.1146/annurev.cellbio.12.1.393

Bendena, W. G., Boudreau, J. R., Papanicolaou, T., Maltby, M., Tobe, S. S., & Chin-Sang, I. D. (2008). A Caenorhabditis elegans allatostatin/galanin-like receptor NPR-9 inhibits local search behavior in response to feeding cues. *Proceedings of the National Academy of Sciences*, *105*(4), 1339–1342. https://doi.org/10.1073/pnas.0709492105

Besseling, J., & Bringmann, H. (2016). Engineered non-Mendelian inheritance of entire parental genomes in C. elegans. *Nature Biotechnology*, *34*(9), 982–986. https://doi.org/10.1038/nbt.3643

Bolger, A. M., Lohse, M., & Usadel, B. (2014). Trimmomatic: a flexible trimmer for Illumina sequence data. *Bioinformatics*, *30*(15), 2114–2120. https://doi.org/10.1093/bioinformatics/btu170

Bolz, D. D., Tenor, J. L., & Aballay, A. (2010). A conserved PMK-1/p38 MAPK is required in caenorhabditis elegans tissue-specific immune response to Yersinia pestis infection. *The Journal of Biological Chemistry*, *285*(14), 10832–10840. https://doi.org/10.1074/jbc.m109.091629

Bond, M. R., Ghosh, S. K., Wang, P., & Hanover, J. A. (2014). Conserved Nutrient Sensor O-GlcNAc Transferase Is Integral to C. elegans Pathogen-Specific Immunity. *PLoS ONE*, *9*(12), e113231. https://doi.org/10.1371/journal.pone.0113231

Brenner, S. (1974). The genetics of Caenorhabditis elegans. *Genetics*, *77*(1), 71–94.

Byars, C. L., Bates, K. L., & Letsou, A. (1999). The dorsal-open group gene raw is required for restricted DJNK signaling during closure. *Development (Cambridge, England)*, *126*(21), 4913–4923.

Calfon, M., Zeng, H., Urano, F., Till, J. H., Hubbard, S. R., Harding, H. P., Clark, S. G., & Ron, D. (2002). IRE1 couples endoplasmic reticulum load to secretory capacity by processing the XBP-1 mRNA. *Nature*, *415*(6867), 92–96. https://doi.org/10.1038/415092a

Campbell, J. C., Polan-Couillard, L. F., Chin-Sang, I. D., & Bendena, W. G. (2016). NPR-9, a Galanin-Like G-Protein Coupled Receptor, and GLR-1 Regulate Interneuronal Circuitry Underlying Multisensory Integration of Environmental Cues in Caenorhabditis elegans. *PLoS Genetics*, *12*(5), e1006050. https://doi.org/10.1371/journal.pgen.1006050

Cao, X., & Aballay, A. (2016). Neural Inhibition of Dopaminergic Signaling Enhances Immunity in a Cell-Non-autonomous Manner. *Current Biology : CB*, *26*(17), 2329–2334. https://doi.org/10.1016/j.cub.2016.06.036

Cao, X., Kajino-Sakamoto, R., Doss, A., & Aballay, A. (2017). Distinct Roles of Sensory Neurons in Mediating Pathogen Avoidance and Neuropeptide-Dependent Immune Regulation. *Cell Reports*, *21*(6), 1442–1451. https://doi.org/10.1016/j.celrep.2017.10.050

Chalfie, M., Tu, Y., Euskirchen, G., Ward, W., & Prasher, D. (1994). Green fluorescent protein as a marker for gene expression. *Science*, *263*(5148), 802–805. https://doi.org/10.1126/science.8303295

Chang, H. C., Paek, J., & Kim, D. H. (2011). Natural polymorphisms in C. elegans HECW-1 E3 ligase affect pathogen avoidance behaviour. *Nature*, *480*(7378), 525–529.

Cheesman, H. K., Feinbaum, R. L., Thekkiniath, J., Dowen, R. H., Conery, A. L., & Pukkila-Worley, R. (2016). Aberrant Activation of p38 MAP Kinase-Dependent Innate Immune Responses Is Toxic to Caenorhabditis elegans. *G3 (Bethesda, Md.)*, *6*(3), 541–549. https://doi.org/10.1534/g3.115.025650

Christophides, G. K., Zdobnov, E., Barillas-Mury, C., Birney, E., Blandin, S., Blass, C., Brey, P. T., Collins, F. H., Danielli, A., Dimopoulos, G., Hetru, C., Hoa, N. T., Hoffmann, J. A., Kanzok, S. M., Letunic, I., Levashina, E. A., Loukeris, T. G., Lycett, G., Meister, S., … Kafatos, F. C. (2002). Immunity-Related Genes and Gene Families inAnopheles gambiae. *Science*, *298*(5591), 159–165. https://doi.org/10.1126/science.1077136

Chuang, C.-F., & Bargmann, C. I. (2005). A Toll-interleukin 1 repeat protein at the synapse specifies asymmetric odorant receptor expression via ASK1 MAPKKK signaling. *Genes & Development*, *19*(2), 270–281. https://doi.org/10.1101/gad.1276505

Chuang, C.-F., VanHoven, M. K., Fetter, R. D., Verselis, V. K., & Bargmann, C. I. (2007). An Innexin-Dependent Cell Network Establishes Left-Right Neuronal Asymmetry in C. elegans. *Cell*, *129*(4), 787–799. https://doi.org/10.1016/j.cell.2007.02.052

Cohen, L. B., & Troemel, E. R. (2015). Microbial pathogenesis and host defense in the nematode C. elegans. *Current Opinion in Microbiology*, *23*, 94–101. https://doi.org/10.1016/j.mib.2014.11.009

Conaway, R. C., & Conaway, J. W. (2011). Function and regulation of the Mediator complex. *Current Opinion in Genetics & Development*, *21*(2), 225–230. https://doi.org/10.1016/j.gde.2011.01.013

Conery, A. L., Larkins-Ford, J., Ausubel, F. M., & Kirienko, N. V. (2014). High-throughput screening for novel anti-infectives using a C. elegans pathogenesis model. *Current Protocols in Chemical Biology*, *6*(1), 25–37. https://doi.org/10.1002/9780470559277.ch130160

Consortium, U. I. G., Barrett, J. C., Lee, J. C., Lees, C. W., Prescott, N. J., Anderson, C. A., Phillips, A., Wesley, E., Parnell, K., Zhang, H., Drummond, H., Nimmo, E. R., Massey, D., Blaszczyk, K., Elliott, T., Cotterill, L., Dallal, H., Lobo, A. J., Mowat, C., … Strachan, D. P. (2009). Genome-wide association study of ulcerative colitis

identifies three new susceptibility loci, including the HNF4A region. *Nature Genetics*, *41*(12), 1330–1334. https://doi.org/10.1038/ng.483

Cook, S. J., Jarrell, T. A., Brittin, C. A., Wang, Y., Bloniarz, A. E., Yakovlev, M. A., Nguyen, K. C. Q., Tang, L. T.-H., Bayer, E. A., Duerr, J. S., Bülow, H. E., Hobert, O., Hall, D. H., & Emmons, S. W. (2019). Whole-animal connectomes of both Caenorhabditis elegans sexes. *Nature*, *571*(7763), 63–71. https://doi.org/10.1038/s41586-019-1352-7

Costantini, T. W., & Baird, A. (2016). Lost your nerve? Modulating the parasympathetic nervous system to treat inflammatory bowel disease. *The Journal of Physiology*, *594*(15), 4097–4098. https://doi.org/10.1113/jp272372

Dierking, K., Polanowska, J., Omi, S., Engelmann, I., Gut, M., Lembo, F., Ewbank, J. J., & Pujol, N. (2011). Unusual regulation of a STAT protein by an SLC6 family transporter in C. elegans epidermal innate immunity. *Cell Host & Microbe*, *9*(5), 425–435. https://doi.org/10.1016/j.chom.2011.04.011

Dijksterhuis, J., Veenhuis, M., & Harder, W. (1990). Ultrastructural study of adhesion and initial stages of infection of nematodes by conidia of Drechmeria coniospora. *Mycological Research*, *94*(1), 1–8. https://doi.org/10.1016/s0953-7562(09)81257-4

Dunbar, T. L., Yan, Z., Balla, K. M., Smelkinson, M. G., & Troemel, E. R. (2012). C. elegans Detects Pathogen-Induced Translational Inhibition to Activate Immune Signaling. *Cell Host & Microbe*, *11*(4), 375–386. https://doi.org/10.1016/j.chom.2012.02.008

Engelmann, I., Griffon, A., Tichit, L., Montañana-Sanchis, F., Wang, G., Reinke, V., Waterston, R. H., Hillier, L. W., & Ewbank, J. J. (2011). A comprehensive analysis of gene expression changes provoked by bacterial and fungal infection in C. elegans. *PloS One*, *6*(5), e19055. https://doi.org/10.1371/journal.pone.0019055

Ercan, S., Giresi, P. G., Whittle, C. M., Zhang, X., Green, R. D., & Lieb, J. D. (2007). X chromosome repression by localization of the C. elegans dosage compensation machinery to sites of transcription initiation. *Nature Genetics*, *39*(3), 403–408. https://doi.org/10.1038/ng1983

Ermolaeva, M. A., & Schumacher, B. (2014). Insights from the worm: the C. elegans model for innate immunity. *Seminars in Immunology*, *26*(4), 303–309. https://doi.org/10.1016/j.smim.2014.04.005

Espelt, M. V., Estevez, A. Y., Yin, X., & Strange, K. (2005). Oscillatory Ca2+ Signaling in the Isolated Caenorhabditis elegans Intestine. *The Journal of General Physiology*, *126*(4), 379–392. https://doi.org/10.1085/jgp.200509355

Estes, K. A., Dunbar, T. L., Powell, J. R., Ausubel, F. M., & Troemel, E. R. (2010). bZIP transcription factor zip-2 mediates an early response to Pseudomonas aeruginosa infection in Caenorhabditis elegans. *Proceedings of the National Academy of Sciences*, *107*(5), 2153–2158. https://doi.org/10.1073/pnas.0914643107

Evans, E. A., Chen, W. C., & Tan, M.-W. (2008). The DAF-2 insulin-like signaling pathway independently regulates aging and immunity in C. elegans. *Aging Cell*, *7*(6), 879–893. https://doi.org/10.1111/j.1474-9726.2008.00435.x

Evans, E. A., Kawli, T., & Tan, M.-W. (2008). Pseudomonas aeruginosa Suppresses Host Immunity by Activating the DAF-2 Insulin-Like Signaling Pathway in Caenorhabditis elegans. *PLoS Pathogens*, *4*(10), e1000175. https://doi.org/10.1371/journal.ppat.1000175

Ewbank, J. J., & Pujol, N. (2016). Local and long-range activation of innate immunity by infection and damage in C. elegans. *Current Opinion in Immunology*, *38*, 1–7. https://doi.org/10.1016/j.coi.2015.09.005

Ewels, P., Magnusson, M., Lundin, S., & Käller, M. (2016). MultiQC: summarize analysis results for multiple tools and samples in a single report. *Bioinformatics*, *32*(19), 3047–3048. https://doi.org/10.1093/bioinformatics/btw354

Feng, Y. J., & Li, Y. Y. (2011). The role of p38 mitogen-activated protein kinase in the pathogenesis of inflammatory bowel disease. *Journal of Digestive Diseases*, *12*(5), 327–332. https://doi.org/10.1111/j.1751-2980.2011.00525.x

Fire, A., Xu, S., Montgomery, M. K., Kostas, S. A., Driver, S. E., & Mello, C. C. (1998). Potent and specific genetic interference by double-stranded RNA in Caenorhabditis elegans. *Nature*, *391*(6669), 806–811. https://doi.org/10.1038/35888

Flanagan, D., Austin, C., Vincan, E., & Phesse, T. (2018). Wnt Signalling in Gastrointestinal Epithelial Stem Cells. *Genes*, *9*(4), 178. https://doi.org/10.3390/genes9040178

Foster, K. J., Cheesman, H. K., Liu, P., Peterson, N. D., Anderson, S. M., & Pukkila-Worley, R. (2020). Innate Immunity in the C. elegans Intestine Is Programmed by a Neuronal Regulator of AWC Olfactory Neuron Development. *Cell Reports*, *31*(1), 107478. https://doi.org/10.1016/j.celrep.2020.03.042

Foster, K. J., McEwan, D. L., & Pukkila-Worley, R. (2020). Measurements of Innate Immune Function in C. elegans. *Methods in Molecular Biology (Clifton, N.J.)*, *2144*, 145–160. https://doi.org/10.1007/978-1-0716-0592-9_13

Friedland, A. E., Tzur, Y. B., Esvelt, K. M., Colaiácovo, M. P., Church, G. M., & Calarco, J. A. (2013). Heritable genome editing in C. elegans via a CRISPR-Cas9 system. *Nature Methods*, *10*(8), 741–743. https://doi.org/10.1038/nmeth.2532

Gravato-Nobre, M. J., Nicholas, H. R., Nijland, R., O'Rourke, D., Whittington, D. E., Yook, K. J., & Hodgkin, J. (2005). Multiple Genes Affect Sensitivity of Caenorhabditis elegans to the Bacterial Pathogen Microbacterium nematophilum. *Genetics*, *171*(3), 1033–1045. https://doi.org/10.1534/genetics.105.045716

Ha, H., Hendricks, M., Shen, Y., Gabel, C. V., Fang-Yen, C., Qin, Y., Colón-Ramos, D., Shen, K., Samuel, A. D. T., & Zhang, Y. (2010). Functional organization of a neural network for aversive olfactory learning in Caenorhabditis elegans. *Neuron*, *68*(6), 1173–1186. https://doi.org/10.1016/j.neuron.2010.11.025

Haenni, S., Ji, Z., Hoque, M., Rust, N., Sharpe, H., Eberhard, R., Browne, C., Hengartner, M. O., Mellor, J., Tian, B., & Furger, A. (2012). Analysis of C. elegans intestinal gene expression and polyadenylation by fluorescence-activated nuclei sorting and 3′-end-seq. *Nucleic Acids Research*, *40*(13), 6304–6318. https://doi.org/10.1093/nar/gks282

Han, S. K., Lee, D., Lee, H., Kim, D., Son, H. G., Yang, J.-S., Lee, S.-J. V., & Kim, S. (2016). OASIS 2: online application for survival analysis 2 with features for the analysis of maximal lifespan and healthspan in aging research. *Oncotarget*, *7*(35), 56147–56152. https://doi.org/10.18632/oncotarget.11269

Hao, Y., Yang, W., Ren, J., Hall, Q., Zhang, Y., & Kaplan, J. M. (2018). C. elegans avoidance of Pseudomonas: thioredoxin shapes the sensory response to bacterially produced nitric oxide. *BioRxiv*, 289827. https://doi.org/10.1101/289827

Hartenstein, V. (2006). The neuroendocrine system of invertebrates: a developmental and evolutionary perspective. *Journal of Endocrinology*, *190*(3), 555–570. https://doi.org/10.1677/joe.1.06964

Haynes, C. M., & Ron, D. (2010). The mitochondrial UPR - protecting organelle protein homeostasis. *Journal of Cell Science*, *123*(22), 3849–3855. https://doi.org/10.1242/jcs.075119

Head, B., & Aballay, A. (2014). Recovery from an acute infection in C. elegans requires the GATA transcription factor ELT-2. *PLoS Genetics*, *10*(10), e1004609. https://doi.org/10.1371/journal.pgen.1004609

Henderson, S. T., & Johnson, T. E. (2001). daf-16 integrates developmental and environmental inputs to mediate aging in the nematode Caenorhabditis elegans. *Current Biology*, *11*(24), 1975–1980. https://doi.org/10.1016/s0960-9822(01)00594-2

Hoeven, R. van der, McCallum, K. C., Cruz, M. R., & Garsin, D. A. (2011). Ce-Duox1/BLI-3 generated reactive oxygen species trigger protective SKN-1 activity via p38 MAPK signaling during infection in C. elegans. *PLoS Pathogens*, *7*(12), e1002453. https://doi.org/10.1371/journal.ppat.1002453

Hoffman, C., & Aballay, A. (2019). Role of neurons in the control of immune defense. *Current Opinion in Immunology*, *60*, 30–36. https://doi.org/10.1016/j.coi.2019.04.005

Hollenbach, E., Neumann, M., Vieth, M., Roessner, A., Malfertheiner, P., & Naumann, M. (2004). Inhibition of p38 MAP kinase-and RICK/NF-κB-signaling suppresses inflammatory bowel disease. *The FASEB Journal*, *18*(13), 1550–1552. https://doi.org/10.1096/fj.04-1642fje

Huang, S. L. B., Saheki, Y., VanHoven, M. K., Torayama, I., Ishihara, T., Katsura, I., Linden, A. van der, Sengupta, P., & Bargmann, C. I. (2007). Left-right olfactory asymmetry results from antagonistic functions of voltage-activated calcium channels and the Raw repeat protein OLRN-1 in C. elegans. *Neural Development*, *2*(1), 24. https://doi.org/10.1186/1749-8104-2-24

Irazoqui, J. E., Ng, A., Xavier, R. J., & Ausubel, F. M. (2008). Role for beta-catenin and HOX transcription factors in Caenorhabditis elegans and mammalian host epithelial-pathogen interactions. *Proceedings of the National Academy of Sciences of the United States of America*, *105*(45), 17469–17474. https://doi.org/10.1073/pnas.0809527105

Irazoqui, J. E., Troemel, E. R., Feinbaum, R. L., Luhachack, L. G., Cezairliyan, B. O., & Ausubel, F. M. (2010). Distinct Pathogenesis and Host Responses during Infection of C. elegans by P. aeruginosa and S. aureus. *PLoS Pathogens*, *6*(7), e1000982. https://doi.org/10.1371/journal.ppat.1000982

Iwasa, H., Han, J., & Ishikawa, F. (2003). Mitogen-activated protein kinase p38 defines the common senescence-signalling pathway. *Genes to Cells*, *8*(2), 131–144. https://doi.org/10.1046/j.1365-2443.2003.00620.x

Janssen, T., Lindemans, M., Meelkop, E., Temmerman, L., & Schoofs, L. (2010). Coevolution of neuropeptidergic signaling systems: from worm to man: Janssen et al. *Annals of the New York Academy of Sciences*, *1200*(1), 1–14. https://doi.org/10.1111/j.1749-6632.2010.05506.x

Jee, C., Lee, J., Lim, J. P., Parry, D., Messing, R. O., & McIntire, S. L. (2012). SEB-3, a CRF receptor-like GPCR, regulates locomotor activity states, stress responses and ethanol tolerance in Caenorhabditis elegans: Stress response in C. elegans. *Genes, Brain and Behavior*, *12*(2), 250–262. https://doi.org/10.1111/j.1601-183x.2012.00829.x

Johnson, G. V. W., & Bailey, C. D. C. (2003). The p38 MAP kinase signaling pathway in Alzheimer's disease. *Experimental Neurology*, *183*(2), 263–268. https://doi.org/10.1016/s0014-4886(03)00268-1

Keating, C. D., Kriek, N., Daniels, M., Ashcroft, N. R., Hopper, N. A., Siney, E. J., Holden-Dye, L., & Burke, J. F. (2003). Whole-Genome Analysis of 60 G Protein-Coupled Receptors in Caenorhabditis elegans by Gene Knockout with RNAi. *Current Biology*, *13*(19), 1715–1720. https://doi.org/10.1016/j.cub.2003.09.003

Kerry, S., TeKippe, M., Gaddis, N. C., & Aballay, A. (2006). GATA Transcription Factor Required for Immunity to Bacterial and Fungal Pathogens. *PLoS ONE*, *1*(1), e77. https://doi.org/10.1371/journal.pone.0000077

Keshet, Y., & Seger, R. (2010). The MAP kinase signaling cascades: a system of hundreds of components regulates a diverse array of physiological functions. *Methods in Molecular Biology (Clifton, N.J.)*, *661*, 3–38. https://doi.org/10.1007/978-1-60761-795-2_1

Kim, D. H. (2018). Signaling in the innate immune response. *WormBook*, 1–35. https://doi.org/10.1895/wormbook.1.83.2

Kim, D. H., Feinbaum, R., Alloing, G., Emerson, F. E., Garsin, D. A., Inoue, H., Tanaka-Hino, M., Hisamoto, N., Matsumoto, K., Tan, M.-W., & Ausubel, F. M. (2002). A Conserved p38 MAP Kinase Pathway in Caenorhabditis elegans Innate Immunity. *Science*, *297*(5581), 623–626. https://doi.org/10.1126/science.1073759

Kim, D., Langmead, B., & Salzberg, S. L. (2015). HISAT: a fast spliced aligner with low memory requirements. *Nature Methods*, *12*(4), 357–360. https://doi.org/10.1038/nmeth.3317

Kim, K. W., Thakur, N., Piggott, C. A., Omi, S., Polanowska, J., Jin, Y., & Pujol, N. (2016). Coordinated inhibition of C/EBP by Tribbles in multiple tissues is essential for Caenorhabditis elegans development. *BMC Biology*, *14*(1), 104. https://doi.org/10.1186/s12915-016-0320-z

Kirienko, N. V., Ausubel, F. M., & Ruvkun, G. (2015). Mitophagy confers resistance to siderophore-mediated killing by Pseudomonas aeruginosa. *Proceedings of the National Academy of Sciences*, *112*(6), 1821–1826. https://doi.org/10.1073/pnas.1424954112

Kirienko, N. V., Cezairliyan, B. O., Ausubel, F. M., & Powell, J. R. (2014). Pseudomonas aeruginosa PA14 pathogenesis in Caenorhabditis elegans. *Methods in Molecular Biology (Clifton, N.J.)*, *1149*, 653–669. https://doi.org/10.1007/978-1-4939-0473-0_50

Komiya, Y., & Habas, R. (2008). Wnt signal transduction pathways. *Organogenesis*, *4*(2), 68–75. https://doi.org/10.4161/org.4.2.5851

Kumar, S., Egan, B. M., Kocsisova, Z., Schneider, D. L., Murphy, J. T., Diwan, A., & Kornfeld, K. (2019). Lifespan Extension in C. elegans Caused by Bacterial Colonization of the Intestine and Subsequent Activation of an Innate Immune Response. *Developmental Cell*, *49*(1), 100-117.e6. https://doi.org/10.1016/j.devcel.2019.03.010

Labed, S. A., Wani, K. A., Jagadeesan, S., Hakkim, A., Najibi, M., & Irazoqui, J. E. (2018). Intestinal Epithelial Wnt Signaling Mediates Acetylcholine-Triggered Host Defense against Infection. *Immunity*, *48*(5), 963-978.e3. https://doi.org/10.1016/j.immuni.2018.04.017

Lakhan, S. E., & Kirchgessner, A. (2010). Neuroinflammation in inflammatory bowel disease. *Journal of Neuroinflammation*, *7*(1), 37. https://doi.org/10.1186/1742-2094-7-37

Lee, K., & Mylonakis, E. (2017). An Intestine-Derived Neuropeptide Controls Avoidance Behavior in Caenorhabditis elegans. *Cell Reports*, *20*(10), 2501–2512. https://doi.org/10.1016/j.celrep.2017.08.053

Lee, S.-H., Wong, R.-R., Chin, C.-Y., Lim, T.-Y., Eng, S.-A., Kong, C., Ijap, N. A., Lau, M.-S., Lim, M.-P., Gan, Y.-H., He, F.-L., Tan, M.-W., & Nathan, S. (2013). Burkholderia pseudomallei suppresses Caenorhabditis elegans immunity by specific degradation of a GATA transcription factor. *Proceedings of the National Academy of Sciences of the United States of America*, *110*(37), 15067–15072. https://doi.org/10.1073/pnas.1311725110

Li, H. (2011). A statistical framework for SNP calling, mutation discovery, association mapping and population genetical parameter estimation from sequencing data. *Bioinformatics*, *27*(21), 2987–2993. https://doi.org/10.1093/bioinformatics/btr509

Li, H. (2018). Minimap2: pairwise alignment for nucleotide sequences. *Bioinformatics*, *34*(18), 3094–3100. https://doi.org/10.1093/bioinformatics/bty191

Li, H., Handsaker, B., Wysoker, A., Fennell, T., Ruan, J., Homer, N., Marth, G., Abecasis, G., & Durbin, R. (2009). The Sequence Alignment/Map format and SAMtools. *Bioinformatics*, *25*(16), 2078–2079. https://doi.org/10.1093/bioinformatics/btp352

Liang, J., Yu, L., Yin, J., & Savage-Dunn, C. (2007). Transcriptional repressor and activator activities of SMA-9 contribute differentially to BMP-related signaling

outputs. *Developmental Biology*, *305*(2), 714–725. https://doi.org/10.1016/j.ydbio.2007.02.038

Liberati, N. T., Fitzgerald, K. A., Kim, D. H., Feinbaum, R., Golenbock, D. T., & Ausubel, F. M. (2004). Requirement for a conserved Toll/interleukin-1 resistance domain protein in the Caenorhabditis elegans immune response. *Proceedings of the National Academy of Sciences*, *101*(17), 6593–6598. https://doi.org/10.1073/pnas.0308625101

Liu, Y., Sellegounder, D., & Sun, J. (2016). Neuronal GPCR OCTR-1 regulates innate immunity by controlling protein synthesis in Caenorhabditis elegans. *Scientific Reports*, *6*(1), 36832. https://doi.org/10.1038/srep36832

Luong, D., Perez, L., & Jemc, J. C. (2018). Identification of raw as a regulator of glial development. *PloS One*, *13*(5), e0198161. https://doi.org/10.1371/journal.pone.0198161

MacNeil, L. T., Pons, C., Arda, H. E., Giese, G. E., Myers, C. L., & Walhout, A. J. M. (2015). Transcription Factor Activity Mapping of a Tissue-Specific In Vivo Gene Regulatory Network. *Cell Systems*, *1*(2), 152–162. https://doi.org/10.1016/j.cels.2015.08.003

Malik, S., & Roeder, R. G. (2010). The metazoan Mediator co-activator complex as an integrative hub for transcriptional regulation. *Nature Reviews. Genetics*, *11*(11), 761–772. https://doi.org/10.1038/nrg2901

Mallo, G. V., Kurz, C. L., Couillault, C., Pujol, N., Granjeaud, S., Kohara, Y., & Ewbank, J. J. (2002). Inducible Antibacterial Defense System in C. elegans. *Current Biology*, *12*(14), 1209–1214. https://doi.org/10.1016/s0960-9822(02)00928-4

Mascarini-Serra, L. (2011). Prevention of soil-transmitted helminth infection. *Journal of Global Infectious Diseases*, *3*(2), 175–182. https://doi.org/10.4103/0974-777x.81696

McCorry, L. K. (2007). Physiology of the Autonomic Nervous System. *American Journal of Pharmaceutical Education*, *71*(4), 78. https://doi.org/10.5688/aj710478

McEwan, D. L., Feinbaum, R. L., Stroustrup, N., Haas, W., Conery, A. L., Anselmo, A., Sadreyev, R., & Ausubel, F. M. (2016). Tribbles ortholog NIPI-3 and bZIP transcription factor CEBP-1 regulate a Caenorhabditis elegans intestinal immune surveillance pathway. *BMC Biology*, *14*(1), 105. https://doi.org/10.1186/s12915-016-0334-6

McEwan, D. L., Kirienko, N. V., & Ausubel, F. M. (2012). Host Translational Inhibition by Pseudomonas aeruginosa Exotoxin A Triggers an Immune Response in

Caenorhabditis elegans. *Cell Host & Microbe*, *11*(4), 364–374. https://doi.org/10.1016/j.chom.2012.02.007

McGhee, J. D., Birchall, J. C., Chung, M. A., Cottrell, D. A., Edgar, L. G., Svendsen, P. C., & Ferrari, D. C. (1990). Production of null mutants in the major intestinal esterase gene (ges-1) of the nematode Caenorhabditis elegans. *Genetics*, *125*(3), 505–514.

Means, T. K., Mylonakis, E., Tampakakis, E., Colvin, R. A., Seung, E., Puckett, L., Tai, M. F., Stewart, C. R., Pukkila-Worley, R., Hickman, S. E., Moore, K. J., Calderwood, S. B., Hacohen, N., Luster, A. D., & Khoury, J. E. (2009). Evolutionarily conserved recognition and innate immunity to fungal pathogens by the scavenger receptors SCARF1 and CD36. *J. Exp. Med.*, *206*(3), 637–653.

Medzhitov, R., & Janeway, C. A. (1998). An ancient system of host defense. *Current Opinion in Immunology*, *10*(1), 12–15. https://doi.org/10.1016/s0952-7915(98)80024-1

Meisel, J. D., & Kim, D. H. (2014). Behavioral avoidance of pathogenic bacteria by Caenorhabditis elegans. *Trends in Immunology*, *35*(10), 465–470. https://doi.org/10.1016/j.it.2014.08.008

Meisel, J. D., Panda, O., Mahanti, P., Schroeder, F. C., & Kim, D. H. (2014). Chemosensation of Bacterial Secondary Metabolites Modulates Neuroendocrine Signaling and Behavior of C. elegans. *Cell*, *159*(2), 267–280. https://doi.org/10.1016/j.cell.2014.09.011

Melo, J. A., & Ruvkun, G. (2012). Inactivation of Conserved C. elegans Genes Engages Pathogen- and Xenobiotic-Associated Defenses. *Cell*, *149*(2), 452–466. https://doi.org/10.1016/j.cell.2012.02.050

Miller, E. V., Grandi, L. N., Giannini, J. A., Robinson, J. D., & Powell, J. R. (2015). The Conserved G-Protein Coupled Receptor FSHR-1 Regulates Protective Host Responses to Infection and Oxidative Stress. *PLOS ONE*, *10*(9), e0137403. https://doi.org/10.1371/journal.pone.0137403

Minevich, G., Park, D. S., Blankenberg, D., Poole, R. J., & Hobert, O. (2012). CloudMap: A Cloud-Based Pipeline for Analysis of Mutant Genome Sequences. *Genetics*, *192*(4), 1249–1269. https://doi.org/10.1534/genetics.112.144204

Miyata, S., Begun, J., Troemel, E. R., & Ausubel, F. M. (2008). DAF-16-Dependent Suppression of Immunity During Reproduction in Caenorhabditis elegans. *Genetics*, *178*(2), 903–918. https://doi.org/10.1534/genetics.107.083923

Mochii, M., Yoshida, S., Morita, K., Kohara, Y., & Ueno, N. (1999). Identification of transforming growth factor-beta - regulated genes in Caenorhabditis elegans by differential hybridization of arrayed cDNAs. *Proceedings of the National Academy of Sciences*, *96*(26), 15020–15025. https://doi.org/10.1073/pnas.96.26.15020

Mogilevski, T., Burgell, R., Aziz, Q., & Gibson, P. R. (2019). Review article: the role of the autonomic nervous system in the pathogenesis and therapy of IBD. *Alimentary Pharmacology & Therapeutics*, *50*(7), 720–737. https://doi.org/10.1111/apt.15433

Moore, R. S., Kaletsky, R., & Murphy, C. T. (2019). Piwi/PRG-1 Argonaute and TGF-β Mediate Transgenerational Learned Pathogenic Avoidance. *Cell*, *177*(7), 1827-1841.e12. https://doi.org/10.1016/j.cell.2019.05.024

Morrison, D. K. (2012). MAP kinase pathways. *Cold Spring Harbor Perspectives in Biology*, *4*(11), a011254–a011254. https://doi.org/10.1101/cshperspect.a011254

Moy, T. I., Conery, A. L., Larkins-Ford, J., Wu, G., Mazitschek, R., Casadei, G., Lewis, K., Carpenter, A. E., & Ausubel, F. M. (2009). High-throughput screen for novel antimicrobials using a whole animal infection model. *ACS Chemical Biology*, *4*(7), 527–533. https://doi.org/10.1021/cb900084v

Murphy, C. T., McCarroll, S. A., Bargmann, C. I., Fraser, A., Kamath, R. S., Ahringer, J., Li, H., & Kenyon, C. (2003). Genes that act downstream of DAF-16 to influence the lifespan of Caenorhabditis elegans. *Nature*, *424*(6946), 277–283. https://doi.org/10.1038/nature01789

Nandakumar, M., & Tan, M.-W. (2008). Gamma-linolenic and stearidonic acids are required for basal immunity in Caenorhabditis elegans through their effects on p38 MAP kinase activity. *PLoS Genetics*, *4*(11), e1000273. https://doi.org/10.1371/journal.pgen.1000273

Nargund, A M, Pellegrino, M. W., Fiorese, C. J., Baker, B. M., & Haynes, C. M. (2012). Mitochondrial Import Efficiency of ATFS-1 Regulates Mitochondrial UPR Activation. *Science*, *337*(6094), 587–590. https://doi.org/10.1126/science.1223560

Nargund, Amrita M, Fiorese, C. J., Pellegrino, M. W., Deng, P., & Haynes, C. M. (2015). Mitochondrial and nuclear accumulation of the transcription factor ATFS-1 promotes OXPHOS recovery during the UPR(mt). *Molecular Cell*, *58*(1), 123–133. https://doi.org/10.1016/j.molcel.2015.02.008

Nathoo, A. N., Moeller, R. A., Westlund, B. A., & Hart, A. C. (2001). Identification of neuropeptide-like protein gene families in Caenorhabditis elegans and other species. *Proceedings of the National Academy of Sciences*, *98*(24), 14000–14005. https://doi.org/10.1073/pnas.241231298

Nemati, R., Mehdizadeh, S., Salimipour, H., Yaghoubi, E., Alipour, Z., Tabib, S. M., & Assadi, M. (2017). Neurological manifestations related to Crohn's disease: a boon for the workforce. *Gastroenterology Report*, *7*(4), 291–297. https://doi.org/10.1093/gastro/gox034

Ng, L., Kaur, P., Bunnag, N., Suresh, J., Sung, I., Tan, Q., Gruber, J., & Tolwinski, N. (2019). WNT Signaling in Disease. *Cells*, *8*(8), 826. https://doi.org/10.3390/cells8080826

Nüsslein-Volhard, C., & Wieschaus, E. (1980). Mutations affecting segment number and polarity in Drosophila. *Nature*, *287*(5785), 795–801. https://doi.org/10.1038/287795a0

O'Donnell, M. P., Fox, B. W., Chao, P.-H., Schroeder, F. C., & Sengupta, P. (2019). Modulation of sensory behavior and food choice by an enteric bacteria-produced neurotransmitter. *BioRxiv*, 735845. https://doi.org/10.1101/735845

O'Donnell, M. P., Fox, B. W., Chao, P.-H., Schroeder, F. C., & Sengupta, P. (2020). A neurotransmitter produced by gut bacteria modulates host sensory behaviour. *Nature*, *583*(7816), 415–420. https://doi.org/10.1038/s41586-020-2395-5

Oka, T., Toyomura, T., Honjo, K., Wada, Y., & Futai, M. (2001). Four SubunitaIsoforms ofCaenorhabditis elegansVacuolar H+-ATPase: CELL-SPECIFIC EXPRESSION DURING DEVELOPMENT. *Journal of Biological Chemistry*, *276*(35), 33079–33085. https://doi.org/10.1074/jbc.m101652200

Ookuma, S., Fukuda, M., & Nishida, E. (2003). Identification of a DAF-16 Transcriptional Target Gene, scl-1, that Regulates Longevity and Stress Resistance in Caenorhabditis elegans. *Current Biology*, *13*(5), 427–431. https://doi.org/10.1016/s0960-9822(03)00108-8

Pagano, D. J., Kingston, E. R., & Kim, D. H. (2015a). Tissue expression pattern of PMK-2 p38 MAPK is established by the miR-58 family in C. elegans. *PLOS Genetics*, *11*(2), e1004997.

Pagano, D. J., Kingston, E. R., & Kim, D. H. (2015b). Tissue expression pattern of PMK-2 p38 MAPK is established by the miR-58 family in C. elegans. *PLoS Genetics*, *11*(2), e1004997. https://doi.org/10.1371/journal.pgen.1004997

Pellegrino, M. W., Nargund, A. M., Kirienko, N. V., Gillis, R., Fiorese, C. J., & Haynes, C. M. (2014). Mitochondrial UPR-regulated innate immunity provides resistance to pathogen infection. *Nature*, *516*(7531), 414–417. https://doi.org/10.1038/nature13818

Pertea, M., Kim, D., Pertea, G. M., Leek, J. T., & Salzberg, S. L. (2016). Transcript-level expression analysis of RNA-seq experiments with HISAT, StringTie and Ballgown. *Nature Protocols*, *11*(9), 1650–1667. https://doi.org/10.1038/nprot.2016.095

Pertea, M., Pertea, G. M., Antonescu, C. M., Chang, T.-C., Mendell, J. T., & Salzberg, S. L. (2015). StringTie enables improved reconstruction of a transcriptome from RNA-seq reads. *Nature Biotechnology*, *33*(3), 290–295. https://doi.org/10.1038/nbt.3122

Peters, J. C., & Harper, A. E. (1985). Adaptation of Rats to Diets Containing Different Levels of Protein: Effects on Food Intake, Plasma and Brain Amino Acid Concentrations and Brain Neurotransmitter Metabolism. *The Journal of Nutrition*, *115*(3), 382–398. https://doi.org/10.1093/jn/115.3.382

Peterson, N. D., Cheesman, H. K., Liu, P., Anderson, S. M., Foster, K. J., Chhaya, R., Perrat, P., Thekkiniath, J., Yang, Q., Haynes, C. M., & Pukkila-Worley, R. (2019). The nuclear hormone receptor NHR-86 controls anti-pathogen responses in C. elegans. *PLoS Genetics*, *15*(1), e1007935. https://doi.org/10.1371/journal.pgen.1007935

Peterson, N. D., & Pukkila-Worley, R. (2018). Caenorhabditis elegans in high-throughput screens for anti-infective compounds. *Current Opinion in Immunology*, *54*, 59–65. https://doi.org/10.1016/j.coi.2018.06.003

Pfaffl, M. W. (2001). A new mathematical model for relative quantification in real-time RT-PCR. *Nucleic Acids Research*, *29*(9), 45e–445. https://doi.org/10.1093/nar/29.9.e45

Portal-Celhay, C., Bradley, E. R., & Blaser, M. J. (2012). Control of intestinal bacterial proliferation in regulation of lifespan in Caenorhabditis elegans. *BMC Microbiology*, *12*(1), 49. https://doi.org/10.1186/1471-2180-12-49

Powell, J. R., & Ausubel, F. M. (2008). Innate Immunity. *Methods in Molecular Biology (Clifton, N.J.)*, *415*, 403–427. https://doi.org/10.1007/978-1-59745-570-1_24

Powell, J. R., Kim, D. H., & Ausubel, F. M. (2009). The G protein-coupled receptor FSHR-1 is required for the Caenorhabditis elegans innate immune response. *Proceedings of the National Academy of Sciences of the United States of America*, *106*(8), 2782–2787. https://doi.org/10.1073/pnas.0813048106

Pujol, N., Cypowyj, S., Ziegler, K., Millet, A., Astrain, A., Goncharov, A., Jin, Y., Chisholm, A. D., & Ewbank, J. J. (2008). Distinct innate immune responses to infection and wounding in the C. elegans epidermis. *Current Biology : CB*, *18*(7), 481–489. https://doi.org/10.1016/j.cub.2008.02.079

Pujol, N., Link, E. M., Liu, L. X., Kurz, C. L., Alloing, G., Tan, M.-W., Ray, K. P., Solari, R., Johnson, C. D., & Ewbank, J. J. (2001). A reverse genetic analysis of components of the Toll signaling pathway in Caenorhabditis elegans. *Current Biology*, *11*(11), 809–821. https://doi.org/10.1016/s0960-9822(01)00241-x

Pujol, N., Zugasti, O., Wong, D., Couillault, C., Kurz, C. L., Schulenburg, H., & Ewbank, J. J. (2008). Anti-fungal innate immunity in C. elegans is enhanced by evolutionary diversification of antimicrobial peptides. *PLoS Pathogens*, *4*(7), e1000105. https://doi.org/10.1371/journal.ppat.1000105

Pukkila-Worley, R. (2016a). Surveillance Immunity: An Emerging Paradigm of Innate Defense Activation in Caenorhabditis elegans. *PLoS Pathog*, *12*(9), e1005795.

Pukkila-Worley, R. (2016b). Surveillance Immunity: An Emerging Paradigm of Innate Defense Activation in Caenorhabditis elegans. *PLOS Pathogens*, *12*(9), e1005795. https://doi.org/10.1371/journal.ppat.1005795

Pukkila-Worley, R., & Ausubel, F. M. (2012a). Immune defense mechanisms in the Caenorhabditis elegans intestinal epithelium. *Current Opinion in Immunology*, *24*(1), 3–9. https://doi.org/10.1016/j.coi.2011.10.004

Pukkila-Worley, R., & Ausubel, F. M. (2012b). Immune defense mechanisms in the Caenorhabditis elegans intestinal epithelium. *Current Opinion in Immunology*, *24*(1), 3–9. https://doi.org/10.1016/j.coi.2011.10.004

Pukkila-Worley, R., Ausubel, F. M., & Mylonakis, E. (2011). Candida albicans infection of Caenorhabditis elegans induces antifungal immune defenses. *PLoS Pathogens*, *7*(6), e1002074. https://doi.org/10.1371/journal.ppat.1002074

Pukkila-Worley, R., Feinbaum, R., Kirienko, N. V., Larkins-Ford, J., Conery, A. L., & Ausubel, F. M. (2012). Stimulation of Host Immune Defenses by a Small Molecule Protects C. elegans from Bacterial Infection. *PLoS Genetics*, *8*(6), e1002733. https://doi.org/10.1371/journal.pgen.1002733

Pukkila-Worley, R., Feinbaum, R. L., McEwan, D. L., Conery, A. L., & Ausubel, F. M. (2014). The Evolutionarily Conserved Mediator Subunit MDT-15/MED15 Links Protective Innate Immune Responses and Xenobiotic Detoxification. *PLoS Pathogens*, *10*(5), e1004143. https://doi.org/10.1371/journal.ppat.1004143

Pukkila-Worley, R., Gerrald, Q. D., Kraus, P. R., Boily, M.-J., Davis, M. J., Giles, S. S., Cox, G. M., Heitman, J., & Alspaugh, J. A. (2005). Transcriptional network of multiple capsule and melanin genes governed by the Cryptococcus neoformans cyclic AMP cascade. *Eukaryot. Cell*, *4*(1), 190–201.

Pukkila-Worley, R., Peleg, A. Y., Tampakakis, E., & Mylonakis, E. (2009). Candida albicans Hyphal Formation and Virulence Assessed Using a Caenorhabditis elegans Infection Model. *Eukaryotic Cell*, *8*(11), 1750–1758. https://doi.org/10.1128/ec.00163-09

Rahme, L., Stevens, E., Wolfort, S., Shao, J., Tompkins, R., & Ausubel, F. (1995). Common virulence factors for bacterial pathogenicity in plants and animals. *Science*, *268*(5219), 1899–1902. https://doi.org/10.1126/science.7604262

Rankin, C. H. (2006). Nematode Behavior: The Taste of Success, the Smell of Danger! *Current Biology*, *16*(3), R89–R91. https://doi.org/10.1016/j.cub.2006.01.025

Reddy, K C, Andersen, E. C., Kruglyak, L., & Kim, D. H. (2009). A Polymorphism in npr-1 Is a Behavioral Determinant of Pathogen Susceptibility in C. elegans. *Science*, *323*(5912), 382–384. https://doi.org/10.1126/science.1166527

Reddy, Kirthi C., Dunbar, T. L., Nargund, A. M., Haynes, C. M., & Troemel, E. R. (2016). The C. elegans CCAAT-Enhancer-Binding Protein Gamma Is Required for Surveillance Immunity. *Cell Reports*, *14*(7), 1581–1589. https://doi.org/10.1016/j.celrep.2016.01.055

Richardson, C. E., Kinkel, S., & Kim, D. H. (2011). Physiological IRE-1-XBP-1 and PEK-1 Signaling in Caenorhabditis elegans Larval Development and Immunity. *PLoS Genetics*, *7*(11), e1002391. https://doi.org/10.1371/journal.pgen.1002391

Richardson, C. E., Kooistra, T., & Kim, D. H. (2010). An essential role for XBP-1 in host protection against immune activation in C. elegans. *Nature*, *463*(7284), 1092–1095. https://doi.org/10.1038/nature08762

Roach, N. P., Sadowski, N., Alessi, A. F., Timp, W., Taylor, J., & Kim, J. K. (2019). The full-length transcriptome of C. elegans using direct RNA sequencing. *BioRxiv*, 598763. https://doi.org/10.1101/598763

Roayaie, K., Crump, J. G., Sagasti, A., & Bargmann, C. I. (1998). The Gα Protein ODR-3 Mediates Olfactory and Nociceptive Function and Controls Cilium Morphogenesis in C. elegans Olfactory Neurons. *Neuron*, *20*(1), 55–67. https://doi.org/10.1016/s0896-6273(00)80434-1

Roberts, A. F., Gumienny, T. L., Gleason, R. J., Wang, H., & Padgett, R. W. (2010). Regulation of genes affecting body size and innate immunity by the DBL-1/BMP-like pathway in Caenorhabditis elegans. *BMC Dev. Biol.*, *10*, 61.

Ron, D., & Walter, P. (2007). Signal integration in the endoplasmic reticulum unfolded protein response. *Nature Reviews Molecular Cell Biology*, *8*(7), 519–529. https://doi.org/10.1038/nrm2199

Rual, J.-F., Ceron, J., Koreth, J., Hao, T., Nicot, A.-S., Hirozane-Kishikawa, T., Vandenhaute, J., Orkin, S. H., Hill, D. E., Heuvel, S. van den, & Vidal, M. (2004). Toward Improving Caenorhabditis elegans Phenome Mapping With an ORFeome-Based RNAi Library. *Genome Research*, *14*(10b), 2162–2168. https://doi.org/10.1101/gr.2505604

Sackton, T. B., Lazzaro, B. P., Schlenke, T. A., Evans, J. D., Hultmark, D., & Clark, A. G. (2007). Dynamic evolution of the innate immune system in Drosophila. *Nature Genetics*, *39*(12), 1461–1468. https://doi.org/10.1038/ng.2007.60

Sagasti, A., Hisamoto, N., Hyodo, J., Tanaka-Hino, M., Matsumoto, K., & Bargmann, C. I. (2001). The CaMKII UNC-43 Activates the MAPKKK NSY-1 to Execute a Lateral Signaling Decision Required for Asymmetric Olfactory Neuron Fates. *Cell*, *105*(2), 221–232. https://doi.org/10.1016/s0092-8674(01)00313-0

Sanahuja, J. C., & Harper, A. E. (1962). Effect of amino acid imbalance on food intake and preference. *American Journal of Physiology-Legacy Content*, *202*(1), 165–170. https://doi.org/10.1152/ajplegacy.1962.202.1.165

Sawin, E. R., Ranganathan, R., & Horvitz, H. R. (2000). C. elegans Locomotory Rate Is Modulated by the Environment through a Dopaminergic Pathway and by Experience through a Serotonergic Pathway. *Neuron*, *26*(3), 619–631. https://doi.org/10.1016/s0896-6273(00)81199-x

Schulenburg, H., & Ewbank, J. J. (2007). The genetics of pathogen avoidance in Caenorhabditis elegans. *Molecular Microbiology*, *66*(3), 563–570. https://doi.org/10.1111/j.1365-2958.2007.05946.x

Sellegounder, D., Liu, Y., Wibisono, P., Chen, C.-H., Leap, D., & Sun, J. (2019). Neuronal GPCR NPR-8 regulates C. elegans defense against pathogen infection. *Science Advances*, *5*(11), eaaw4717. https://doi.org/10.1126/sciadv.aaw4717

Sellegounder, D., Yuan, C.-H., Wibisono, P., Liu, Y., & Sun, J. (2018). Octopaminergic Signaling Mediates Neural Regulation of Innate Immunity in Caenorhabditis elegans. *MBio*, *9*(5), e01645-18. https://doi.org/10.1128/mbio.01645-18

Shapira, M., Hamlin, B. J., Rong, J., Chen, K., Ronen, M., & Tan, M.-W. (2006). A conserved role for a GATA transcription factor in regulating epithelial innate immune responses. *Proceedings of the National Academy of Sciences*, *103*(38), 14086–14091. https://doi.org/10.1073/pnas.0603424103

Shen, X., Ellis, R. E., Lee, K., Liu, C.-Y., Yang, K., Solomon, A., Yoshida, H., Morimoto, R., Kurnit, D. M., Mori, K., & Kaufman, R. J. (2001). Complementary Signaling Pathways Regulate the Unfolded Protein Response and Are Required for C. elegans Development. *Cell*, *107*(7), 893–903. https://doi.org/10.1016/s0092-8674(01)00612-2

Shivers, R. P., Kooistra, T., Chu, S. W., Pagano, D. J., & Kim, D. H. (2009). Tissue-Specific Activities of an Immune Signaling Module Regulate Physiological Responses to Pathogenic and Nutritional Bacteria in C. elegans. *Cell Host & Microbe*, *6*(4), 321–330. https://doi.org/10.1016/j.chom.2009.09.001

Shivers, R. P., Pagano, D. J., Kooistra, T., Richardson, C. E., Reddy, K. C., Whitney, J. K., Kamanzi, O., Matsumoto, K., Hisamoto, N., & Kim, D. H. (2010). Phosphorylation of the conserved transcription factor ATF-7 by PMK-1 p38 MAPK regulates innate immunity in Caenorhabditis elegans. *PLoS Genetics*, *6*(4), e1000892. https://doi.org/10.1371/journal.pgen.1000892

Shivers, R. P., Youngman, M. J., & Kim, D. H. (2008). Transcriptional responses to pathogens in Caenorhabditis elegans. *Current Opinion in Microbiology*, *11*(3), 251–256. https://doi.org/10.1016/j.mib.2008.05.014

Shtonda, B. B., & Avery, L. (2006). Dietary choice behavior in Caenorhabditis elegans. *Journal of Experimental Biology*, *209*(1), 89–102. https://doi.org/10.1242/jeb.01955

Singh, J., & Aballay, A. (2019). Microbial Colonization Activates an Immune Fight-and-Flight Response via Neuroendocrine Signaling. *Developmental Cell*, *49*(1), 89-99.e4. https://doi.org/10.1016/j.devcel.2019.02.001

Singh, V., & Aballay, A. (2009). Regulation of DAF-16-mediated Innate Immunity in Caenorhabditis elegans. *Journal of Biological Chemistry*, *284*(51), 35580–35587. https://doi.org/10.1074/jbc.m109.060905

Sluder, A. E., Mathews, S. W., Hough, D., Yin, V. P., & Maina, C. V. (1999). The nuclear receptor superfamily has undergone extensive proliferation and diversification in nematodes. *Genome Research*, *9*(2), 103–120.

Sommeren, S. van, Visschedijk, M. C., Festen, E. A. M., Jong, D. J. de, Ponsioen, C. Y., Wijmenga, C., & Weersma, R. K. (2010). HNF4α and CDH1 are associated with ulcerative colitis in a Dutch cohort. *Inflammatory Bowel Diseases*, *17*(8), 1714–1718. https://doi.org/10.1002/ibd.21541

Sowa, J. N., Jiang, H., Somasundaram, L., Tecle, E., Xu, G., Wang, D., & Troemel, E. R. (2020). The Caenorhabditis elegans RIG-I Homolog DRH-1 Mediates the Intracellular

Pathogen Response upon Viral Infection. *Journal of Virology*, *94*(2). https://doi.org/10.1128/jvi.01173-19

Styer, K. L., Singh, V., Macosko, E., Steele, S. E., Bargmann, C. I., & Aballay, A. (2008). Innate immunity in Caenorhabditis elegans is regulated by neurons expressing NPR-1/GPCR. *Science (New York, N.Y.)*, *322*(5900), 460–464. https://doi.org/10.1126/science.1163673

Sun, J, Singh, V., Kajino-Sakamoto, R., & Aballay, A. (2011). Neuronal GPCR Controls Innate Immunity by Regulating Noncanonical Unfolded Protein Response Genes. *Science*, *332*(6030), 729–732. https://doi.org/10.1126/science.1203411

Sun, Jingru, Liu, Y., & Aballay, A. (2012). Organismal regulation of XBP-1-mediated unfolded protein response during development and immune activation. *EMBO Reports*, *13*(9), 855–860. https://doi.org/10.1038/embor.2012.100

SUN, S.-C., & FAYE, I. (1992). Cecropia immunoresponsive factor, an insect immunoresponsive factor with DNA-binding properties similar to nuclear-factor KB. *European Journal of Biochemistry*, *204*(2), 885–892. https://doi.org/10.1111/j.1432-1033.1992.tb16708.x

Tan, M.-W., Mahajan-Miklos, S., & Ausubel, F. M. (1999). Killing of Caenorhabditis elegans by Pseudomonas aeruginosa used to model mammalian bacterial pathogenesis. *Proceedings of the National Academy of Sciences*, *96*(2), 715–720. https://doi.org/10.1073/pnas.96.2.715

Taubert, S., Gilst, M. R. V., Hansen, M., & Yamamoto, K. R. (2006). A Mediator subunit, MDT-15, integrates regulation of fatty acid metabolism by NHR-49-dependent and -independent pathways in C. elegans. *Genes & Development*, *20*(9), 1137–1149. https://doi.org/10.1101/gad.1395406

Taubert, S., Hansen, M., Gilst, M. R. V., Cooper, S. B., & Yamamoto, K. (2005). The Mediator Subunit MDT-15 Confers Metabolic Adaptation to Ingested Material. *PLoS Genetics*, *preprint*(2008), e40. https://doi.org/10.1371/journal.pgen.0040040.eor

Taubert, S., Hansen, M., Gilst, M. R. V., Cooper, S. B., & Yamamoto, K. R. (2008). The Mediator Subunit MDT-15 Confers Metabolic Adaptation to Ingested Material. *PLoS Genetics*, *4*(2), e1000021. https://doi.org/10.1371/journal.pgen.1000021

Taubert, S., Ward, J. D., & Yamamoto, K. R. (2011). Nuclear hormone receptors in nematodes: Evolution and function. *Molecular and Cellular Endocrinology*, *334*(1–2), 49–55. https://doi.org/10.1016/j.mce.2010.04.021

Tenor, J. L., & Aballay, A. (2008). A conserved Toll-like receptor is required for Caenorhabditis elegans innate immunity. *EMBO Reports*, *9*(1), 103–109. https://doi.org/10.1038/sj.embor.7401104

Torayama, I., Ishihara, T., & Katsura, I. (2007). Caenorhabditis elegans Integrates the Signals of Butanone and Food to Enhance Chemotaxis to Butanone. *Journal of Neuroscience*, *27*(4), 741–750. https://doi.org/10.1523/jneurosci.4312-06.2007

Tran, A., Tang, A., O'Loughlin, C. T., Balistreri, A., Chang, E., Villa, D. C., Li, J., Varshney, A., Jimenez, V., Pyle, J., Tsujimoto, B., Wellbrook, C., Vargas, C., Duong, A., Ali, N., Matthews, S. Y., Levinson, S., Woldemariam, S., Khuri, S., … VanHoven, M. K. (2017). C. elegans avoids toxin-producing Streptomyces using a seven transmembrane domain chemosensory receptor. *ELife*, *6*, e23770. https://doi.org/10.7554/elife.23770

Troemel, E. R. (2011). New models of microsporidiosis: infections in Zebrafish, C. elegans, and honey bee. *PLoS Pathogens*, *7*(2), e1001243. https://doi.org/10.1371/journal.ppat.1001243

Troemel, E. R., Chu, S. W., Reinke, V., Lee, S. S., Ausubel, F. M., & Kim, D. H. (2006). p38 MAPK Regulates Expression of Immune Response Genes and Contributes to Longevity in C. elegans. *PLoS Genetics*, *2*(11), e183. https://doi.org/10.1371/journal.pgen.0020183

Troemel, E. R., Félix, M.-A., Whiteman, N. K., Barrière, A., & Ausubel, F. M. (2008). Microsporidia Are Natural Intracellular Parasites of the Nematode Caenorhabditis elegans. *PLoS Biology*, *6*(12), e309. https://doi.org/10.1371/journal.pbio.0060309

Troemel, E. R., Kimmel, B. E., & Bargmann, C. I. (1997). Reprogramming Chemotaxis Responses: Sensory Neurons Define Olfactory Preferences in C. elegans. *Cell*, *91*(2), 161–169. https://doi.org/10.1016/s0092-8674(00)80399-2

Troemel, E. R., Sagasti, A., & Bargmann, C. I. (1999). Lateral Signaling Mediated by Axon Contact and Calcium Entry Regulates Asymmetric Odorant Receptor Expression in C. elegans. *Cell*, *99*(4), 387–398. https://doi.org/10.1016/s0092-8674(00)81525-1

VanHoven, M. K., Huang, S. L. B., Albin, S. D., & Bargmann, C. I. (2006). The Claudin Superfamily Protein NSY-4 Biases Lateral Signaling to Generate Left-Right Asymmetry in C. elegans Olfactory Neurons. *Neuron*, *51*(3), 291–302. https://doi.org/10.1016/j.neuron.2006.06.029

Visvikis, O., Ihuegbu, N., Labed, S. A., & Luhachack, L. G. (2014). Innate host defense requires TFEB-mediated transcription of cytoprotective and antimicrobial genes. *Immunity*.

Vowels, J. J., & Thomas, J. H. (1992). Genetic analysis of chemosensory control of dauer formation in Caenorhabditis elegans. *Genetics*, *130*(1), 105–123.

Wang, W., Chen, J. X., Liao, R., Deng, Q., Zhou, J. J., Huang, S., & Sun, P. (2002). Sequential Activation of the MEK-Extracellular Signal-Regulated Kinase and MKK3/6-p38 Mitogen-Activated Protein Kinase Pathways Mediates Oncogenic ras-Induced Premature Senescence. *Molecular and Cellular Biology*, *22*(10), 3389–3403. https://doi.org/10.1128/mcb.22.10.3389-3403.2002

Ward, J. D. (2014). Rapid and Precise Engineering of theCaenorhabditis elegansGenome with Lethal Mutation Co-Conversion and Inactivation of NHEJ Repair. *Genetics*, *199*(2), 363–377. https://doi.org/10.1534/genetics.114.172361

Ward, S., Thomson, N., White, J. G., & Brenner, S. (1975). Electron microscopical reconstruction of the anterior sensory anatomy of the nematodecaenorhabditis elegans. *The Journal of Comparative Neurology*, *160*(3), 313–337. https://doi.org/10.1002/cne.901600305

Ware, R. W., Clark, D., Crossland, K., & Russell, R. L. (1975). The nerve ring of the nematodeCaenorhabditis elegans: Sensory input and motor output. *The Journal of Comparative Neurology*, *162*(1), 71–110. https://doi.org/10.1002/cne.901620106

Wasserman, S. A. (1993). A conserved signal transduction pathway regulating the activity of the rel-like proteins dorsal and NF-kappa B. *Molecular Biology of the Cell*, *4*(8), 767–771. https://doi.org/10.1091/mbc.4.8.767

Wehrwein, E. A., Orer, H. S., & Barman, S. M. (2011). Comprehensive Physiology. *Comprehensive Physiology*, *6*(3), 1239–1278. https://doi.org/10.1002/cphy.c150037

Wes, P. D., & Bargmann, C. I. (2001). C. elegans odour discrimination requires asymmetric diversity in olfactory neurons. *Nature*, *410*(6829), 698–701. https://doi.org/10.1038/35070581

White, J. G., Southgate, E., Thomson, J. N., & Brenner, S. (1986). The structure of the nervous system of the nematode Caenorhabditis elegans. *Philosophical Transactions of the Royal Society of London. B, Biological Sciences*, *314*(1165), 1–340. https://doi.org/10.1098/rstb.1986.0056

Wingett, S. W., & Andrews, S. (2018). FastQ Screen: A tool for multi-genome mapping and quality control. *F1000Research*, *7*, 1338. https://doi.org/10.12688/f1000research.15931.2

Wong, D., Bazopoulou, D., Pujol, N., Tavernarakis, N., & Ewbank, J. J. (2007). Genome-wide investigation reveals pathogen-specific and shared signatures in the response of Caenorhabditis elegans to infection. *Genome Biology*, *8*(9), R194. https://doi.org/10.1186/gb-2007-8-9-r194

Xia, Z., Dickens, M., Raingeaud, J. l, Davis, R. J., & Greenberg, M. E. (1995). Opposing Effects of ERK and JNK-p38 MAP Kinases on Apoptosis. *Science*, *270*(5240), 1326–1331. https://doi.org/10.1126/science.270.5240.1326

Yu, S., Avery, L., Baude, E., & Garbers, D. L. (1997). Guanylyl cyclase expression in specific sensory neurons: A new family of chemosensory receptors. *Proceedings of the National Academy of Sciences*, *94*(7), 3384–3387. https://doi.org/10.1073/pnas.94.7.3384

Yu, Y., Zhi, L., Wu, Q., Jing, L., & Wang, D. (2016). NPR-9 regulates the innate immune response in Caenorhabditis elegans by antagonizing the activity of AIB interneurons. *Cellular & Molecular Immunology*, *15*(1), 27–37. https://doi.org/10.1038/cmi.2016.8

Zarubin, T., & Han, J. (2005). Activation and signaling of the p38 MAP kinase pathway. *Cell Research*, *15*(1), 11–18. https://doi.org/10.1038/sj.cr.7290257

Zhang, Y., Lu, H., & Bargmann, C. I. (2005). Pathogenic bacteria induce aversive olfactory learning in Caenorhabditis elegans. *Nature*, *438*(7065), 179–184. https://doi.org/10.1038/nature04216

Zugasti, O., Bose, N., Squiban, B., Belougne, J., Kurz, C. L., Schroeder, F. C., Pujol, N., & Ewbank, J. J. (2014). Activation of a G protein–coupled receptor by its endogenous ligand triggers the innate immune response of Caenorhabditis elegans. *Nature Immunology*, *15*(9), 833–838. https://doi.org/10.1038/ni.2957

Zugasti, O., & Ewbank, J. J. (2009a). Neuroimmune regulation of antimicrobial peptide expression by a noncanonical TGF-beta signaling pathway in Caenorhabditis elegans epidermis. *Nat. Immunol.*, *10*(3), 249–256.

Zugasti, O., & Ewbank, J. J. (2009b). Neuroimmune regulation of antimicrobial peptide expression by a noncanonical TGF-β signaling pathway in Caenorhabditis elegans epidermis. *Nature Immunology*, *10*(3), 249–256. https://doi.org/10.1038/ni.1700